The Ph.D. Thesis

Study on the Improvement of Interior Illumination Distribution by Using Lighting Equipment on Window in order to Use Daylight

Akita University

February, 2018

李 承霖

Chenglin Li

Abstract

Lighting is always necessary during the operation hours from morning to night in an office building and generally, the amount of electric power consumed by lighting is about 20% to 30% of the total electric power consumption. Therefore, the positive effect of using daylight for energy saving in office, and the development of a system that utilizes daylight positively is attracting attention. When developing a lighting device in practice, the season, weather and many other factors have to be considered. For example, when using daylight, direct sunlight entering the room is often dazzling and cannot be used directly. And, in the case of Akita City, the solar altitude angle (the angle between the sunbeam and the earth plane) depends on the season, it is about 75 °at noon of the summer solstice where the sun is the highest, while it is about 30 ° on the winter solstice. Furthermore, solar azimuth angle moves from east in morning to west in the evening. Due to this, the angle of light entering rooms from the windows also changes, which may affect the indoor lighting environment as well. In order to solve these problems, it is necessary to develop a window system using daylight combined with seasonal strong light shielding.

In this research, I have aimed to reflect the direct sunlight incident on the ceiling by attaching angle-changeable reflecting plates (blind-reflectors) to the window, and use the reflected diffused light from rough material of the ceiling for room lighting. In order to avoid dazzling daylight from the window and create a comfortable indoor environment, reflector angle that can be adjusted accordingly with changes in the solar angle of all seasons is needed and it is necessary to obtain the illuminance distribution of the work surface when designing the actual lighting. However, the angle of incident light from the window and the amount of incident light flux change gradually. In order to find out the illuminance distribution in various situations, it is necessary to spend enormous amount of time and cost in designing by performing actual measurements and calculation manually.

Therefore, in order to reduce the time and cost to manually measure and calculate these illuminance distributions, a simulation of illuminance distribution using the Monte Carlo method was performed. In preparing the simulator, I made it possible such that lighting fixtures, rooms, windows and etc. can be freely set and installed. In addition, an illuminance distribution simulator was created that can display the illuminance distribution chart after calculating the reflector angle with sunlight. The function to simulate changes in solar angle depending on the season and time zone was also calculated. In this simulator, the Monte Carlo method was used because compared with other methods, it can reproduce the properties of light with higher precision on a computer, and calculate the illuminance distribution by simulating various conditions in the room desired for virtual space. However, in order to obtain excellent calculation results, enormous calculation time is required. On the other hand,

in this study, by using a new Monte Carlo method for the photon flux generation method from lighting fixtures, fluorescent lamps of various shapes can be reproduced with a point light source, and the calculation speed of the illuminance distribution can be shortened with a simulator. First, the validity of the lighting fixture and the validity of the window by comparing the measured value and the simulation value was compared using this simulator. This method was used to investigate the illuminance distribution in the indoor space. From the simulation results, the indoor lighting environment when changing the solar angle and the reflector's angle in the window was compared. And thus, the possibility of reducing the power consumption was testified.

A model space of a typical laboratory of Akita University was considered in this research work and calculation of illuminance distribution was performed. These simulation works meet the indoor lighting standards described in 「Lighting standard JIS Z 9110: 2010」 of the Japanese Industrial Standard (JIS). The sun angle used in the simulation was based on the solar altitude angle and solar azimuth angle at Akita University and the solar flux amount was also calculated from the measured values. In order to avoid problems such as sunset, this research used daylight in the time zone from 9:00 to 15:00 throughout the whole year. The illuminance distribution on the work surface was compared for the cases of with and without any reflectors installed in the window. From the results, one can understand that the lighting in the room was comfortable when the reflectors were installed in the window. And the effectiveness of the blind reflectors was also confirmed.

In the window system whereby reflectors were installed, the design of the reflectors is important. For example, when designing a reflector, if the width is too long, the daylight that can be reflected on the ceiling will be blocked, and the amount of light taken into the room will reduce. On the other hand, when the width of the reflector is too short, daylight illuminating the workplace through the reflectors will be too dazzling. In order to improve the practicality and performance of the reflector system, I have performed several simulation works to understand the dimensions of the blind reflectors and their installation process in a manner so that the highest amount of light is reflected on the ceiling. As a result, parameters such as the number of blind reflecting plates, length, distance, etc. were determined for real environment in order to get a better lighting system. In actual simulation, since comfortable lighting environment can be obtained, it is installed so that incident light can be reflected to the center of the ceiling. In this research, the JIS illuminance reference values was set as the target values, and by applying the knowledge of the change in the indoor environment due to the change of the position of the sunlight, the horizontal and vertical angle of the slat of the blind reflector was adjusted and the angles which satisfy the comfortable lighting environment under each environment was measured.

From these results, the amount of energy saving which can be achieved by comparing power consumption when using daylight was examined. In the near future, by improving the window

system with reflectors, better energy saving effect is expected which will contribute to a sustainable energy saving society.

Contents

Chapter 1

Introduction

1-1 Background

In recent years, various natural problems such as the thinning of the ozone layer and global warming are aggravating and CO_2 reduction has become an important issue. Globally, the problem of energy shortage has been particularly prominent in countries with rapid economy development. It is important to solve the problem of energy saving not only in Japan but also for other countries in order to achieve sustainable social and economic development. As a large amount of energy is consumed in the field of building lighting, the importance of energy conservation has become even more prominent.

In recent years, it is becoming more common for us to rely on artificial lighting during the daytime even when daylight can be obtained at places such as office buildings. The idea of daytime artificial lighting is to shield direct sunlight to prevent dazzling daylight entering through the window and to further create a high quality illumination environment. The consumption of electric power due to illumination is 20-30% of the total electric power consumption in office buildings as illumination system runs from morning till night [1]. Along with this, the cooling load increases as illumination system dissipates heat in the office rooms. This phenomenon occurs not only in summer but also in other seasons as well. Thus, the use of natural sunlight may pave way for energy saving system of office buildings [2].

As we know, natural light is an inexhaustible natural energy source, and it is also a clean energy which doesn’t cause pollution. The use of natural light as a building lighting energy is the biggest energy saving method. Therefore, natural light source should be used as the lighting energy of buildings as much as possible when the conditions permits. And natural light has several merits compared to artificial lighting.

Full spectrum lighting, such as sunlight, can provide a lot of nutrition to the human body. Many people may have known that natural light contributes to the production of vitamin C. But not everyone knows the effect of sunlight on the production level of vitamin D in the body. Vitamin D is a kind of essential vitamin that helps relieve depression, helps absorb other vitamins and minerals, and is also believed to prevent some types of cancer. Because vitamin D is produced when sunlight comes in contact with skin, short exposure to natural light every day will make it easier for you to get enough vitamin D and help your body resist various diseases [3-6].

Phototherapy is also helpful in the treatment of various types of anxiety. For example, tension and depression associated with seasonal affective disorders are exacerbated by the lack of natural light. People who like to stay indoors and do not touch the sunlight have the risk of

developing this disease and it may lead to complete depression or panic disorder. In fact, getting in contact the natural light for 15-20 minutes a day can be a good way to avoid this kind of problems [7-9].

A study found that employees who work near windows or skylights tend to be less negative and are more likely to focus on their work, and are more creative and happier in their work [10]. In addition, exposure to natural light can also bring practical benefits to many people. For example, getting sunlight into the room helps to reduce the dependence on the lights, which will undoubtedly save a lot of electricity. Working under natural light is more likely to see details than under a light. In addition, there are also theories stating that getting in contact with natural light helps to accelerate the recovery of colds and other diseases [11-13].

In this way, using natural light during actual life and work is important not only for reducing the power consumption of lighting equipment but also for living in a comfortable lighting environment leading to better health. In office buildings, the most common daylighting method is using daylight from the window, and it is common to use it together with artificial lighting. In addition, light is also accompanied by heat, not only to take in light from the window well but also to control the amount of light that enters the room as a measure against dazzling light and heat in order to maintain a comfortable indoor environment. It is thought that the effect of energy saving on the entire office space is great from such daylighting method, and the development of a lighting device which actively utilizes daylight is attracting attention. Again, Bodart and De Herde evaluated the impact of the reduction of lighting power costs on global energy consumption levels, and reported the potential for cutting artificial lighting power costs by 50–80% if daylight is actively incorporated in office buildings [14].

It has been reported that daylight-illumination methods are important for energy saving in buildings by using daylight entering into the rooms from window [14]. For example, Ming-Chin Ho et.al. estimated that 70% of lighting power cost reduction might be possible by using daylight with sun shading devices [15]. Previous works with using daylight illumination methods to reduce the energy consumption of buildings in a variety of indoor environments includes using specular reflectors [15], daylighting film [16, 17], various blinds [18-22], and so on[23-30].

Ming-Chin Ho’s group used daylight and artificial lighting together by using sun-shading system combined with large reflection plates in various ways. According to a survey, it is possible to save up to 70% in subtropical classrooms like Taiwan [15]. Takuma BAN’s group and Masaki Nishimura’s group confirmed the energy saving effect when they reflected the dazzled sunlight to the ceiling using a daylighting film and lighting by diffusing light from the ceiling [16, 17]. Furthermore, the group of Takuma Ban not only confirmed the energy saving effect by using daylight but also evaluated from the perspective of solar heat control [16]. In recent years, studies of blinds that are compatible with solar shielding and daylight control have been actively conducted [18-22]. A blind slat angle control system which helps in conserving

energy and provides comfortability to its users has already been developed [21]. There are various researches on daylight utilization [14-30], and the use of daylight is roughly divided into two kinds, which are direct use and indirect use.

The direct use of natural light is in close coordination with the field of civil engineering. To optimize the usage of building windows by using the methods of converting outdoor natural light into interior light, common window lighting are mainly made up of side window lighting and scuttle lighting. Indirect use of natural light in the control system refers to the use of light, light transmission equipment, astigmatism to match the amount of natural light with artificial light to provide a comfortable lighting environment. For example, the use of lighting film, blinds and so on.

In previous works, there were almost no situations where the energy saving rate was 100%. Artificial lighting is also necessary due to factors such as insufficient illuminance and uniformity, even when using daylight while working indoors. The author measured the amount of sunlight entering the room from the window of the actual office environment at each time zone in order to examine if it is possible to create a comfortable indoor lighting environment simply by using sunlight entering from the actual window. The measurement took place in a typical laboratory of Akita University, and the window was roughly facing south. And in order to avoid glaring sunlight during sunrise and sunset, the daylight hours was set from 9:00 to 15:00. From the measurement results, it was revealed that the amount of incident daylight in almost all time zones is larger than the luminous flux amount of artificial lighting within any lighting time period in any season. In other words, if the sunlight coming from the window is used well, it is considered that a comfortable lighting environment can be created without artificial lighting.

However, in the previous research, there are few situations where only daylight is used. It is thought that the cause is low daylighting rate. In the conventional daylighting method, in the case of the direct use method, the sunlight is not directly used, instead it is the scattered rays after reflection on walls or ceiling that are used. When sunlight enters the room, the consumption rate of sunlight is high due to absorption and shielding etc. in facilities with various lighting means. In the case of using a reflector, the daylighting rate is good, but glaring light concentrates in local areas in the room, so the degree of homogeneity decreases. In order to create a comfortable lighting environment, it is necessary to shield a part of dazzling daylight, combine it with artificial lighting, and increase the degree of uniformity. In the case of daylighting films, sunlight is absorbed or blocked partially when light passes through the lighting film. The light entering the room is a part of the incident daylight. In the case of blinds, by adjusting the angle, the amount of light entering the room can be adjusted, but the incident sunlight on the blind surface is diffuse reflection, and a considerable amount of daylight is reflected out of the room. Likewise, other daylighting methods are unable to raise the lighting

rate due to such problems. Another problem is the conduction of sunlight. The incident sunlight concentrates on the window side, so it can not reach the back of the room.

In order to solve these problems, it is necessary to develop a window system combining the use of daylight with seasonal strong light shielding. Therefore, in this research, a method of using daylight with angle adjustable blind reflectors is proposed. One of the reasons on why research on angle adjustable blinds is active in recent years is its convenience. Since it is attached to the inner side of the window, it has less influence on the working environment and storage is convenient. In this research, the incident sunlight is reflected to the ceiling by setting a few angle adjustable blind reflectors on the window, and the diffuse light reflected from the rough material of the ceiling is used for room lighting. In this case, it is possible to catch almost all light in the room, since it utilizes ceiling diffused light, it can be expected that the ratio of uniformity is high. And since the angle of the blinds is adjustable, it is possible to secure a large lighting rate according to the movement of the sun which constantly changes throughout the day.

And now, products such as smartphones and cars are getting more and more intelligent. Currently, products with high intelligence are already made [31-36]. Therefore, the daylighting system is also made intelligent such that the blind reflectors are able to adjust its angle automatically according to the movement of the sun and becomes a daylighting system that can be used in the future to provide a comfortable indoor lighting environment at any time. Also, as the sun passes the same place on the same day almost every year [37, 38], the azimuth and elevation angle of the sun of any time of the year can be calculated. Correspondingly, the change in angle of the reflector can also be easily calculated. Furthermore, this intelligent system can be used in various fields. For example, in the case of solar power generation, by using such a reflector control system, to concentrate sunlight to a single location, it increases the utilization rate of solar power generation panels and also the number of panels can be reduced.

1-2 Investigation method

When developing a lighting device in practice, the season, weather and many other factors have to be considered. For example, when using daylight, direct sunlight entering the room is often dazzling and cannot be used directly. And, in the case of Akita City, the solar altitude angle (the angle between the sunbeam and the earth plane) depends on the season, it is about 75 °at noon on the summer solstice where the sun is the highest, while it is about 30 °on the winter solstice. Furthermore, solar azimuth angle moves from east in morning to west in the evening [37-41]. Due to this, the angle of light entering rooms from the windows also changes, which may affect the indoor lighting environment as well. When taking in light from the window, it is necessary to know the change of the indoor environment due to the change of the position of the sun and

to consider the arrangement of the lighting equipment to satisfy the comfortable lighting environment under each environment. In order to solve these problems, it is necessary to develop a window system using daylight combined with seasonal strong light shielding.

In this research, the incident sunlight is reflected to the ceiling by attaching angle-changeable reflecting plates (blind-reflectors) to the window, and the reflected diffused light from rough material of the ceiling is used for room lighting. In order to avoid dazzling daylight from the window and create a comfortable indoor environment, reflector angle that can be adjusted accordingly with changes in the solar angle of all seasons is needed and it is necessary to obtain the illuminance distribution of the work surface when designing the actual lighting. However, the angle of incident light from the window and the amount of incident light flux change gradually. In order to find out the illuminance distribution in various situations, it is necessary to spend enormous amount of time and cost in designing by performing actual measurements and calculation manually.

Therefore, optical simulation by computer has been used in recent years in order to reduce the time and cost of actually measuring and manually calculating these illuminance distributions. This is to reproduce the nature and physical phenomenon of light on a computer and to calculate the illuminance and illuminance distribution by simulating various conditions in a room in a virtual space. In recent years, as the performance of the computer have improved rapidly, various illumination distribution simulators using difference calculation methods have been developed.

At present, many professional lighting design software have been developed abroad. 3ds MAX, DIAlux, AGI32, Rayfront and other three dimensional design software for lighting design are also quite effective. But in general, there is no graphic design for AutoCAD in the field of lighting design. Photoshop is also another dominant software in the industry of image processing. The various software have their own advantages and disadvantages.

In a previous research conducted in the author's laboratory, a simulator for room lighting was created and used for lighting design without sunlight [42-49]. In the current research, in order to investigate the indoor conditions in all seasons, an illuminance distribution simulator was built so that sunlight can be used using the Monte Carlo method based on the previous simulator [2, 50]. In preparing the simulator, it was made such that lighting fixtures, rooms, windows and etc. can be freely set and installed. In addition, an illuminance distribution simulator that can display the illuminance distribution chart after calculating the reflector angle with sunlight was created. The function to simulate changes in solar angle depending on the season and time zone was also calculated. In this simulator, the Monte Carlo method was used because compared with other methods, it can reproduce the properties of light with higher precision on a computer, and calculate the illuminance distribution by simulating the various desired conditions for the room in the virtual space [51-55]. However, in order to obtain excellent calculation results, enormous calculation time is required. On the other hand, in this study, by using a new Monte

Carlo method for the photon flux generation method from lighting fixtures, fluorescent lamps of various shapes can be reproduced with a point light source, and the calculation speed of the illuminance distribution can be shortened with a simulator. First, the validity of the lighting fixture and the validity of the window by comparing the measured value and the simulation value was done using this simulator. This method was used to investigate the illuminance distribution in the indoor space. From the simulation results, the indoor lighting environment when changing the solar angle and the reflector's angle in the window was compared. And thus, the possibility of reducing the power consumption was testified.

1-3 Purpose

In this research, a versatile illuminance distribution simulator by using the Monte Carlo method was developed and used to compare the difference in interior lighting environment by changing the angle of the reflector based on the sun angle for all seasons. It was also evaluate the possibility of reduction of power consumption. The specifics are as follows.

1：Creation of illumination distribution simulator using Monte Carlo method

By using the Monte Carlo method, it is possible to create a highly versatile simulator capable of conducting complicated simulations. In this research, parameters such as lighting fixtures, windows, reflectors, sun, etc. can be freely set, and after completion of calculation, an illuminance distribution simulator which can display the illuminance distribution map is created. Before actual simulation, both the validity of the lighting fixture and the validity of the window were verified by comparing the measured value and the simulation value using the created simulator.

2：Changes to the indoor lighting environment and evaluation of the amount of power consumption reduction when it is possible to take light from the window

Using the created illuminance distribution simulator, the illuminance of the observation surface in the case of installing windows and lighting fixture on the ceiling in the model space and the case where no windows are installed in the model space were compared and examined. Together with the results from the actual environment, this study simulated the following three situations in the simulator, and the changes in the indoor lighting environment and the amount of power consumption reduction in the case of daylight adoption were examined. The amount of light flux and the sun angle used during the simulation are all measured values

- **Without direct Sunlight (no Reflector)**

Alike a cloudy day, the incident light through the window is not dazzling and it can be used without installing any reflector on the window.

- **With direct Sunlight (with reflector)**
  Alike a sunny day, the incident light through the window is dazzling and it is necessary for the sunlight from the window to by reflect to the ceiling by using reflectors. The reflectors were controlled by adjusting the vertical angle of the blind reflector.
- **With direct sunlight (with many rows of reflectors)**
  Here, in order to further improve the performance of the reflecting plate, a large number of rows of reflecting plates are controlled by adjusting two types of angle which are the vertical and horizontal angle, and all the incident daylight were reflected to the center of the ceiling.

These three situations were simulated all year round and compared with the case when daylighting from the window is not possible, and the amount of power consumption reduction was evaluated. The ultimate goal of this research is to produce a comfortable lighting environment for an indoor room just by using daylight from the window.

References

[1] The Energy Conservation Center - Energy saving of office buildings - Characteristics of energy consumption of office buildings- https://www.eccj.or.jp/office_bldg/01.html. (in Japanese) ECCJ 省エネルギーセンター ― オフィスビルの省エネルギー ― 1. オフィスビルのエネルギー消費の特徴 ― https://www.eccj.or.jp/office_bldg/01.html

[2] L. Chenglin, M. Kabir: “Development of an Indoor Illuminance Distribution Simulator by using the Monte Carlo Method”, Global Journal of Engineering Science and Research Management, ISSN 2277-9655, vol.4, no.13, pp. 85-94 (2017)

[3] Ola Engelsen: “The Relationship between Ultraviolet Radiation Exposure and Vitamin D Status”, Nutrients, ISSN 2072-6643, pp482-495 (2010)

[4] Jörg Reichrath and Bernd Nürnberg: “Understanding positive and negative effects of solar UV-radiation: A challenge and a fascinating perspective”, Universitätsklinikum des Saarlandes, Homburg/Saar, Germany (2008)

[5] F.R. de Gruijl (INVITED): “Health Effects from Solar UV Radiation”, Radiation Protection Dosimetry, Vol. 72, No. 3–4, pp. 177–196 (1997)

[6] Robyn Lucas, Tony McMichael, Wayne Smith, Bruce Armstrong: “Solar Ultraviolet Radiation - Global burden of disease from solar ultraviolet radiation” Environmental Burden of Disease Series, No. 13, pp1-9 (2006)

[7] Japan Interior Industry Association: “Illumination・color design for elderly people~ Considering harmony between light and color~,” pp. 12-32 (1999) (in Japanese)
社団法人　インテリア産業協会 :「高齢者のための照明・色彩設計~光と色彩の調和を考える~」，pp12-32 (1999)
[8] Jacob Liberman O.D. Ph.D.: “Light: Medicine of the Future: How We Can Use It to Heal Ourselves NOW”, pp. 4-13 (1990)
[9] Misako Okawa: “Bright light treatment for sleep disorders in the elderly”, Lighting Research and Technology, vol.81, no.12 (1997) (in Japanese)
大川匡子:「光 による高齢者の睡眠障害の治療」，照明学会誌 第 81 巻 第 12 号，平成 9 年
[10] Sean Sanders, Ph.D.; Jackie Oberst, Ph.D.: “Changing perspectives on daylight: Science, technology, and culture”, Science, pp. 4-32 (2017)
[11] Dag O. Hessen: “Solar radiation and the evolution of life”, Solar Radiation and Human Health, The Norwegian Academy of Science and Letters, pp. 123-136 (2008)
[12] Juzeniene, Asta & Brekke, Pål & Dahlback, Arne & andersson-engels, Stefan & Reichrath, Jörg & Moan, Kristin & Holick, Michael & Grant, William & Moan, Johan: “Solar radiation and human health”, Reports on Progress in Physics. Pp32-44 (2011)
[13] Caradee Y. Wright, Mary Norval, Beverley Summers, Lester Davids, Gerrie Coetzee, Matthew O. Oriowo: “The impact of solar ultraviolet radiation on human health in sub-Saharan Africa”, South African Journal of Science, Vol 108 No.11 (2012)
[14] M. Bodart, A. De Herde: “Global energy savings in offices buildings by the use of Daylighting”, Energy and Buildings 34, pp. 421–429 (2002)
[15] Ming-Chin Ho, Che-Ming Chiang, Po-Cheng Chou, Kuei-Feng Chang, Chia-Yen Lee: “Optimal sun-shading design for enhanced daylight illumination of subtropical classrooms”, Energy and Buildings 40,pp. 1844–1855 (2008)
[16] Takuma BAN, Takashi INOUE, Norihisa MORIYA, Ryo AKAIKE, Misato SASAHARA, Takehiro TAKASHIMA, Yasushi WATANABE: “Proposal of Shielding Solar Radiation and Simple Daylighting Method by Using Film”, Techinical Papers of Annual Meeting the Society of Heating,Air-conditioning and Sanitary Engineers of Japan, Vol 10 (2014) (in Japanese)
伴 琢磨，井上 隆，守谷 徳久，赤池 亮，笹原 海里，高島 武大 : “採光フィルムによる日射熱制御及び昼光利用の提案”，空気調和・衛生工学会大会学術講演論文集，第10巻 (2014)
[17] Masaki NISHIMURA, Takashi INOUE, Kazuki YAMADA, Yoshinori KAIGUCHI, Kozo TAKASE, Motohiro KOSUGI, Kouta KOBAYASHI: “Study on effectiveness of daylighting film in an actual office”, Techinical Papers of Annual Meeting the Society of Heating,Air-conditioning and Sanitary Engineers of Japan, Vol 10 (2016) (in Japanese)

西村 昌城，井上 隆，山田 一樹，開口 善典，高瀬 幸造，小杉 太洋：“採光フィルムの実空間導入時の有効性に関する検討”，空気調和・衛生工学会大会学術講演論文集，第 10 巻 (2014)

[18] Kumiko Toshi, Takashi Akimoto, Yukihiko Nakajima, Michiya Suzuki, Tatsuo Oka: “Field Measurements on Efficiency of Gradation Blind (Venetian Blinds with Slats Having Different Angles)”, Journal of Asian Architecture and Building Engineering, No.7, pp. 83−86 (1999) (in Japanese)

登石 久美子，中島 幸彦，秋元 孝之，鈴木 道哉，竹林 芳久，岡 建雄：“グラデーションブランイド(角度変化型ブラインド)の性能実測”，日本建築学会技術報告，5 巻 7 号，pp. 83-86 (1999)

[19] Ryo Akaike, Takashi Inoue, Masayuki Ichinose, Katsuki Izumi, Daiki Iwasaki: “Study on combination control of blind and lighting to reflect changes in natural light environment”, Lighting Research and Technology, vol.98, no.5, pp. 218-224 (2014) (in Japanese)

赤池 亮，井上 隆，一ノ瀬 雅之，泉 克樹，岩崎 大輝：“昼光の色味を反映させる照明・ブラインド制御に関する研究”，照明学会誌 98 巻 5 号，pp. 218-224 (2014)

[20] Yoshikazu Nakane, Tadashi Doi and Kei Yokota: “Study on Lighting Designing Based on Daylight (Part 2) -Examination on Lighting Design Method Based on Daylight from Window with Light-diffusing-fixed slats 8lind.一”, Annual report of the sciences of living, Osaka City University, pp. 139-145 (1983) (in Japanese)

中根，芳一，土井 正，横田 圭：“昼光利用照明設計のための基礎研究(その 2)~ 光拡散性固定羽線ブラインド使用による昼光照明設計法の有効性の検討~”，大阪市立大学生活科学部紀要・第 31 巻，pp. 139-145 (1983)

[21] NIKKEN SEKKEI: “Development the System for Daylight Use by Blind Angle Control in Consideration of energy saving and Comfortable environment at NIKKEN SEKKEITOKYO BUILDING”, The Journal of the Institute of Electrical Installation Engineers of Japan, Vol.26, no.7, pp. 526-528 (2006) (in Japanese)

日建設計，松下電工：“日建設計東京ビルにおける省エネルギーと快適性を考慮したブラインドスラット角制御による昼光利用システムの開発”，電気設備学会誌，26 巻 7 号，pp. 526-528 (2006)

[22] Masayuki Ichinose, Takashi Inoue: “Window system combing solar shading and utilization of daylight”, Architectural Institute of Japan, vol.39, pp. 87-91(2009) (in Japanese)

一ノ瀬雅之，井上隆：“自然光利用と日射遮蔽を両立する窓システム”，日本建築学会環境工学委員会熱シンポジウム 39 巻，pp. 87-91 (2009)

[23] Sermin Onayg, Onder Guler: “Determination of the energy saving by daylight responsive lighting control systems with an example from Istanbul”, Building and Environment vol.38, pp. 973 – 977 (2003)

[24] Michele Zinzi, Alessandro Mangione: “The daylighting contribution in the electric lighting energy uses: EN standard and alternative method comparison”, Energy Procedia vol.78, pp. 2663–2668 (2015)
[25] Arman Hashemi: “Daylighting and solar shading performances of an innovative automated reflective louvre system”, Building and Environment vol.82, pp. 607 – 620 (2014).
[26] D.H.W. Li, J.C. Lam, Evaluation of lighting performance in office buildings with daylighting controls, Energy and Buildings 33 (2001) 793–803
[27] T. Inoue: “Solar shading and daylighting by means of autonomous responsive dimming glass: practical application”, Energy and Buildings vol.35, pp. 463–471 (2003)
[28] A.Tsangrassoulis, A.Kontadakis, L.Doulos: “Assessing Lighting Energy Saving Potential from Daylight Harvesting in Office Buildings Based on Code Compliance & Simulation Techniques: A Comparison”, Procedia Environmental Sciences, vol.38, pp. 420-427 (2017)
[29] Ngoc Hai Vu and Seoyong Shin: “A Large Scale Daylighting System Based on a Stepped Thickness Waveguide”, Energies 2016, 9(2), 71; doi:10.3390/en9020071
[30] P. Tsikra, E. Andreou: “Investigation of the Energy Saving Potential in Existing School Buildings in Greece. The role of Shading and Daylight Strategies in Visual Comfort and Energy Saving”, Procedia Environmental Sciences, vol.38, pp. 204 – 211(2017)
[31] Carlo Giovannella, Mihai Dascalu, Federico Scaccia: “Smart City Analytics: state of the art and future perspectives”, Interaction Design and Architecture(s) Journal -, N.20, pp. 72-87 (2014)
[32] Abdelhamied A.Ateya, Ammar Muthanna, Irina Gudkova, Abdelrahman Abuarqoub, Anastasia Vybornova and Andrey Koucheryavy: “Development of Intelligent Core Network for Tactile Internet and Future Smart Systems”, J. Sens. Actuator Netw, doi:10.3390/jsan7010001 (2017)
[33] Lennart Bochmann, Timo Bänziger, Andreas Kunz, Konrad Wegener: “Human-robot Collaboration in Decentralized Manufacturing Systems: An Approach for Simulation-based Evaluation of Future Intelligent Production”, Procedia CIRP, Vol.62, pp.624-629 (2017)
[34] Ricardo Jardim-Goncalves, David Romero & Antonio Grilo: “Factories of the future: challenges and leading innovations in intelligent manufacturing”, International Journal of Computer Integrated Manufacturing, Vol.30 Issue 1, pp. 4 – 14 (2017)
[35] Georgios Lilis, Gilbert Conus, Nastaran Asadi, Maher Kayal: “Towards the next generation of intelligent building: An assessment study of current automation and future IoT based systems with a proposal for transitional design”, Sustainable Cities and Society, Vol.28, pp. 473-481 (January 2017)
[36] Marco Venturelli, Guido Borghi, Roberto Vezzani, Rita Cucchiara: “Deep Head Pose Estimation from Depth Data for In-car Automotive Applications”, DIEF - University of Modena and Reggio Emilia, arXiv:1703.01883v1 [cs.CV] 6 Mar 2017
[37] The National Astronomical Observatory of Japan (NAOJ) http://www.nao.ac.jp

[38] Lee Jin You, Roger: “Yong Heavenly Mathematics GEK 1506 - Sun and Architecture”, pp.1-14

[39] Masahiro Kajikawa: “On the Calculating Diagrams of Solar Altitude and Solar Azimuth on the Northern Hemisphere”, Geophysical bulletin of Hokkaido University, No.13, pp. 71-98 (1965) (in Japanese)

梶川 正弘:「北半球における太陽高度角および方位角の計算図の作成」, 北海道大学地球物理学研究報告, No.13, pp. 71-98 (1965)

[40] David B.Ampratwum, Atsu S.S.Dorvlo: “Estimation of solar radiation from the number of sunshine hours”, Applied Energy, Volume 63, Issue 3, pp. 161-167, July 1999

[41] Philip Scherrer & Deborah Scherrer, Stanford Solar Center: “Solstice and Equinox (Sun track) Season Model”

[42] L.Chen,M.Suzuki, N.Yoshimura: “Study on Optimal Lighting Configuration and Aberration of Inspection System by Monte Carlo Method”, J.Light & Visual Environment, vol.23, No.1, pp.20-28 (1999)

[43] L.Chen,X.Wang,M.Suzuki,N.Yoshimura: “Optimizing the Lighting in Automatic Inspection System using Monte Carlo Method”, Jpn.J.Appl.Phys.vol.38, No.10, pp.6123-6129 (1999)

[44] L. Chen, M. Suzuki and N. Yoshimura: “An Application of Monte Carlo Method on Simulating Optical Aberration of Automatic Inspection System,” *Jpn. J. Appl. Phys.*, vol.**38**, No.4A, pp. 2155-2160 (1999)

[45] M. Suzuki, N. Yoshimura, O. Kimura and M. Awata: “Monte Carlo simulation for Color Changes Caused by an Inter-reflection Light”, Lighting Research and Technology, vol.78, no.2, pp.65-71 (1994) (in Japanese)

鈴木 雅史, 吉村 昇, 木村 修, 粟田 昌延 : “モンテカルロ法を用いた相互反射光による色彩変化のシミュレーション”, 照明学会誌 / 78 巻 (1994) 2 号

[46] L. Chen, M. Suzuki, T. Goda and N. Yoshimura: “Luminous intensity characteristics of luminaires: Monte Carlo simulation”, International journal of Lighting Research and Technology, vol.30, no.4, pp.159-164 (1998)

[47] M. Suzuki, K. Akazawa and Noboru Yoshimura: “Luminous Intensity Distribution of Luminaires with Specular Reflectors”, Lighting Research and Technology, vol.88, no.2, pp.85-90 (2004) (in Japanese)

鈴木雅史, 赤澤幸造, 吉村昇: “鏡面反射を有する照明器具の配光特性” ,照明学会誌, 88 巻 2 号, pp.85-90 (2004)

[48] Masafumi Suzuki, Takashi Yamaguchi, Hidemasa Nakajima, Noboru Yoshimura: “The Back Light Simulation of the Direct Method LCD - Consideration in the Arrangement of the Fluorescent Lamp”, Journal of Environmental Engineering, Vol.35, No.5, pp.361-363 (2001) (in Japanese)

鈴木雅史　山口隆志　中嶋秀正　吉村昇：“直下型液晶ディスプレイのバックライトシミュレーション　-蛍光ランプの配置における一考察-”，照明学会誌，85 巻 5 号, pp.361-363 (2001)

[49] L.Chen, X.Wang, M.Suzuki and N.Yoshimura: “Comparison of Direst and Indirect Photometric Descriptions in Monte Carlo Lighting Simulation”, Jpn.J.Appl.Phys, vol.39, No.8, pp.4786-4792 (2000)

[50] L. Chenglin and M. Kabir: “The Use of Daylight for Interior Illumination System with Window Shade Reflector”, International Journal of Engineering Sciences & Research Technology, ISSN 2277-9655, Vol.6, No.5, pp.7-14 (2017)

[51] M. I. Disney, P. Lewis, P. R. J. North: “Monte Carlo ray tracing in optical canopy reflectance modelling”, Remote Sensing Reviews，Volume 18, 2000 - Issue 2-4, pp163-196 (2009)

[52] Henrik Wann Jensen: “Monte Carlo Ray Tracing”, University of California, San Diego, pp.1-14 (2003)

[53] Lawrence, David E: “Cluster-Based Bounded Influence Regression”, Statistics, Chapter 8.Monte Carlo Simulation pp.1-3 (2016)

[54] Gabriel A. Terejanu: “Tutorial on Monte Carlo Techniques”, Department of Computer Science and Engineering University at Buffalo, Buffalo, NY 14260

[55] Dirk P. Kroese: “Monte Carlo Methods”, Department of Mathematics School of Mathematics and Physics, The University of Queensland, pp 9-12

Chapter 2

Simulation method

In this chapter, I will briefly describe how light is defined in illumination engineering and explain how light is handled on computers.

2-1 Photometric value and the units [1-6]

Radiation is a kind of energy, but light is a form of electromagnetic radiation that is visible to the human eye. Therefore, the amount of light luminance is not a physical value but a kind of psychophysical value. Various Units about light (i.e. the definition of photometric values and its units) are described below.

1：Luminous flux

Luminous flux describes the total amount of light emitted by a light source. It differs from

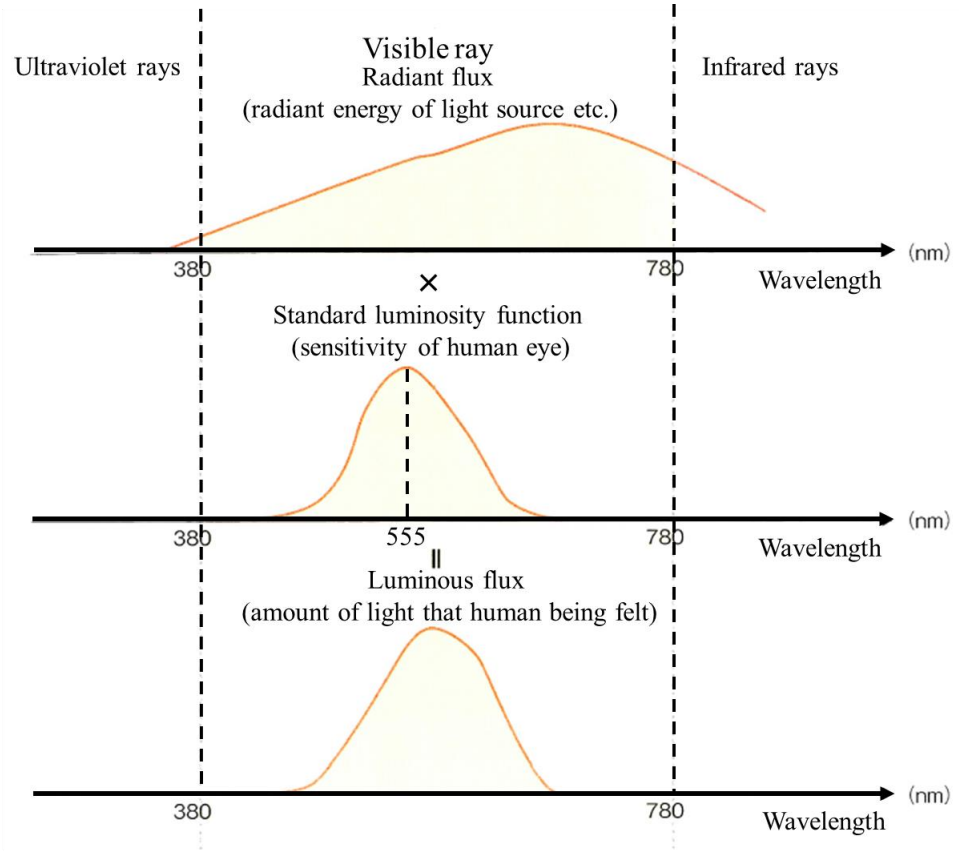

Fig. 2-1 Idea of luminous flux [2]

radiant flux such that luminous flux is the sensitivity of the human eye towards the different wavelengths of light. It was determined internationally, that a standard function called luminosity function was set by the CIE (Commission Internationale de l'Ĕclairage). The human eye is sensitive to a portion of the magnetic spectrum with wavelength between 380 to 780 nanometers. The maximum sensitivity is the yellow green light which wavelength is 555 nm (frequency 540 THz) (Fig. 2-1).

A luminous flux φ is a value obtained by measuring the radiant flux in the visible wavelength range with reference to the sensitivity of the eye which use the luminosity function $V(\lambda)$ described in eq. (2-1).

$$\varphi = \mathrm{K}m \int_{380}^{780} V(\lambda)P(\lambda)d\lambda \qquad (2\text{-}1)$$

In the eq. (2-1), the unit of luminous flux φ: lumen [lm], $P(\lambda)$: The spectral radiant flux (Power per unit wavelength width of radiant flux at wavelength λ) [W/nm], λ：Wavelength [nm], Km：Conversion factor of radiant flux and luminous flux at wavelength of maximum visual sensitivity, 683 lm/W. The image diagram is shown in Fig. 2-1.

By using the equation above, the luminous flux is measured as the amount of radiant flux sensed by the human eyes, which is the basis of the following photometric amount. The luminous flux emitted from the actual light source is shown in the following Table 2-1.

2：Luminous intensity

An object that emits light is called a light source. We will refer a point or size of negligible distance (1/10 or less of the length of light fixture) as a point light source.

Luminous fluxes are emitted to all directions from this point light source. The luminous flux included in the unit solid angle in a certain direction (1 steradian [sr]), i.e. the solid angle density of the luminous flux is called Luminous intensity. The unit for measuring luminous intensity is called candela [cd]. It is defined as one of the base units in the International System of Units. In order to handle light, the effect of radiation toward human vision must be taken

Table 2-1 The luminous flux of some light sources

Light source		Luminous flux［lm］
Sun		3.6×10^{28}
Incandescent lamps	40W	485
White fluorescent lamp	40W	3000
Fluorescent mercury lamp	40W	1400

into account. The luminosity is the base unit because a special candle was used for the initial metering standard. The luminous intensity is calculated by using luminous flux in eq. (2-2) and has since become the current base unit being used for luminous intensity.

In Fig. 2-2, if there exists a luminous flux dφ [lm] in the small solid angle at a certain direction, the luminous intensity I [cd] in the direction of the arrow of this light source is expressed by the following equation.

$$I = \frac{d\varphi}{d\omega}, \quad d\varphi = I \cdot d\omega \tag{2-2}$$

The approximate luminous intensity values of actual light sources are shown in the following Table 2-2.

A point light source having equal luminous intensity in all directions is a uniform point source. If luminosity is expressed as I_0 [cd] and the total solid angle around one point is 4π [sr], the total luminous flux φ[lm] emitted from this light source is described by eq. (2-3)

$$\varphi = 4\pi I_0 \quad [\mathrm{lm}] \tag{2-3}$$

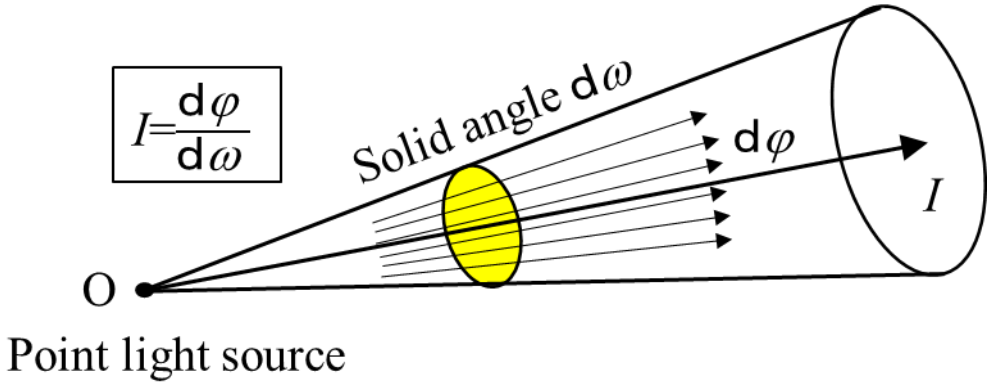

Fig. 2-2 Definition of luminous intensity

Table 2-2 The luminous intensity of a representative light source

Light source		luminous intensity［cd］
Sun		2.8×10^{27}
Incandescent lamps	40W	40
White fluorescent lamp	40W	330
Fluorescent mercury lamp	40W	110
Fluorescent mercury lamp	40W	1800

3：Illuminance

The density of luminous flux incident on a certain surface is called illuminance. Certainly, the brightness of the surface varies depending on the magnitude of the illuminance. The unit of illuminance is lux [lx], and 1 lx is the illuminance when 1 lm of light is incident on the plane of lm^2.

In Fig. 2-3, the illuminance E [lx] of the point P is expressed by the following equation when the luminous flux incident on the small area dS [m^2] around the point P on the irradiated surface is dφ [lm].

$$E = \frac{\mathrm{d}\varphi}{\mathrm{d}S}, \quad \mathrm{d}\varphi = E \cdot \mathrm{d}S \tag{2-4}$$

Again, the illuminance E at all points on the inner surface of the sphere is calculated by the following equation when a uniform point source of luminosity I [cd] is placed at the center of the sphere of radius R [m]

$$E = \frac{\mathrm{d}\varphi}{\mathrm{d}S} = \frac{4\pi I}{4\pi R^2} = \frac{I}{R^2} \quad [\mathrm{lm}] \tag{2-5}$$

Illuminance on the inner surface of the sphere is proportional to the luminous intensity of the light source and inversely proportional to the square of the radius. Likewise, when the luminous intensity in one direction of a point light source is I [cd], the relationship between the distance R [m] and the illuminance E_n on the plane perpendicular to the direction of light is,

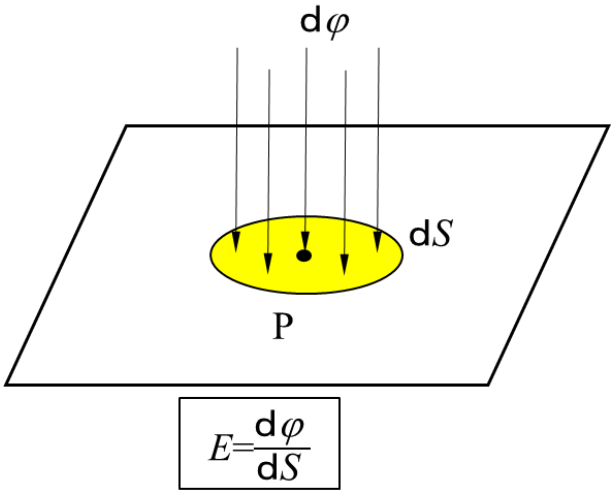

Fig. 2-3 Concept of illuminance

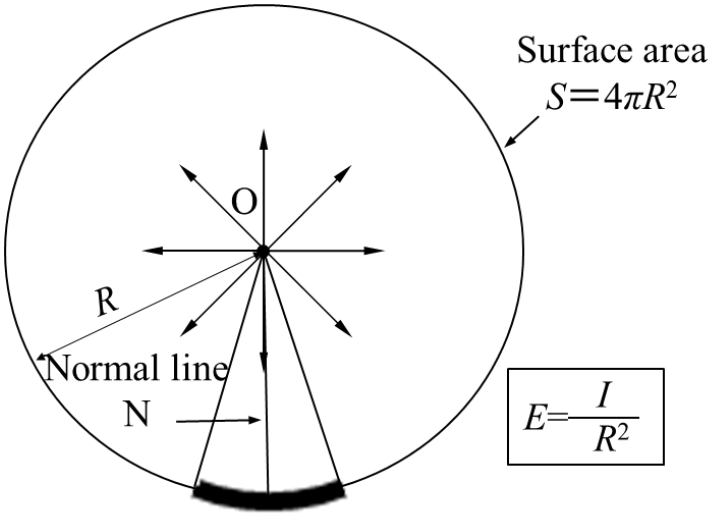

Fig. 2-4 Concept of uniform point light source and spherical illuminance

$$E_n = \frac{I}{R^2} \quad [\mathrm{lm}] \tag{2-6}$$

This relationship is called inverse square law of illuminance (Refer to Fig. 2-4 for the concept of this relationship. The subscript *n* of E_n in eq. (2-6) represents the direction of incident light is the direction normal to the surface).

If the light source is not dot-shaped, and the distance to a certain object is small, this inverse square law cannot be applied. In that case, it is sufficient to divide the light source into elements of smaller area and consider them as point light sources and calculate the illuminance (eq. (2-7)).

Next, as shown in Fig. 2-5, when a luminous flux φ [lm] parallel to the normal direction of the surface is incident to the area S [m^2] on a certain plane, the illuminance E_n of this surface is expressed by the following equation.

$$E_n = \frac{\varphi}{S} \quad [\mathrm{lx}] \ (=[\mathrm{lm/m^2}]) \tag{2-7}$$

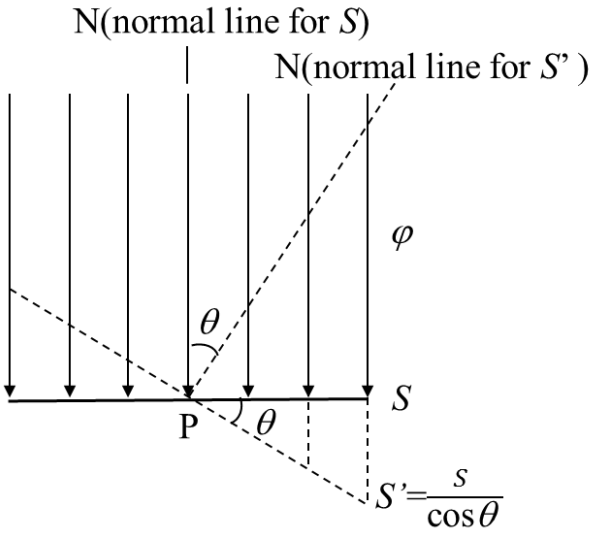

Fig. 2-5 Law of the incident angle cosine

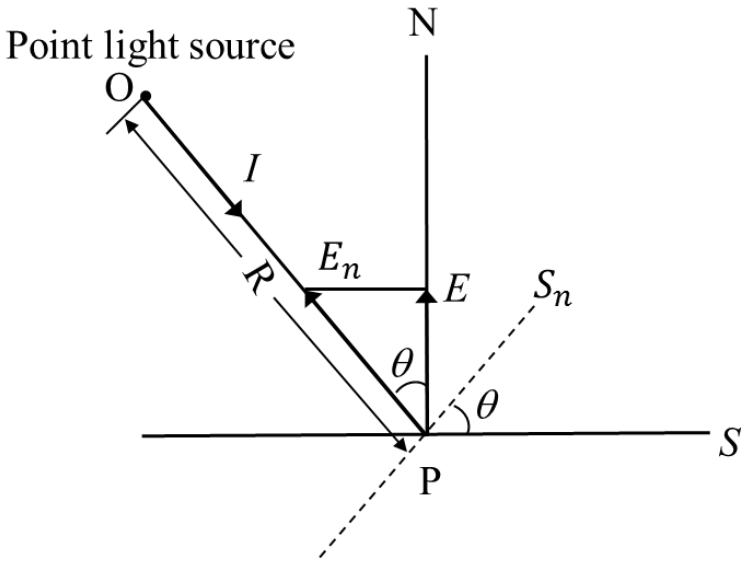

Fig. 2-6 Illuminance by point light source

If this plane gradient is 0, the area where the luminous flux φ strikes becomes $S'=S/\cos\theta$. Therefore, the illuminance E' on the S' plane is,

$$E' = \frac{\varphi}{S'} = \frac{\varphi}{s/\cos\theta} = E_n \cos\theta \tag{2-8}$$

In other words, the angle of inclination of the surface, i.e. the cosine of light incidence of angle θ is proportional to the illuminance E' (this is called the incident angle cosine law).

Furthermore, as shown in Fig. 2-6, the luminous flux from the point light source with luminosity I [cd] is considered to be a parallel ray near the point P when light enters point P on the plane S from the direction forming the angle θ with the normal PN. Therefore, the

Table 2-3 Example of illumination values

Light source or place	Illumination［lx］
Direct sunlight	About 100 thousand
Cloudy	30～70 thousand
Rain cloudy	10～30 thousand
Shade・Blue sky light	10～20 thousand
Full moon night	About 0.2
Starry star	About 0.0003
Office	500～1000

illuminance E on the plane S is expressed by the following equation.

$$E = E_n \cos\theta = \frac{I}{R^2}\cos\theta \tag{2-9}$$

Here, E_n: Illuminance of plane S_n with OP as normal (Called normal illuminance).
The illuminance E in the case where there are a plurality of point light sources, illuminance E can be calculated by summing the illuminance of all the point light sources using the following equation. The general representation of the illuminance of light source is shown in Table 2-3.

$$E = \sum E_{ni}\cos\theta_i = \sum \frac{I}{R^2}\cos\theta_i \tag{2-10}$$

Here, subscript i: The i^{th} point light source.
As shown in the Table 2-3, the illuminance in the actual lighting environment is several ten thousand lx in the outdoors under a clear sky, whereas approximately 0.2 lx under the full moon night, and several hundred lx in the office and classroom desk.

4：Luminance

The amount representing the brightness of the shining or illuminated surface is luminance. In Fig. 2-7, the luminance L_a of a certain direction α with a small area dS of a certain surface is calculated by dividing the luminous intensity I_a [cd] in that direction by the orthogonal projection area (the apparent area viewed from the α direction) dS'（=dS cosθ） divided by unit meter. In other words, it is the area density of luminous intensity (unit is cd/m^2 (candela

per square meter)) and is expressed by the following equation.

$$L_\alpha = \frac{I_\alpha}{\mathrm{d}S\cos\alpha} \qquad [\mathrm{cd/m^2}] \tag{2-11}$$

The luminance is irrelevant to the distance from the eyes.

We recognize objects by the difference in luminance, and in the case of uniform luminance, the object will look like a flat plate. The general representation of the luminance of light source is shown in Table 2-4.

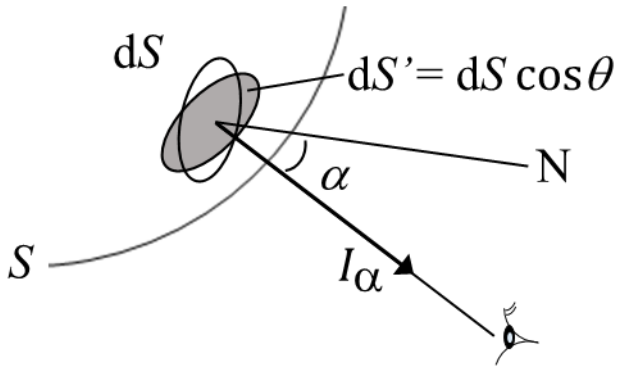

Fig. 2-7 Definition of luminance

Table 2-4 Example of luminance

Light source or place	luminance［cd/m^2］
Zenith sun (On the ground)	1.65×10^9
Blue sky light (Clear sky)	5000
Blue sky light (Fine day)	10000
Blue sky light (Standard cloudy weather)	1700
Incandescent lamp (100W clear)	4×10^6
Fluorescent lamp (40W White)	9000
Mercury lamp (400W clear)	4×10^8
Mercury lamp (400W Fluorescent form)	1×10^5

5：Luminous radiance

The luminous flux diverging from the unit area of a certain surface is called luminous flux divergence.

Let the small area of any point on this surface be dS [m^2] and the luminous flux diverging from there be dφ [lm], the luminous radiance M at that point is expressed by the following equation.

$$M = \frac{\mathrm{d}\varphi}{\mathrm{d}S} \quad [\mathrm{lm/m^2}] \tag{2-12}$$

6：Complete diffusion surface

A surface with uniform luminance as viewed from any direction is called a complete diffusion surface or an even diffusing surface. In Fig. 2-8: The luminous intensity in the normal direction of a minute area dS [m^2] of a light emitting surface is represented by dI_n [cd], L_n [cd/m^2] is the luminance in that direction. Let the luminosity and luminance in the direction forming the normal and the angle θ be dI_θ[cd] and L_θ [cd/m^2] respectively and they can be calculated using the following equations.

$$L_n = \frac{\mathrm{d}I_n}{\mathrm{d}S}, \quad L_\theta = \frac{\mathrm{d}I_\theta}{\mathrm{d}S\cos\theta} \tag{2-13}$$

On the complete diffusion surface, as the brightness is not dependent on its direction, L_θ and dI_θ can be represented as eq. (2-14).

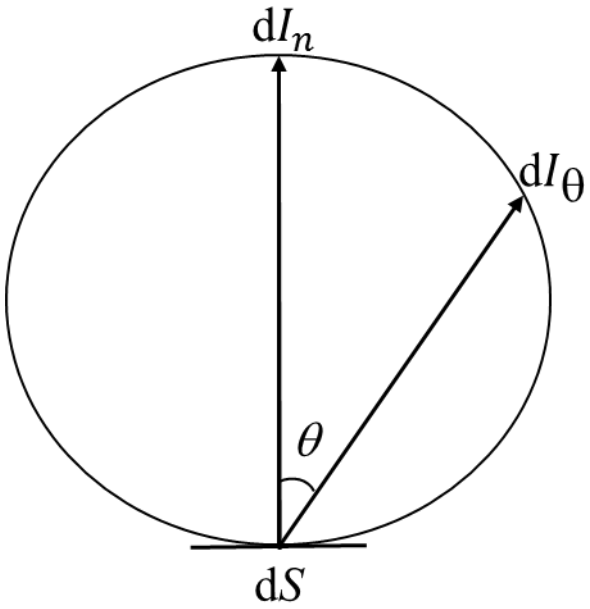

Fig. 2-8 Idea of Complete diffusion plane

$$L_\theta = L_n, \quad \mathrm{d}I_\theta = \mathrm{d}I_n \cos\theta \tag{2-14}$$

Therefore, the trajectories of light intensity become a spherical surface. This is called Lambert's cosine law.

On the complete diffusion plane, there is a relationship between luminance L [cd/m^2] and luminous radiance M [lm/m^2] as shown below.

$$M = \pi L \tag{2-15}$$

2-2 Monte Carlo ray tracing

Monte Carlo ray tracing is one of the simulation methods which simulate the light's characteristics on the screen by using the random numbers. It can simulate the illumination system in an easy and very accurate way. Here, I will introduce Monte Carlo ray tracing method and its calculation process.

2-2-1 Ray tracing simulation method

The ray tracing algorithm is one of the numerous techniques that exists to render images with computers. It is well-known for the generation of high-quality images, making it the defector standard for high-quality rendering and for almost all lighting simulation systems [7].
The first ray tracing algorithm used for rendering was presented by Arthur Appel in 1968 [8] and this algorithm had been called "ray casting" since that time. The idea of ray casting is about shooting rays from the eye, one ray per pixel, and find the blocked path between the ray and the closest object. Previous algorithms traced rays from the eye to the scene until they reached an object, but the ray color was determined without considering the properties of light which affects the result of the algorithm. Turner Whitted continued this process and made an important research breakthrough in 1979 [9]. This method perfectly simulates the properties of light. In nature, the light emitted by the light source propagates forward and finally reaches a surface that hinders it from spreading continuously. We can consider "light" as a photon flow that is transmitted in the same path. In full vacuum, this light will be a straight line. But in reality, there are three factors affecting the light path, i.e. absorption, reflection and refraction. The surface of an object may reflect all or part of the light in one or more directions. It may also absorb some light, which reduces the intensity of the reflected or refracted light. If the surface of the object is transparent or translucent, it will refract part of the light in different directions, and absorb some or all of the spectrum and emit radiation.
The ray tracing simulation method in this research starts from the light source, a light is emitted from a point which is the light source to the scene. The starting point of the light is the coordinates of the light source and the direction is described by a unit vector. There are three possibilities when a light reaches the surface of an object:

- If the surface of the object at the current intersection is an absolute blackbody, the light will be absorbed 100% and the tracking ends.
- If the surface of the current intersection is a specular surface or diffuse surface, the tracking continues in the direction of the reflected unit vector.
- If the surface of the object at the current intersection is a regular transmission surface, the tracking continues in the direction of its regular transmission.

A ray tracing model is shown in Fig. 2-9 and the ray tracing simulation algorithm will be explained later.

Ray tracing algorithm make a realistic simulation of lighting over other rendering methods (such as scan line rendering or ray casting). Effects such as reflections and inter reflection, which are difficult to simulate using other algorithms, are a natural result of the ray tracing algorithm. The computational independence of each ray makes ray tracing amenable to parallelization. [10, 11]

As the properties of light are perfectly reproduced on the computer by ray tracing simulation, this method is not only used for optical design, but also for long wavelength applications such as microwave design and radio system, and also for short wavelength fields such as ultraviolet or X ray optics [12].

On the other hand, in order to simulate light accurately and physically, it is necessary to calculate the locus of a myriad of light emitted from the light source and the direction of a ray is determined by random number (Monte Carlo method). The more tracks one has, the more accurate results gets. For this reason, ray tracing is well known for its long rendering times, often the calculation time needs minutes to hours for a single frame. Hence a serious disadvantage of ray tracing is that the simulation performance depends on the computer machine. But recent progress in hardware of the computers has paved the way of using ray tracing simulation method in illumination system.

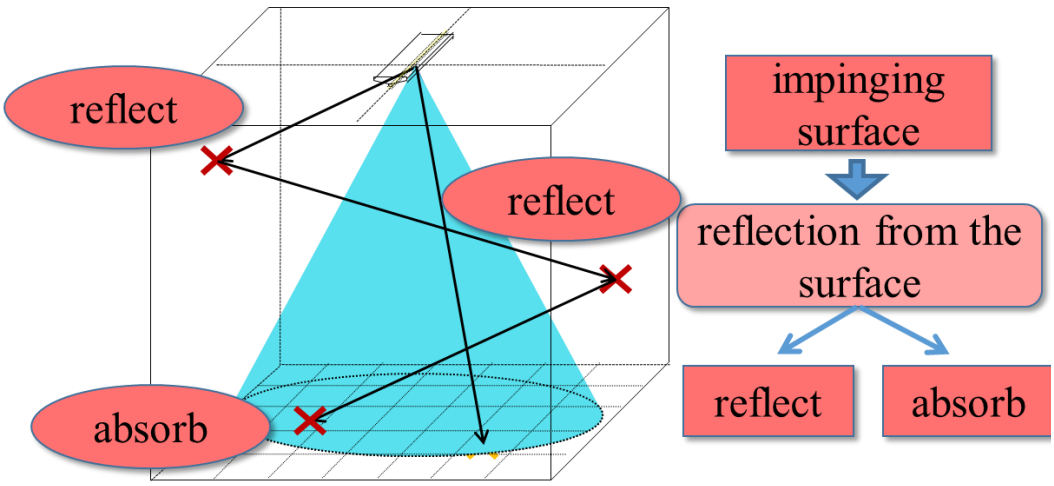

Fig. 2-9 Ray tracing model

2-2-2 Monte Carlo method

The “Monte Carlo” name is derived from the name of a city-state, Principality of Monaco, which is well known for its casinos. This method is named because the roulette wheel is the simplest mechanical device for generating random numbers [13]. Since the simulation process involves generating chance variables and exhibits random behaviors, it has been called Monte Carlo simulation. Monte Carlo simulation is a powerful statistical analysis tool and widely used in both non-engineering and engineering fields. It was initially used to solve neutron diffusion problems in atomic bomb work at Alamos Scientific Laboratory in 1944. Monte Carlo simulation has been applied to diverse problems ranging from the simulation of complex physical phenomena such as atom collisions to the simulation of traffic flow and Dow Jones forecasting. Monte Carlo is also suitable for solving complex engineering problems because it can deal with a large number of random variables, various distribution types, and highly nonlinear engineering models [14].

A simple and well known example of Monte Carlo simulation is the method for determination of the ratio of circumference and the radius of a circle i.e. π. A uniform random number sequences uniformly distributed between 0 and 1 generates many points on the two-dimensional coordinates as shown in Fig. 2-10. If these coordinates determined by random numbers are X_i and Y_i, the points representing them are always uniformly distributed inside the square of area 1 as shown in Fig. 2-10. Let N be the total number of these points, and let M be the total number of those points those exist inside the circle with a radius of 1 with the origin at the center, since each point is uniformly distributed within the figure. The area ratio of a quarter circle is expressed by M / N [15]. Therefore,

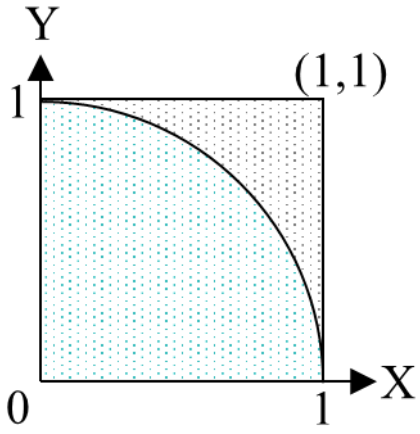

Fig. 2-10 Calculation of π by Monte Carlo method

$$\pi = \frac{M}{N} \times 4 \tag{2-16}$$

π will be calculated by this equation. It is obvious that if the number of points to be generated is increased, the calculation accuracy will be further improved. Such this method is a probabilistic statistical method, it is a very effective means in solving a complex event.

In this research, Monte Carlo method is used for the algorithm of the developed illumination distribution simulator. When the Monte Carlo method is used for optical simulation, actual light (photon) emitted from the light source is replaced with countless direction vectors as shown in Fig. 2-11. These photons travel straight through the interior space according to the direction vectors. The number of times the photon enters the eyes is the luminous intensity at that position, and the number of photon fluxes incident on a specific area of a wall or floor is the illuminance in that portion. The point where these photons are generated and the vector component are determined by using appropriate probability distribution. Therefore, the real light is perfectly reproduced on the computer by Monte Carlo ray tracing simulation.

The main advantages and disadvantages in optical simulation by the Monte Carlo method are showed below.

< advantages > :

- Since the main part of the calculation algorithm is an iterative sentence, it is relatively easy to create and change programs.
- There is versatility such that it is possible to calculate complicated simulation conditions with many light sources and diffusion surfaces (please see 2-1).

< disadvantages > :

- Because most algorithms are iterative sentences, calculation time tends to depend on the performance of the machine which is used
- The accuracy of the simulation result is susceptible to the influence of the number of calculations, and unless a sufficient number of calculations are given, the error increases due to the influence of the bias of the probability distribution.

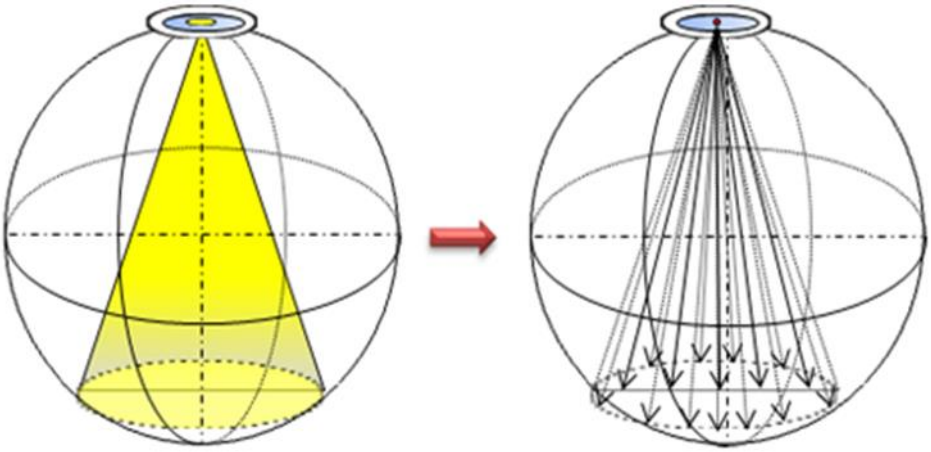

(a) Light with specific distribution (b) Photon fluxes along the distribution

Fig. 2-11 Optical simulation by Monte Carlo method.

Recently, with the development of the computers, the calculation speed and performance has increased rapidly. In this, we solved the disadvantages of the Monte Carlo method to some extent.

2-2-3 Random numbers

Monte Carlo simulation method is one of them which provide the light's characteristics on the virtual screen by using the random numbers. So firstly, we should choose a good random generator.

The way a good random generator is chosen is like choosing a new car whereby for some people or applications, speed is preferred, while for others robustness and reliability are more important. In the Monte Carlo simulation, the distributional properties of random generators are of utmost importance, whereas unpredictability is crucial in coding and cryptography [16]. Even though "random variable" implies that the value is unpredictable, the distribution may be well known. The probability of a given value can be known from the distribution of a random variable[17]. When PC generates a random number, it always generates a number with a algorithm containing certain rules, so random number generated by PC is called pseudorandom numbers.

A good random number generator depends on many factors. A variety of random number generators is available, as different applications may require different properties of the random generator. A good uniform random number generator possesses the below characteristics [16]:

1. *Statistical tests*: A generator should produce a stream of uniform random numbers that is indistinguishable from a genuine uniform iid (Independent and Identically Distributed)

sequence. Although from a theoretical point of view this criterion is too imprecise and even infeasible, from a practical point of view this means that the generator should pass a battery of simple statistical tests designed to detect deviations from uniformity and independence.

2. *Theoretical support*: A good generator should be based on sound mathematical principles, allowing for a rigorous analysis of essential properties of the generator.

3. *Reproducible*: An important property of a good generator is that it can reproduce the random numbers. This is essential for testing and variance reduction techniques. Physical generation methods cannot be repeated unless the entire stream is recorded.

4. *Fast and efficient*: The generator should produce random numbers in a fast and efficient manner, and require little storage in computer memory. Many Monte Carlo techniques for optimization and estimation require billions or more random numbers. Current physical generation methods are no match for simple algorithmic generators in terms of speed.

5. *Large period*: The period of a random number generator should be extremely large — on the order of 10^{50}— in order to avoid problems with duplication and dependence. Most early algorithmic random number generators were fundamentally inadequate in this respect.

6. *Multiple streams*: In many applications it is necessary to run multiple independent random streams in parallel. A good random number generator should have easy provisions for multiple independent streams.

7. *Cheap and easy*: A good random number generator should be cheap and not require expensive external equipment. In addition, it should be easy to install, implement, and run.

8. *Not produce 0 or 1*: A desirable property of a random number generator is that both 0 and 1 are excluded from the sequence of random numbers. This is to avoid division by 0 or other numerical complications [16].

Actually, when this pseudorandom number is used for optical simulation, rational numbers from 0 to 1 are usually generated, i.e. if there is a pseudorandom number *rand ( )* that generates a numeric value from 0 to R_{MAX} (arbitrary natural number), the equation as shown in here:

$$\xi = \frac{rand\ (\,)}{R_{MAX}} \tag{2-17}$$

Here, ξ is a random number taking a rational number from 0 to 1. For example, if anybody wants to generate angle θ from 0 to 2π with uniform probability, as the equation will be like below

$$\theta = 2\pi \cdot \xi \tag{2-18}$$

2-3 Procedure of illuminance calculation and program flow

In the case of performing illumination calculation using the Monte Carlo ray tracing method, it is possible to treat the radiation characteristics of the light source, reflection and absorption of light using random numbers. Illumination calculation in the model space by Monte Carlo simulation is performed by simulating the individual photon flux flight paths emitted from the light source and tracking from the light source.

Here, we describe the procedure of illuminance calculation using the Monte Carlo method and the flow of the program in this portion.

1：Procedure for calculating illuminance

The calculation procedure of illuminance distribution in this research is as follows (Fig. 2-12).The illuminance *E* [lx] of each surface of the observation surface is obtained as follow [18].

$$E = \frac{F \times k}{N} \times N' \times \frac{1}{S} \tag{2-19}$$

Here, *F*: The total luminous flux of the light source [lm], *k*: Lighting efficiency (The ratio of the luminous flux actually emitted from the lighting fixture among the light source luminous flux) [%], *N*: Number of initial radiated photon flux from light source, *N'*: Number of incident photon flux to each surface element *S*: Surface area [m^2].

As described in section 2-1, illuminance is the amount of light flux per unit area of the surface. Therefore, the number of photon fluxes incident on each surface element is proportional to illuminance as shown in eq. (2-19).

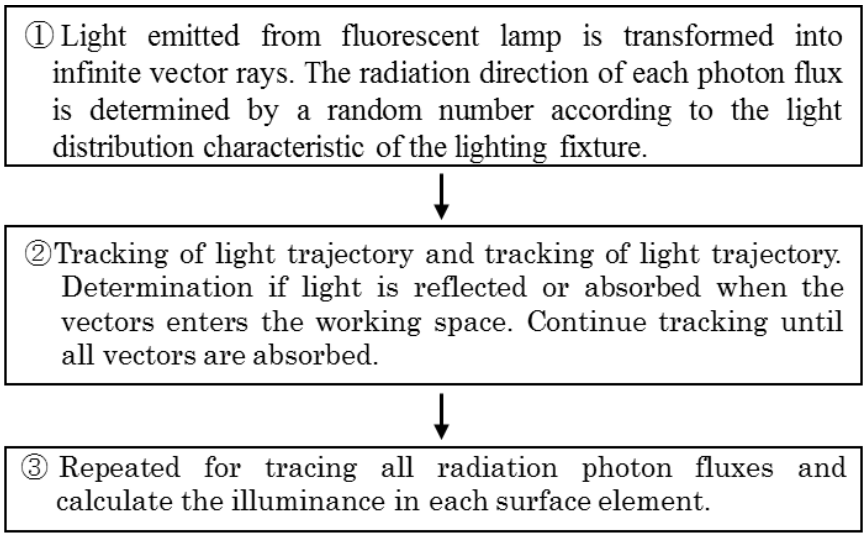

Fig. 2-12 Illuminance calculation procedure by Monte Carlo method

2-4 Representation method of lighting equipment

In this study, as the Light distribution characteristics of lighting are known, the horizontal angle φ and the vertical angle θ are determined by the data of its light distribution characteristics, and emit the photon flux vector directly from the point light source in that direction .

Here, a specific method will be described.

2-4-1 Light distribution characteristics of lighting equipment

The first thing one needs to know in applying this method is the light distribution characteristics of the lighting equipment. Light distribution is the distribution of luminous intensity that shows how light is emitted to the space from the lighting equipment, and it is expressed by a radar graph called light distribution curve.

The light distribution of the equipment can be visualized as a virtual sphere with its center at the center of the lighting as shown in Fig. 2-13. The direction of point P on the spherical surface is determined by the horizontal angle φ and the vertical angle θ. In general, the vertical angle directly below the equipment is θ = 0°and the horizontal angle is set in the counterclockwise direction of the reference direction φ = 0°. Distribution of light on the vertical plane *V* forming the horizontal angle φ is called vertical light distribution, and it shows the relationship between the vertical angle θ and the luminous intensity $I(\theta)$ in that direction [2,3,5,18-20].

Generally, as shown in Fig. 2-13, the light distribution of the lighting is measured by using the vertical light distribution when viewing the lighting horizontally in three directions (φ = 0°, 45°, 90°) , the vertical angle θ represent in intervals of 5°or 10°. An example of the light distribution curve is shown in Fig. 2-14 and Fig. 2-15.

Each lighting maker has disclosed the light distribution curve of the lighting equipment of the company and other characteristics (light source, light flux, instrument efficiency, etc.) in the catalog, and the data necessary for calculating by this simulator can be obtained possibility.

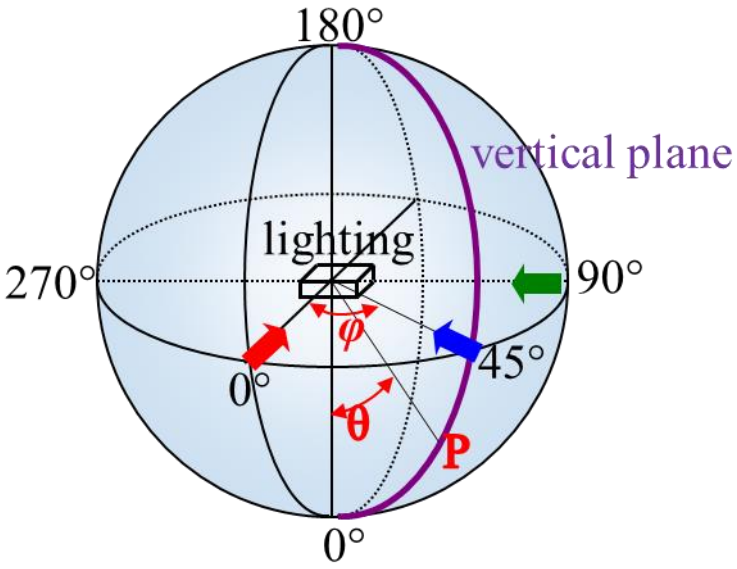

Fig. 2-13 Representation of light distribution

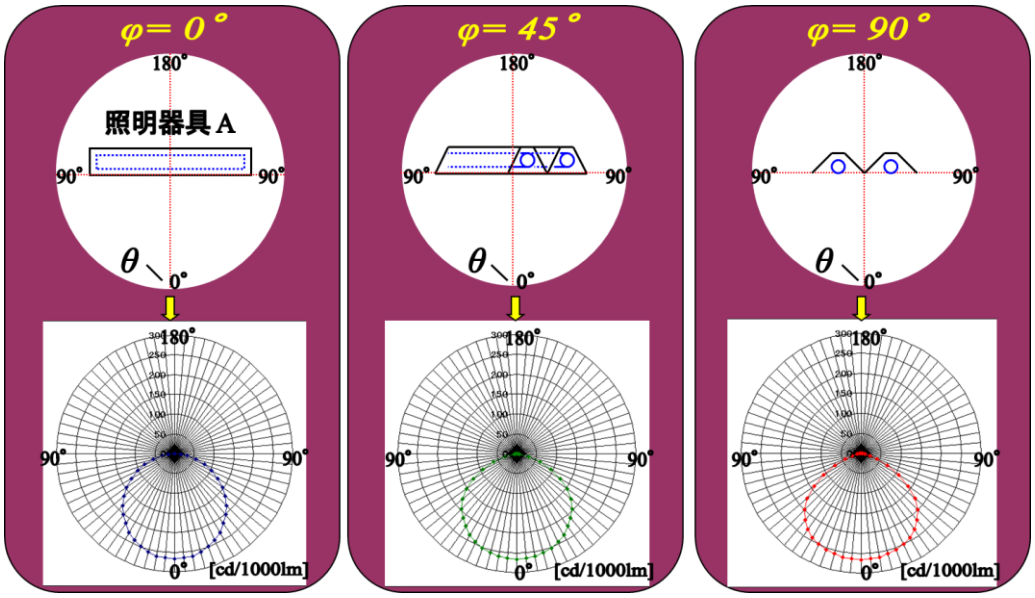

Fig. 2-14 Expression of the light intensity (light intensity) and its direction (horizontal angle φ, vertical angle θ) by a curve

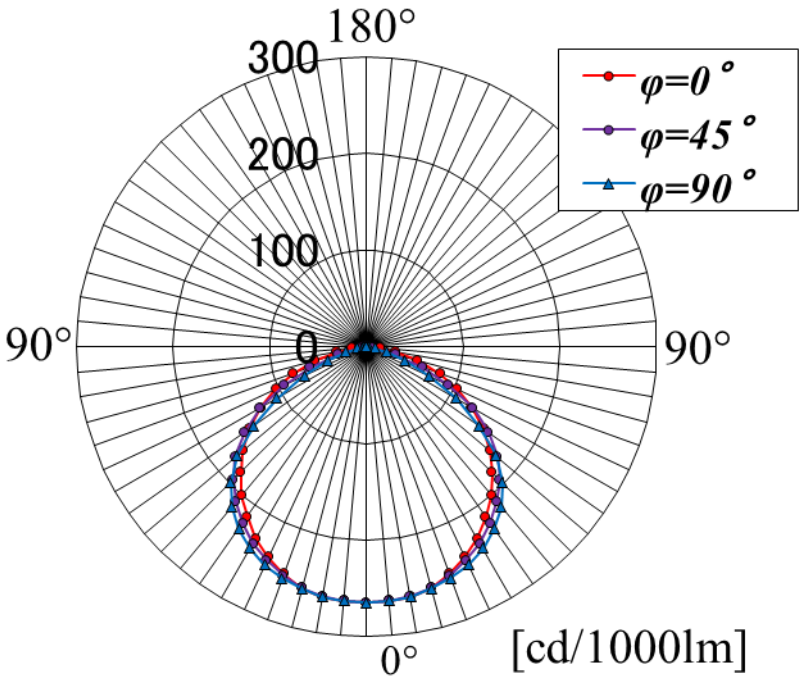

Fig. 2-15 Light distribution curve

2-4-2 Creation of photon flux distribution

As described in previous, each photon flux has an equal luminous flux. Therefore, in order to generate a photon flux according to the light distribution (luminous intensity distribution) of the lighting, it is necessary to distribute the luminous flux in all directions of the space from the center of lighting equipment. Therefore, the light flux distribution is created from the light distribution curve of the lighting equipment by the following procedure. Here, it will be explained by using the light intensity value of the light distribution curve in Fig. 2-15.

1：Interpolation of light distribution (Luminous intensity distribution)

As described in the previous section, generally, it is possible to know the luminous intensity distribution as viewed from three directions ($\varphi_{a,\,b,\,c}$ = 0 °, 45 °, 90 °) of the lighting equipment respectively. This luminosity value set is as shown in Table 2-5 with respect to the horizontal angle φ and the vertical angle θ, and the horizontal angle φ is expanded at intervals of 5 °and the values are interpolated in Table 2-6.

Table 2-5 Luminous intensity distribution (measured value)

Luminous intensity [cd]			
θ \ φ	φ_a = 0 °	φ_b = 45 °	φ_c = 90 °
0 °	265	265	265
5 °	264	264	264
10 °	263	262	263
15 °	258	258	259
20 °	250	252	255
25 °	240	244	249
30 °	229	235	241
35 °	215	223	230
40 °	201	210	217
45 °	184	195	199
50 °	167	177	175
55 °	148	154	142
60 °	126	127	107
65 °	103	94	71
70 °	81	62	42
75 °	55	31	22
80 °	31	7	9
85 °	15	2.5	3
90 °	0	0	0

Coefficient a, b, c is obtained from luminous intensity values in three directions with respect to a certain vertical angle θ, and calculate the quadratic curve $I(\varphi)$ of light intensity in the horizontal direction using approximate function (eq. (2-20)).

$$I(\varphi) = a\varphi^2 + b\varphi + c \qquad (2\text{-}20)$$

Luminous intensity $I(\varphi)$ for each horizontal angle φ (0 °, 5 °, 10 °,..., 90 °) is obtained from eq. (2-20) and this is done for each vertical angle θ.

Table 2-6 Luminous intensity distribution of horizontal angle φ interpolated in an interval of 5 °

Luminous intensity [cd] (0°~45°)

θ \ φ	0°	5°	10°	15°	20°	25°	30°	35°	40°	45°
0°	265.0	265.0	265.0	265.0	265.0	265.0	265.0	265.0	265.0	265.0
5°	264.0	264.0	264.0	264.0	264.0	264.0	264.0	264.0	264.0	264.0
10°	263.0	263.0	263.0	262.0	262.0	262.0	262.0	262.0	262.0	262.0
15°	258.0	258.0	258.0	258.0	258.0	258.0	258.0	258.0	258.0	258.0
20°	250.0	250.0	250.0	251.0	251.0	251.0	251.0	251.0	252.0	252.0
25°	240.0	240.0	241.0	241.0	242.0	242.0	243.0	243.0	244.0	244.0
30°	229.0	230.0	230.0	231.0	232.0	232.0	233.0	234.0	234.0	235.0
35°	215.0	216.0	217.0	218.0	218.0	220.0	220.0	221.0	222.0	223.0
40°	201.0	202.0	203.0	204.0	205.0	206.0	207.0	208.0	209.0	210.0
45°	184.0	186.0	187.0	188.0	190.0	191.0	192.0	193.0	194.0	195.0
50°	167.0	169.0	170.0	172.0	173.0	174.0	175.0	176.0	175.0	177.0
55°	148.0	150.0	151.0	152.0	153.0	154.0	154.0	154.0	154.0	154.0
60°	126.0	127.0	128.0	129.0	129.0	129.0	129.0	129.0	128.0	127.0
65°	103.0	103.0	102.0	102.0	101.0	100.0	99.0	97.0	96.0	94.0
70°	81.0	79.0	77.0	75.0	73.0	71.0	68.0	66.0	64.0	62.0
75°	55.0	52.0	48.0	45.0	42.0	40.0	37.0	35.0	33.0	31.0
80°	31.0	27.0	23.0	20.0	17.0	14.0	12.0	10.0	8.0	7.0
85°	15.0	13.0	11.0	9.0	8.0	6.0	5.0	4.0	3.0	3.0
90°	0.0	0.0	0.0	0.0	0.0	0.0	0.0	0.0	0.0	0.0

Luminous intensity [cd] (45°~90°)

θ \ φ	45°	50°	55°	60°	65°	70°	75°	80°	85°	90°
0°	265.0	265.0	265.0	265.0	265.0	265.0	265.0	265.0	265.0	265.0
5°	264.0	264.0	264.0	264.0	264.0	264.0	264.0	264.0	264.0	264.0
10°	262.0	262.0	262.0	262.1	262.2	262.3	262.4	262.6	262.8	263.0
15°	258.0	258.1	258.1	258.2	258.3	258.4	258.6	258.7	258.8	259.0
20°	252.0	252.3	252.6	252.9	253.2	253.5	253.9	254.2	254.6	255.0
25°	244.0	244.5	245.0	245.6	246.1	246.7	247.2	247.8	248.4	249.0
30°	235.0	235.7	236.3	237.0	237.7	238.3	239.0	239.7	240.3	241.0
35°	223.0	223.8	224.6	225.4	226.2	227.0	227.8	228.5	229.3	230.0
40°	210.0	210.9	211.7	212.6	213.4	214.1	214.9	215.6	216.3	217.0
45°	195.0	195.8	195.5	197.1	197.6	198.1	198.4	198.7	198.9	199.0
50°	177.0	177.4	177.6	177.7	177.6	177.4	177.0	176.5	175.8	175.0
55°	154.0	153.6	152.9	152.0	150.9	149.6	148.0	145.2	144.2	142.0
60°	127.0	125.8	124.4	122.7	120.7	118.5	116.0	113.3	110.3	107.0
65°	94.0	92.1	80.1	87.9	85.5	82.9	80.2	77.3	74.2	71.0
70°	62.0	58.8	57.6	55.4	53.2	51.0	48.8	46.5	44.3	42.0
75°	31.0	29.3	27.7	26.3	25.1	24.1	23.3	22.7	22.3	22.0
80°	7.0	5.9	5.2	4.8	4.7	4.9	5.4	6.3	7.5	9.0
85°	2.5	1.9	1.5	1.2	1.1	1.2	1.4	1.8	2.3	3.0
90°	0.0	0.0	0.0	0.0	0.0	0.0	0.0	0.0	0.0	0.0

2：Converting luminous intensity distribution to luminous flux distribution

The luminous intensity I [cd] in each direction of the obtained luminous intensity distribution (Table 2-6) is calculated by considering the virtual spherical surface as shown in Fig. 2-16, if we consider the luminous flux incident on the micro area dS [m^2] in each direction as dF [lm], it can be expressed by the following equation.

$$I = \frac{\mathrm{d}F}{\mathrm{d}S} \tag{2-21}$$

Therefore, the luminous flux dF [lm] in each direction is obtained by the eq. (2-18). The micro area dS [m2] is smallest at the vertical angle θ = 0 to 5 °and maximum at θ = 85 to 90 °, when we consider the vertical plane V (Fig. 2-16) at a certain horizontal angle φ where different size is obtained from different vertical angle.

$$\mathrm{d}F = I \cdot \mathrm{d}S \tag{2-22}$$

In this way, the luminous intensity distribution in Table 2-6 can be converted into luminous flux distribution.

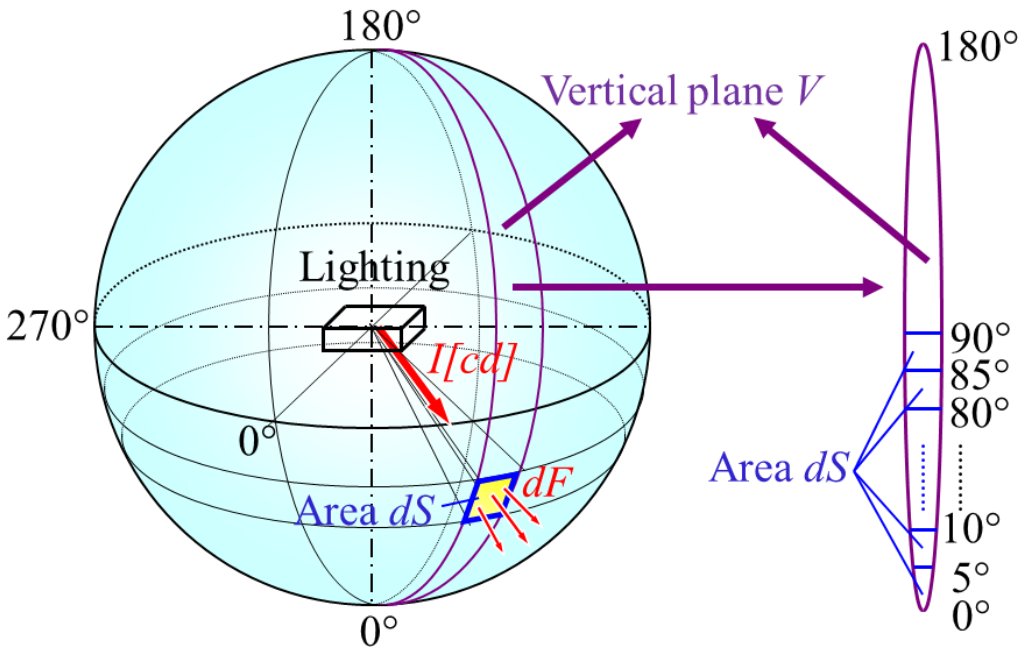

(a) Light intensity distribution (b) Vertical face of sphere

Fig. 2-16 Converting luminous intensity distribution to luminous flux distribution

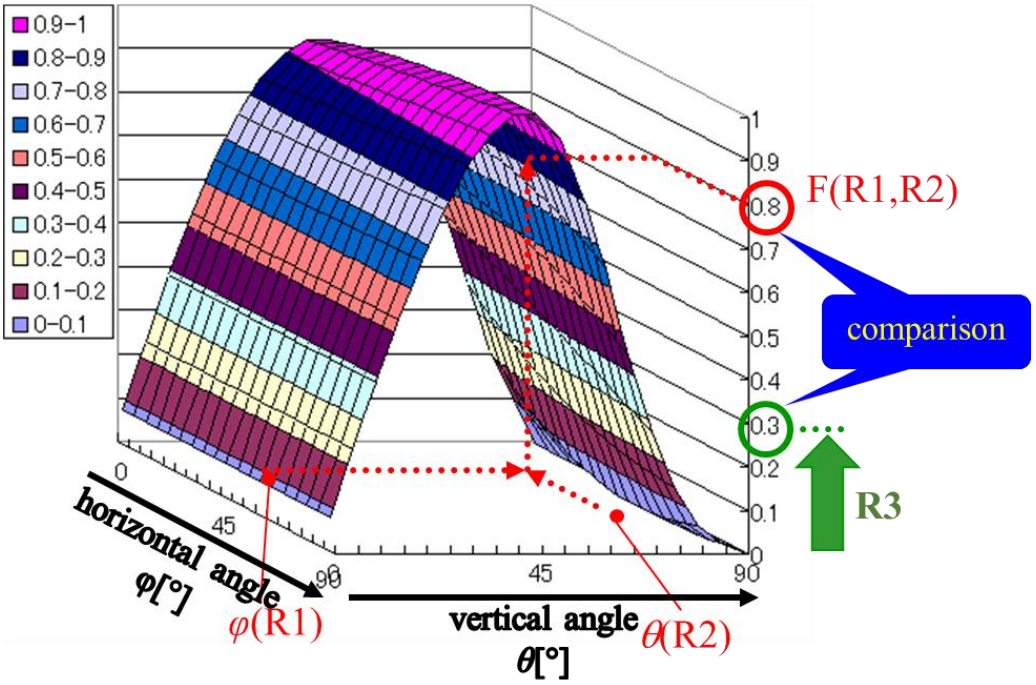

Fig. 2-17 Luminous flux distribution of lighting equipment and rejection method

2-4-3 Radial direction of photon flux

When each value of the luminous flux distribution obtained in the previous section is divided by the maximum value in the distribution and normalized to 0 to 1, a luminous flux distribution diagram is obtained as shown in Fig. 2-17. The procedure for emitting a photon flux directly from a point light source in the direction according to this luminous flux distribution (probability distribution) will be described below.

For the probability distribution function $F(\varphi, \theta)$, if the maximum value of this distribution is 1,

(1) Each variable φ and θ is determined by a uniform random number in an appropriate section (R_1, R_2).

(2) Find the coordinates F (R_1, R_2) determined in (1) (R_1, R_2), compare it with the uniform random number in the section. If F (R_1, R_2)> R_3, the random number is adopted following this distribution, and emit a photon flux from the point source in the direction of the corresponding φ, θ (Fig. 2-18). For other options, it can be negligible.

By repeating (1) and (2), a random number according to the luminous flux distribution can be obtained.

In this way, the radiation direction of the photon flux about an arbitrary distribution can be determined.

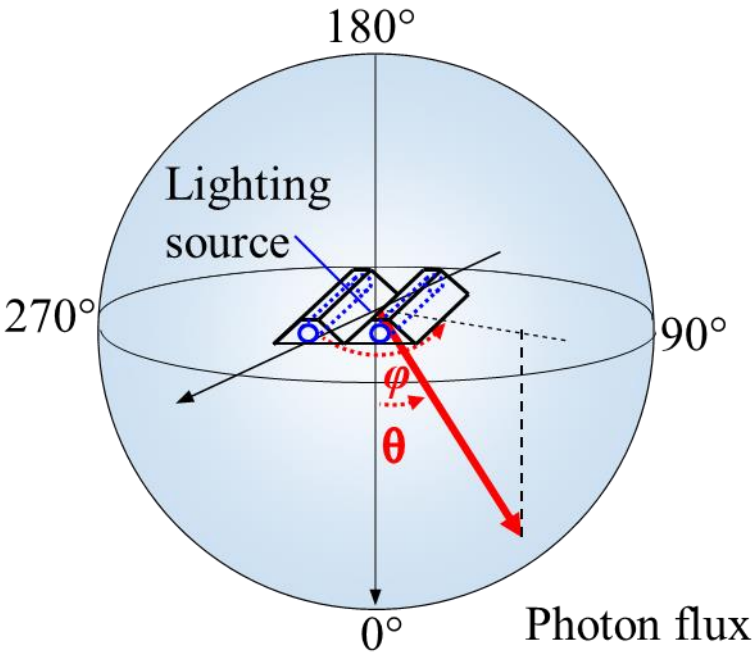

Fig. 2-18 Radiation from point source

2-5 Determination of radiation vector

The photon flux is calculated with vector after transforming the light into photon flux. In this research work, the point light source is assumed as equivalent diffusion point light source. The photon flux vector from the light source represents diffusion reflection and radiosity from the light source on XYZ space. The calculation method will be discussed below where V is the unit vector, θ and φ are vertical angle and azimuthal angle respectively in eq. (2-19).

The angles θ and φ are determined by uniform random numbers ξ in the range of 0~1 as we have assumed the light source as the radiation of Lambert-like light by following the eq. (2-20).

The vivid descriptions of these equations are eq. (2-20) is available from geometric relationship in Fig. 2-19 [21, 22]. However, the values of θ and φ vary with the eq. (2-21).

$$\left.\begin{aligned} Vy &= \sin\theta \cdot \cos\varphi \\ Vy &= \sin\theta \cdot \sin\varphi \\ Vz &= \cos\theta \end{aligned}\right\} \quad (2\text{-}23)$$

$$\left.\begin{aligned} \theta &= \frac{1}{2}\cos^{-1}(1-2\xi) \\ \varphi &= 2\pi\xi \end{aligned}\right\} \quad (2\text{-}24)$$

$$\left.\begin{aligned} 0 \le \theta < \pi/2 \\ 0 \le \varphi < 2\pi \end{aligned}\right\} \quad (2\text{-}25)$$

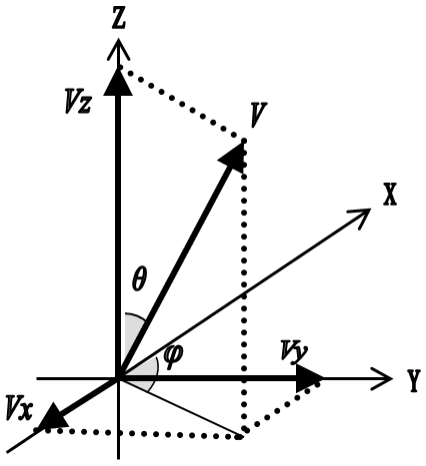

Fig. 2-19 Determination of radiant vector

2-6 Determination of incident coordinates of photon flux

The photon flux emitted from the light source travels straight through the model space. The direction of this photon flux is represented by a direction vector: $\overrightarrow{V} = (V_x, V_y, V_z)$. At this time, the trajectory of the photon flux is represented by a straight line using the radiation point coordinates and the direction vector, and the intersection of this straight line and each surface of the model space is the incident coordinate of the photon flux. Below, the method to determine the incidence and coordinates of the photon flux on each surface constituting the model space is shown.

Let X_s, Y_s, Z_s be the radiation coordinates of the photon flux, the X, Y, Z coordinates of the photon flux are calculated using the parameters t as shown in eq. (2-26).

$$\left.\begin{aligned} X &= Xs + Vx \cdot t \\ Y &= Ys + Vy \cdot t \\ Z &= Zs + Vz \cdot t \end{aligned}\right\} \tag{2-26}$$

Assuming an indoor environment surface is a plane, the collision between the photon flux and each surface can be determined using the general plane eq. (2-27).

$$aX + bY + cZ + d = 0 \tag{2-27}$$

X, Y, Z : intersection coordinates
a, b, c : normal vector of the relevant planes
d : constant

X, Y and Z is substituted in eq. (2-26), and parameter t is solved by

$$t = -\frac{aX_s + bY_s + cZ_s + d}{aV_x + bV_y + cV_z} \tag{2-28}$$

If the parameter t in eq. (2-28) exists at $t > 0$, the photon flux collides with the plane and it does not exist. The actual colliding coordinates are determined by substituting t in each of the expressions eq. (2-26).

2-7 Vector conversion

The reflector flux at a reflector plane needs again a vector transformation. The transformation will use again the Lambert reflection shown in Fig. 2-17. The transformation will be changed according to the position of the coordinates of the reflector plane and the shape. The vector $\overrightarrow{V}$ (V_x, V_y, V_z) described at sections 2-5 and 2-6, is a unit vector to the surface. Therefore, this vector needs to rotate along with the *X* and *Y* axes by an angle θ inclined to the *Z* axis described in Lambert plane in Fig. 2-17 (b) for vector transformation at the plane [23]. Here, the values of the vector transformation rotated along with the *X* axis will be shown below. The value of *X* axis will not be changed as it has rotated along with *X* axis. So, the values of *Y* and *Z* axis will be changed by using linear transformation with the angle θ (please see Fig. 2-20).The transformed values are shown by eq. (2-29).

$$\left.\begin{aligned} Vx' &= Vx \\ Vy' &= Vy \cdot \cos\theta - Vz \cdot \sin\theta \\ Vz' &= Vz \cdot \cos\theta + Vy \cdot \sin\theta \end{aligned}\right\} \quad (2\text{-}29)$$

2-8 Detection of reflection and absorption of photon flux

When the photon flux enters in the room and collides to the room's surface plane, then it is necessary to know whether the photon flux is reflected or absorbed by the plane.

In this work, there are two general types of reflection: diffuse and specular, as shown in Fig. 2-21 and Fig. 2-22. A diffuse reflection, sometimes called Lambertian scattering or diffusion, occurs when a rough or matte surface reflects the light at many different angles. A specular reflection, such as what you see in a mirror or a polished surface, occurs when light is reflected away from the surface at the same angle as the incoming light's angle [24].

The decision of reflection absorption for a photon flux will be decided by another random

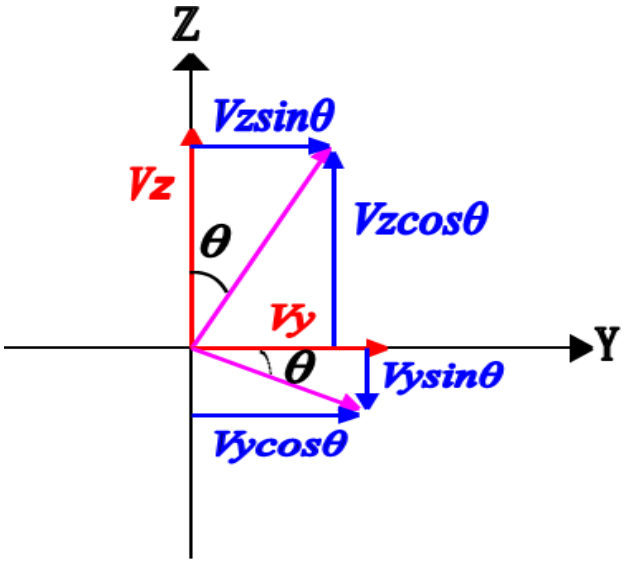

(a) 2D change

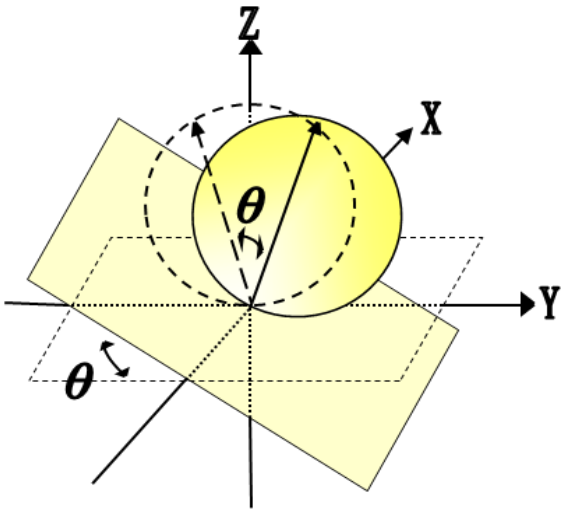

(b) 3D change

Fig. 2-20 Reflection vector

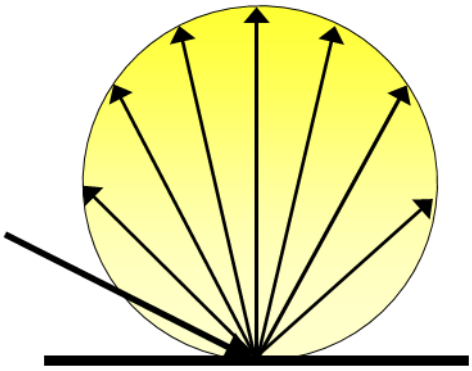

(a) Lambertian scattering

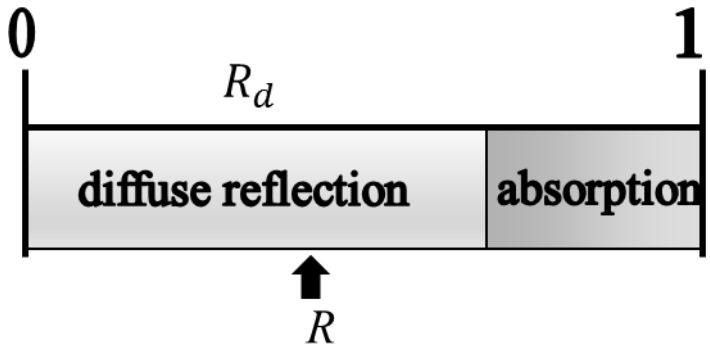

(b) Reflection/absorption (Diffuse)

Fig. 2-21 Setting of diffuse reflection

number R_d (0-1) with considering the reflection rate R of the planes described before in this paper (Fig. 2-21).

Lambert reflector plane is mainly a rough plane, which acts a new point source when a photon flux collides on it. The new trajectory of the photon flux is calculated with the cosine of Lambert's law. And the vector's change of photon flux will be reference by section 2-4, 2-5 and 2-7.

Specular reflections demonstrate the law of reflection, which states that the angle between the incident ray and a line that is normal (perpendicular) to the surface is equal to the angle between the reflected ray and the normal. Please see Fig. 2-22. The angle between an incident ray and the normal is called the incident angle, denoted by the symbol θ. The angle between a reflected ray and the normal is called the reflected angle, denoted by the symbol θ'[24]. In this research, the ratio of specular reflection

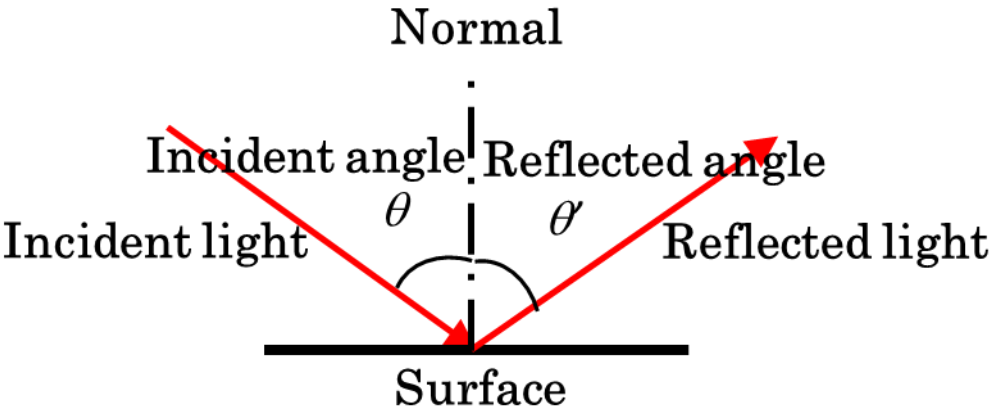

(a) Specular reflection

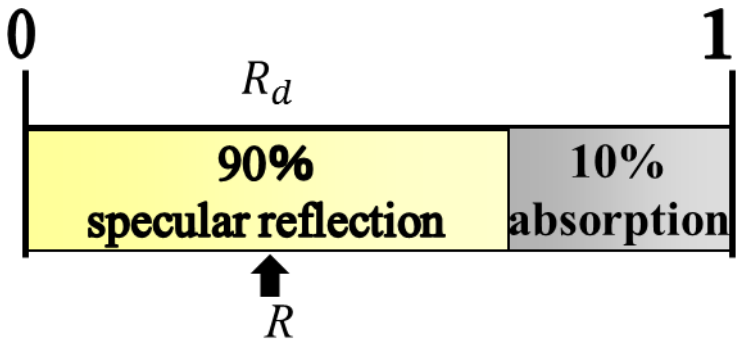

(b) Reflection/absorption(Specular)

Fig. 2-22 Setting of specular reflection

2-9 Radiation distribution characteristics of reflected light[23]

As mentioned in the previous section, in this research, reflection from an indoor environment surface can be considered as complete diffuse reflection. Therefore, in consideration of the radiation distribution characteristic of light from the surface, it is necessary to revise the probability distribution of the generated angle. In order to reproduce Lambert's cosine law described in section 2-1 in the program, it is necessary to revise the probability distribution for the vertical angle θ. Here, this principle of the revised probability distribution will be described. First, if the luminous intensity in the vertical direction is represented by the eq. (2-2), the luminous intensity I_θ when the vertical component tilted by θ is

$$I_\theta = I_n \cos\theta \tag{2-30}$$

Let us consider a sphere centered on a point light source with a radius of 1 as shown in Fig. 2-23. The band-like area ΔS created when this sphere makes one rotation around the Z axis represented by θ is

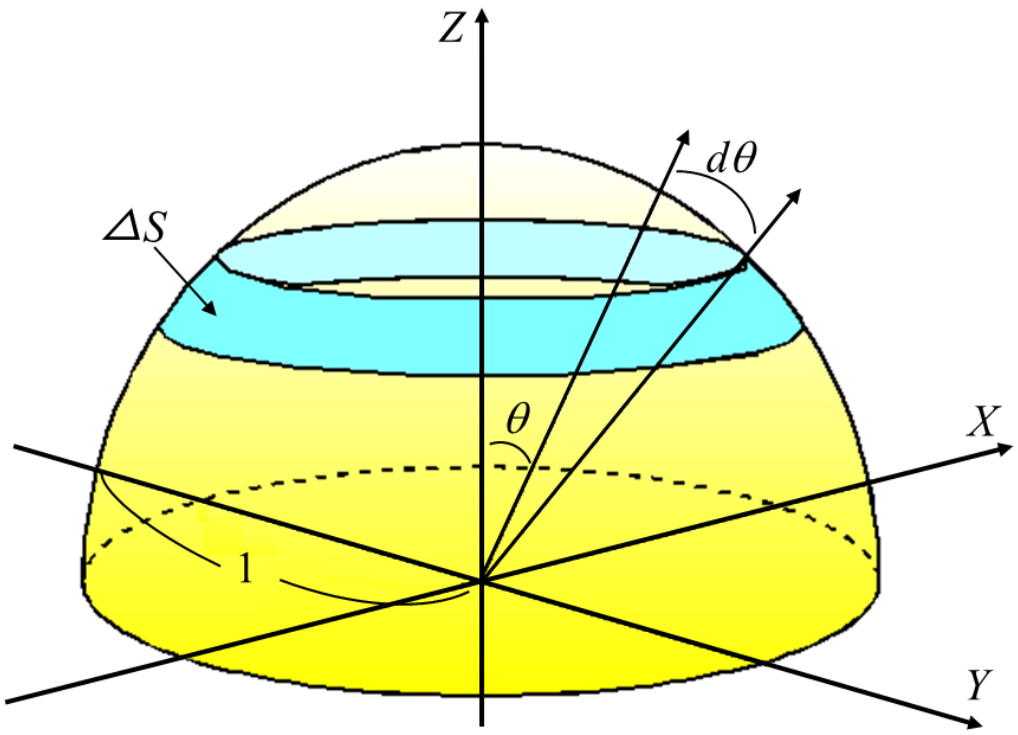

Fig. 2-23 The area on the spherical surface

$$\Delta S = 2\pi sin\theta d\theta \tag{2-31}$$

If the light intensity I_n of the vertical component is 1 [cd] and the light flux that passes through ΔS is expressed by the function $N(\theta)$ with an angle θ, the eq. (2-30) and (2-31) substituted into the new equation

$$N(\theta) = I_\theta \Delta S = 2\pi sin\theta d\theta cos\theta \tag{2-32}$$

Let total luminous flux N be the total luminous flux at $0 < \theta < \pi / 2$

$$N = 2\pi \int_0^{\frac{\pi}{2}} sin\theta cos\theta d\theta \tag{2-33}$$

Hence, the probability $P(a, b)$ of the light flux incident on the annular zone with the condition $a < \theta < b$ is

$$P(a,b) = \frac{2\pi \int_a^b sin\,\theta cos\,\theta d\,\theta}{N} \tag{2-34}$$

Therefore, the cumulative distribution function $F(y)$ that can obtain an arbitrary probability distribution in a specific angle section is

$$F(y) = \frac{2\pi}{N} \int_0^y sin\theta cos\theta d\theta \tag{2-35}$$

Here, if you compute eq. (2-35) with $F(y)$ as the uniform random number sequence x in the interval [0,1], that is, $x = F(y)$

$$x = sin^2 y = \frac{1}{2}(1 - cos2y) \tag{2-36}$$

Therefore, the angle y satisfying this condition is

$$y = \frac{1}{2} cos^{-1}(1 - 2x) \tag{2-37}$$

The value that satisfy x can be obtained by this equation.
That is, if ξ is a random number from 0 to 1, the vertical angle θ is

$$\theta = \frac{1}{2} cos^{-1}(1 - 2\xi) \tag{2-38}$$

By fulfilling the above conditions, this phenomenon can be reproduced in the simulation. Also, since the horizontal angle φ has the same distribution of occurrence in all directions, by simply using the random number ξ

$$\varphi = 2\pi\xi \tag{2-39}$$

The angle is will be within the range of 0 to 2π.

References

[1] Kouiti Ikeda，Akio. Kobara: “Optical technology and lighting design - From foundation to interior design”, The Institute of Elcetric Engineers of Japan, pp.1-7 (2004) (in Japanese)
池田　紘一，小原　章男：「光技術と照明設計　－基礎からインテリアデザインまで－」，電気学会，pp.1-7（2004）
[2] Institute of Architectural Space Lighting Planning: “Lighting Design of the House”, pp.16-25 (in Japanese)
建築空間照明計画研究会：「住まいの照明設計」pp.16-25
[3] The Illuminating Engineering Institute of Japan: “New · Lighting classroom-Lighting basic knowledge-Intermediate level”, pp.11－pp.15 (in Japanese)
社団法人　照明学会：「新・照明教室　照明の基礎知識　中級編」pp.11－pp.15
[4] NICHIA -Light Emitting Diode: “Optical Unit and Calculation”, SE-AP00041, pp.1-6 (2016)
[5] Rüdiger Ganslandt and Harald Hofmann, : “Handbook of Lighting Design”, ERCO Edition, Published by: Verlag Vieweg, 1992, ISBN 3-528-08895-8,pp.37-42
[6] Hamamatsu: “Photomultiplier Tubes Basics And Applications”, pp.4-9
[7] Ingo Wald, Timothy J.Purcell, Jörg Schmittler, Carsten Benthin, Philipp Slusallek: “Realtime Ray Tracing and its use for Interactive Global Illumination”, EUROGRAPHICS 2003, pp.1-3 (2003)
[8] Appel A: “Some techniques for shading machine renderings of solids”, AFIPS Conference Proc. 32, pp.37-45 (1968)
[9] Whitted T: “An improved illumination model for shaded display”, Proceedings of the 6th annual conference on Computer graphics and interactive techniques (1979)

[10] J.-C. Nebel: “A New Parallel Algorithm Provided by a Computation Time Model”, Eurographics Workshop on Parallel Graphics and Visualisation, 24–25 September 1998, Rennes, France

[11] Robert L. Cook, Thomas Porter, Loren Carpenter: “Distributed Ray Tracing”, Computer Graphic, Vol.18, No.3 (1984)

[12] M. I. Disney, P. Lewis, P. R. J. North: “Monte Carlo ray tracing in optical canopy reflectance modelling”, Remote Sensing Reviews, Vol. 18, 2000 - Issue 2-4, pp1-13 (2009)

[13] Ilya M. Sobol’: “A Primer for the Monte Carlo Method”, CRC Press, pp1-2 (1994)

[14] Lawrence, David E: “Cluster-Based Bounded Influence Regression”, Statistics, Chapter 8.Monte Carlo Simulation pp.1-3 (2016)

[15] Gabriel A. Terejanu: “Tutorial on Monte Carlo Techniques”, Department of Computer Science and Engineering University at Buffalo, Buffalo, NY 14260, pp1-3

[16] Dirk P. Kroese: “Monte Carlo Methods”, Department of Mathematics School of Mathematics and Physics, The University of Queensland, pp 9-12

[17] F. James, “Monte Carlo Theory and Practice”, Rep. Prog. Phys., Vol. 43, pp1147-1153 (1980)

[18] The Illuminating Engineering Institute of Japan: “University course - Lighting engineering (new edition) ”, Ohmsha, pp.76～89(1997) (in Japanese)

照明学会編：「大学課程　照明工学(新版)」，オーム社，p.76～89 (1997)

[19] Kouiti Ikeda, Akio. Kobara: “Optical technology and lighting design - From foundation to interior design - ”, The Institute of Elcetric Engineers of Japan, pp. 151-162 (2004) (in Japanese)

池田　紘一，小原　章男：「光技術と照明設計　－基礎からインテリアデザインまで－」，電気学会（2004）pp.151-162

[20] “LED light distribution comparison study”, U.S. ENVIRONMENTAL PROTECTION AGENCY, Washington, DC

[21] M. Suzuki, N. Yoshimura, O. Kimura and M. Awata: “Monte Carlo simulation for Color Changes Caused by an Inter-reflection Light”, Lighting Research and Technology, vol.78, no.2, pp.65-71 (1994) (in Japanese)

[21] 鈴木 雅史, 吉村 昇, 木村 修, 栗田 昌延：“モンテカルロ法を用いた相互反射光による色彩変化のシミュレーション”，照明学会誌 / 78 巻 (1994) 2 号

[22] L. Chenglin, M. Kabir: “Development of an Indoor Illuminance Distribution Simulator by using the Monte Carlo Method”, Global Journal of Engineering Science and Research Management, ISSN 2349-4506, Vol.4, No.3, pp.85-94 (2017)

[23] Zenta Usiyama, Tooru Kusakawa: “Simulation optics for optical designers and engineers”, Tokai University Press, pp189-196 (in Japanese)

牛山 善太、草川 徹：「シミュレーション光学～多様な光学系設計のために～」東海

大学出版会, pp.189～196, 2003 年
[24] Alma E. F. Taylor: “Illumination Fundamentals”, the Lighting Research Center, Optical Research Associates, pp.9-12 (2000)

Chapter 3

Illumination distribution simulator

By using the Monte Carlo method, I have developed a highly versatile illuminance distribution simulator that can be applied to complicated geometric simulations. In this section, I will explain the characteristics and operation procedure of the created illuminance distribution simulator. The validity of the illuminance distribution simulator was examined by comparing the measured values with the simulation results for an actual environment. The basic knowledge and procedures on lighting design when designing the lighting environment in the office will also be explained in this chapter.

3-1 Summary of illuminance distribution simulator

1. System requirement

Programming languages have been developed very rapidly since the early 1950's. More than 200 programming languages have been invented so far [1]. Furthermore, with the rapid development of hardware technology, processors are getting faster and faster, and more and more powerful programming languages are capable to meet the requirements of more efficient program design for various applications [2]. Among these languages, C# is a language extended based on C language and C++, it is said that it is the most excellent in function and productivity when compared with other languages. The features of C# include the following.

- Memory management is automated by the garbage collection function.
- JAVA functions are provided.
- Operating speed equal to or higher than Visual Basic can be expected [3,4]

With these features in mind, I developed an illuminance distribution simulator with C# language using Visual Studio 2015.

2. Features of the simulator created in this research

I have been working on the research of the development of illuminance distribution simulator. The biggest difference with the previously created simulator is the use of sunlight coming in from windows and installation of blind-like reflectors in the window. Until now, simulations have been carried out by installing lighting equipment (point light source, line light source, and surface light source) on the ceiling, but in this study I installed a window on the wall and devised it so that I can efficiently utilize daylight reflected from the window [5-9].

The utilization of daylight from the window was designed to cope with cloudy and sunny days.

In the case of cloudy days, the daylight entering through the window is diffuse light and is harmless to the human eyes. Therefore, it can be used directly as it is natural light. On the other hand, direct usage of daylight on sunny days is too dazzling, and in many cases it cannot be used for working indoor environment. In order to conserve energy, it is necessary to install reflectors, artificial lighting equipment and windows for this research. One of the biggest consideration in this research is the factor of sunlight which varies depending on the season and time zone. For example, in Akita City, the altitude of the sun (the angle between the sunbeam and horizontal plane) is about 75° in summer noon, whereas it is only 30° in winter and thus it varies according to seasons [10]. As the strength of sunlight varies depending on the season and time zone, it is necessary to be able to freely change the width and angle of the blind shaped reflectors placed under the window.

In this research, in order to develop a window system capable of utilizing daylight and shielding strong light which varies depending on the season, I have created an illuminance distribution simulator that can perform under these complex conditions. The features that were considered are listed below.

- The size of the room can be freely changed
- The type of light source of lighting fixtures can be selected
- Windows can be installed on the wall
- The size of the window can be freely changed
- The type of sunlight entering through the window (direct light or diffused light) and strength can be changed
- Change in solar altitude for each season can be simulated
- The number of blind reflectors can be freely changed
- The width and angle of the blind-shaped reflectors can be freely changed
- Illuminance distribution can be calculated automatically

3. Concept of light (surface light source) incident from the window

This simulator can deal with natural light which enters through the window as can be seen in Fig. 3-1. And the 3D coordinate system of model space simulation is shown in Fig. 3-2. Here, the concept of light (surface light source) incident from this window will be described.

In this study, the window that I installed in this simulation program has very good transmittance ability. And the light beam that will transmit through the window will be directed to the ceiling and will be reflected there. As a result, the light will be simulated as a sum of point light sources as shown in Fig. 3-3.

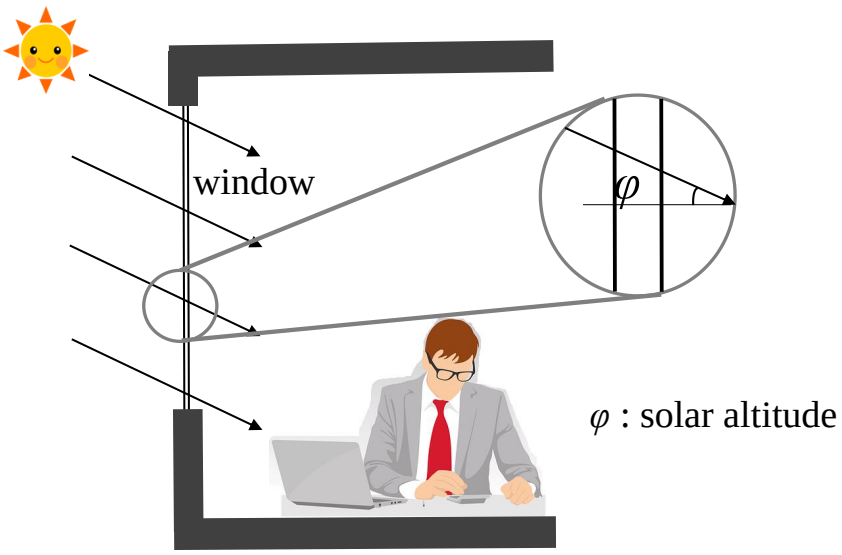

Fig. 3-1 Solar altitude and incident light from the window

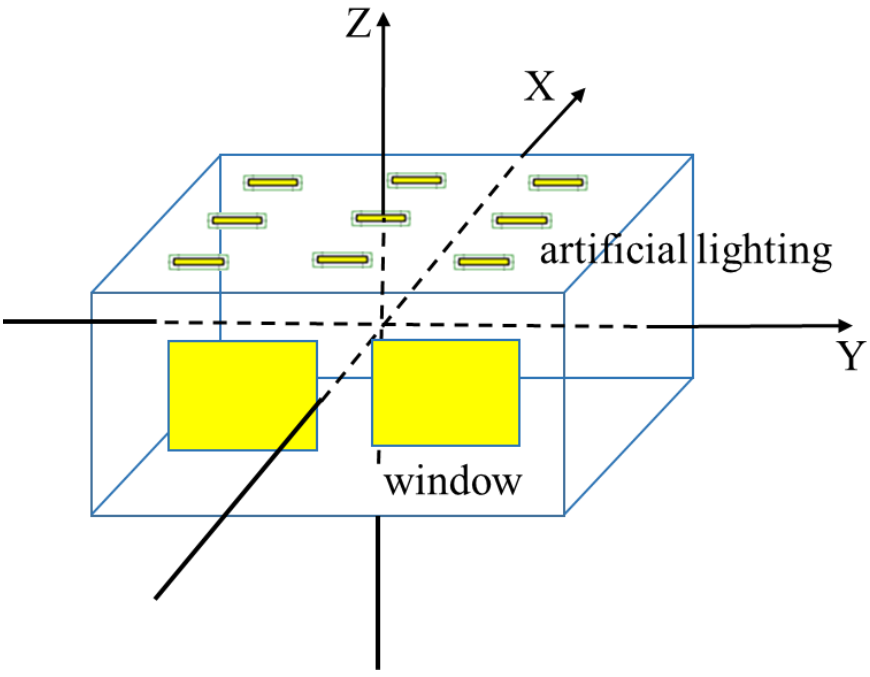

Fig. 3-2 Model space simulation

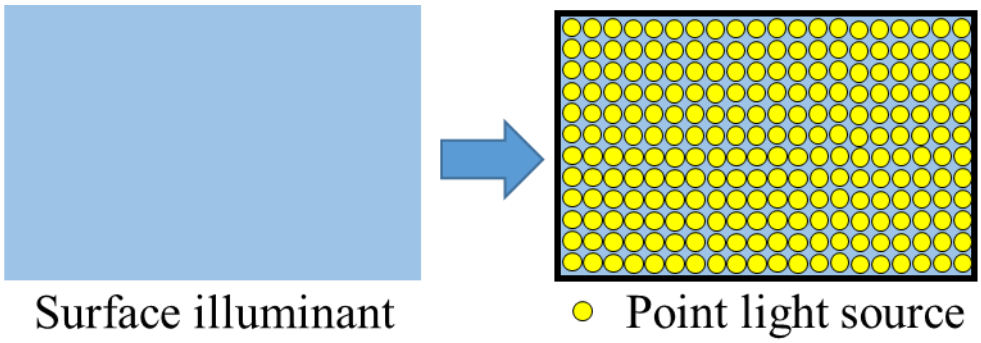

Fig. 3-3 Surface assumed as a collection of point light source

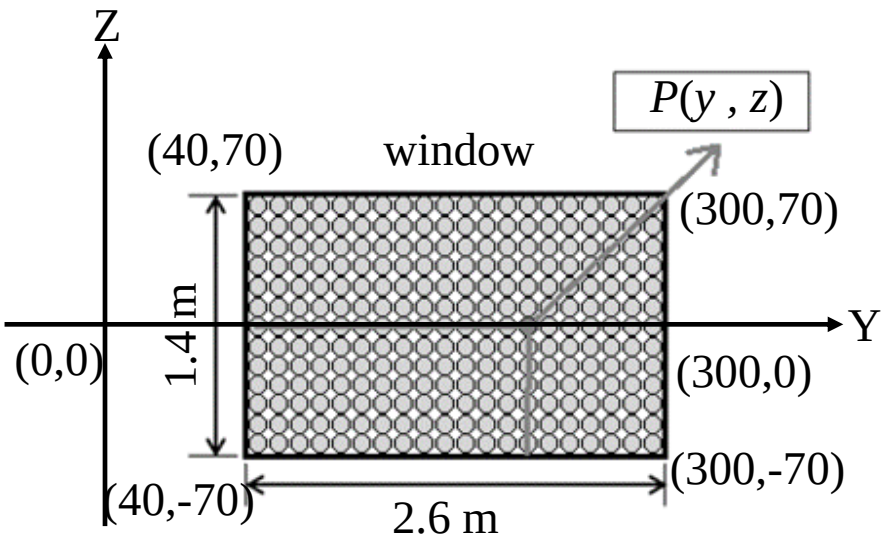

Fig. 3-4 Determination of a photon flux point (for one window)

The point light sources are selected by 2 coordinates of axes Y and Z on the window surface as shown in Fig. 3-4 [11]. e.g. A point P (y, z) on the window is selected in a way, where y and z fulfill the conditions of $40 \leq y \leq 300$ and $-70 \leq z \leq 70$ (the other is $-300 \leq y \leq -40$ and $-70 \leq z \leq 70$)respectively where the size of one window is 2.6×1.4 m. The point P is selected by generating random numbers and the natural light that comes through window is simulated. The number of calculations is set as 50,000,000 times for each window. This calculation number is larger than that of fluorescent lamp as it is a surface light source compared to a point light source. The angle of photon flux will be changed according to the sunlight elevation angle. For a cloudy day, the light source is modeled with random numbers with diffusion light.

3-2 Operating procedure of the illuminance distribution simulator

The illuminance distribution simulator operates with the flow as shown in Fig. 3-5. Each specific operation method will be described in the operation procedures (1) to (9).

(1) Dimension input of model space

When constructing the model space, a simulation model as shown in Fig. 3-6 (b) can be constructed by inputting the height, width and depth of the room from the keyboard as numerical values as shown in Fig. 3-6 (a). It is also possible to increase or decrease the value

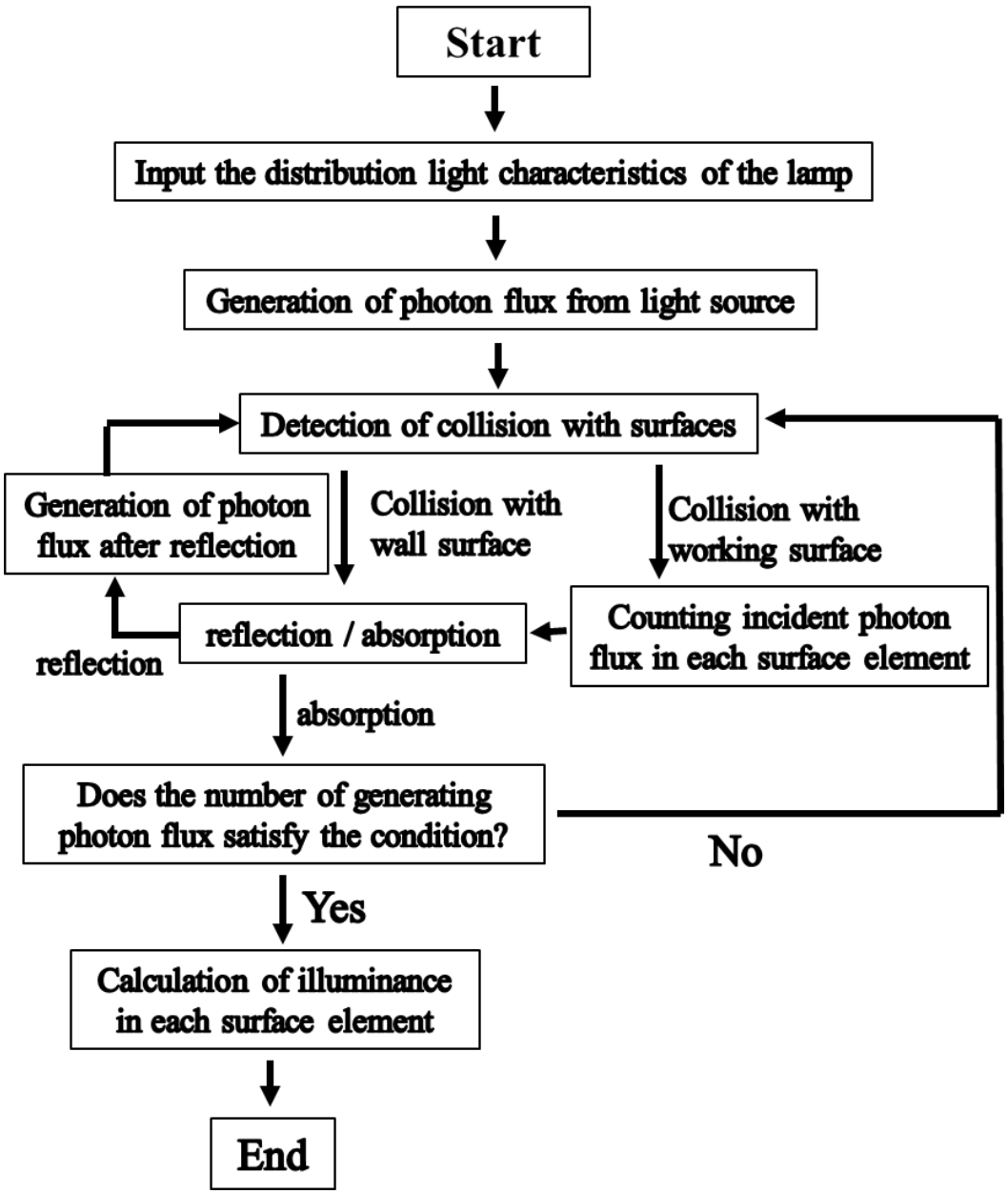

Fig. 3-5 Flow chart of illuminance distribution simulator

with the arrows at the right end of the text box. With this, I can simulate room in any size.

(2) Reflectance input

Here, it is possible to freely input the reflectance of the wall, the ceiling, and the work surface. In this study, I have set the values based on a typical laboratory at Akita University for the simulation. The reflectance was set at 80%, 70%, 40% after investigating the materials used such as laboratory walls and ceilings [12].

(3) Window input

This research is based on a typical laboratory at Akita University and two windows were installed on the wall as shown in Fig. 3-8 (b). The dimension of the window to be set on the wall was inputted as a numerical value from the keyboard as shown in Fig. 3-8 (a). In the actual simulation, simulation was performed by assuming the window as a surface light source. The efficiency of the surface light source and the number of luminous fluxes were inputted in the form as shown in Fig. 3-8(a).

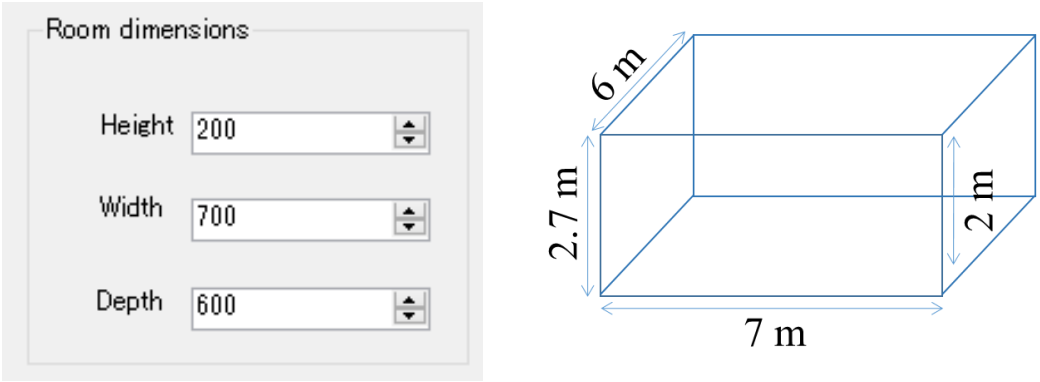

(a) Input form (b) Model space

Fig. 3-6 Model space input

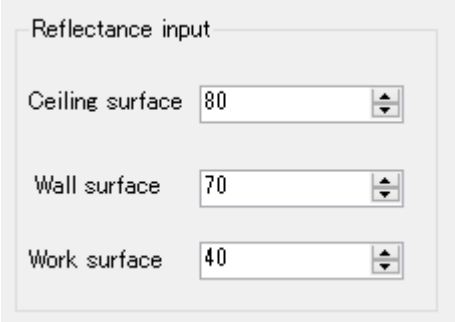

Fig. 3-7 Reflectance input

(4) Solar angle input

Unlike previously created simulators, the simulator in this research can simulate the sunlight from windows for energy saving. However, solar altitude angle and solar azimuth angle change depending on the season and time zone. Therefore, it is necessary to investigate solar altitude angle and solar azimuth angle when in actual simulation. The solar altitude used in this simulation is the solar angle at Akita University which will be further explained later. Here, the height and azimuth of the sun are inputted numerically from the keyboard as shown in Fig. 3-9.

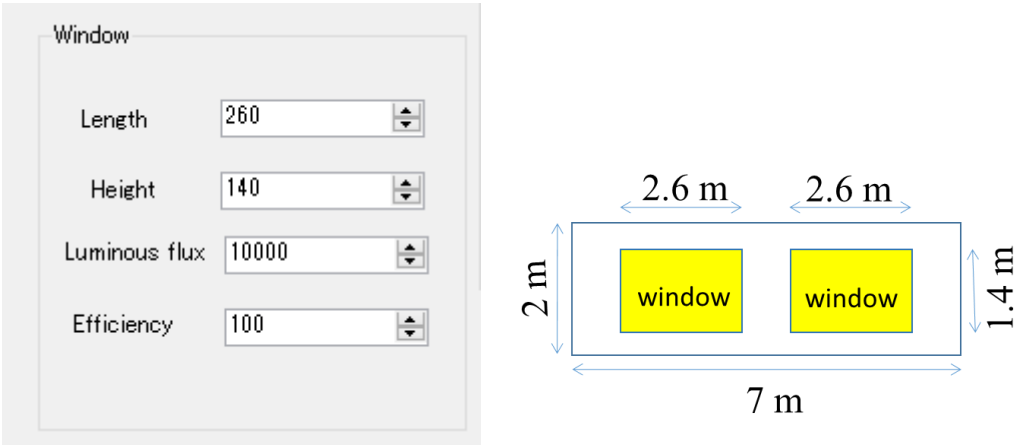

(a) Input form (b) Window

Fig. 3-8 Window input

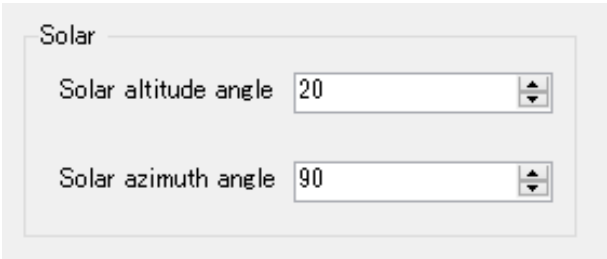

Fig. 3-9 Input form for solar altitude angle and solar azimuth angle

(5) Setting of reflector

Fig. 3-10 (a) shows the mechanism for controlling daylight entering from the window. As shown in the figure, dazzling sunlight coming from the window is reflected to the ceiling by blind reflectors, and it is supplemented as indoor lighting as diffused light. Reflectors are installed as shown in Fig. 3-10 (a), and the angle can be freely changed, thereby controlling incident sunlight. Further explanation will be made in Chapter 4. Here, numerical values related to the blind-shaped reflection plate installed in the window are inputted from the keyboard as shown in Fig. 3-10(b).

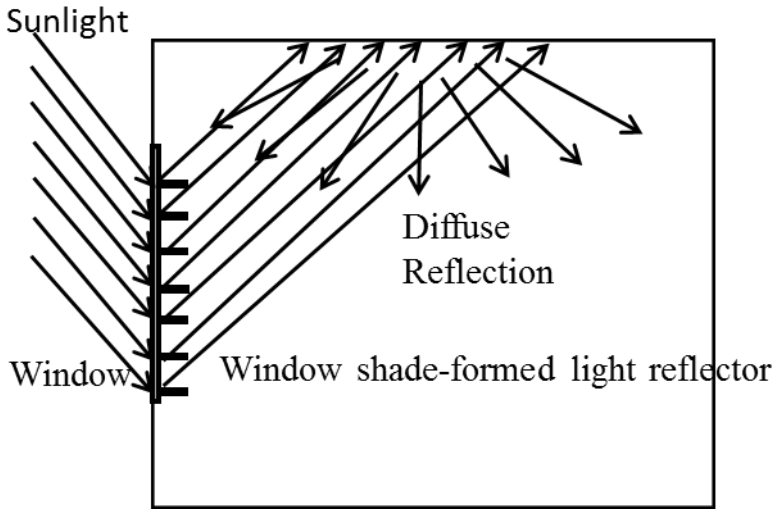

(a) Using of daylight

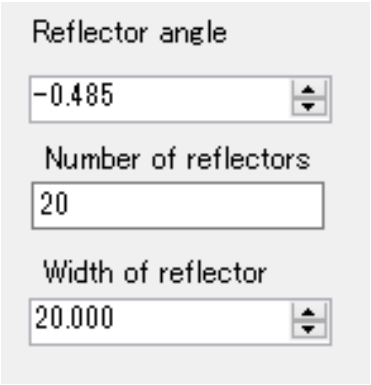

(b) Input form

Fig. 3-10 Setting of Reflectors

(6) Setting of lighting

All lighting makers disclose the light distribution curve of the lighting equipment of their companies and light characteristics (light source, light flux, instrument efficiency, etc.) in catalogs, etc.

In this research, the light distribution characteristics of the lighting equipment used are downloaded from the company catalog, and the file is automatically read by the simulator. Here, I use luminaires efficiency and luminous flux etc. from the catalog and input it in the form shown in Fig. 3-11.

(7) Input of surface elements

As shown in Fig. 3-12 (a), the size of the surface element is set to an appropriate size with respect to the dimension of the model space. In this research, surface element is the element unit area of a work surface, the smaller the surface element is, the higher the accuracy of the illuminance distribution chart is, and the lighting environment will look more beautiful. For example, as shown in Fig. 3-12 (b), when the size of the work surface is 600 x 600 cm^2 and the size of the surface element is 50 x 50 cm^2, the room is divided by 12 x 12 and the illuminance is calculated and the illuminance distribution chart is made. When measuring the surface element, the illuminance of surface element can be calculated by measuring the illuminance at four points of the surface element square as shown in Fig. 3-12 (b). The calculation method is described in section 3-3-1.

(8) Illuminance calculation and result data storage

After setting the above conditions, calculation is initialized by clicking the “Calculation” button as shown in the form of Fig. 3-13. The result is displayed in the text box after calculation is completed. When you press the save button, the result is saved as csv file in a predefined path on the computer. When you press the end button, the program will end automatically.

(9) Illuminance distribution chart

In order to make a good lighting environment in this research, an illuminance distribution chart was made from the result obtained explained in the previous section. An example of the resulting illuminance distribution chart is shown in Fig. 3-14. From this illuminance distribution chart, you can see the lighting condition of the work surface. This research creates illuminance distribution map in MATLAB.

MATLAB is the abbreviation of Matrix Laboratory, a commercial mathematical software produced by the The MathWorks company in the United States. Compared with other software, its matrix calculation and graphic processing are the strengths of MATLAB [13].

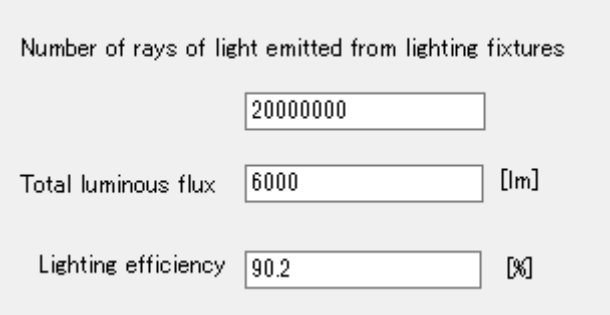

Fig. 3-11 Input form for lighting information

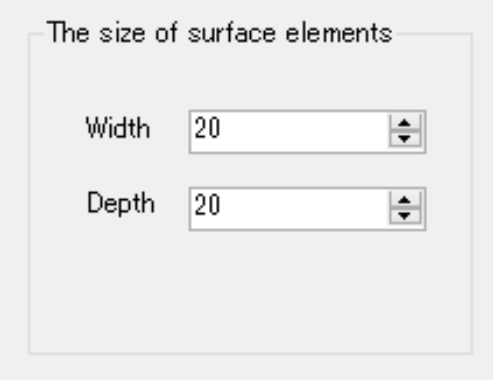

(a) Input form for surface elements

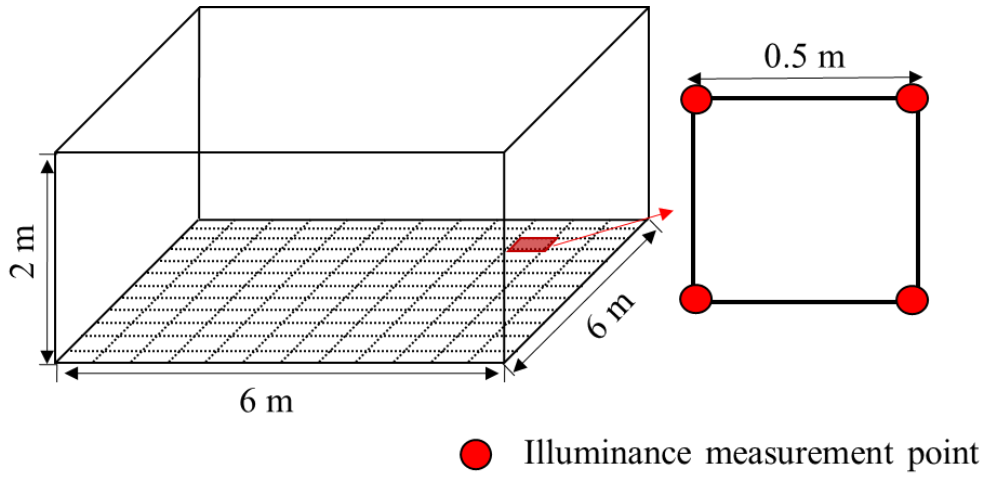

(b) Example of surface elements

Fig. 3-12 Surface elements

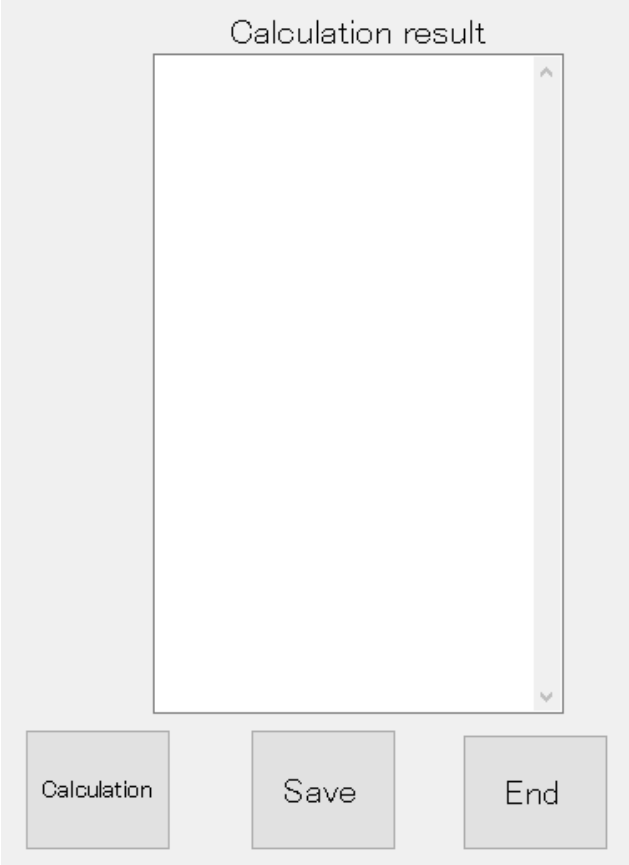

Fig. 3-13 Illuminance calculation and result storage

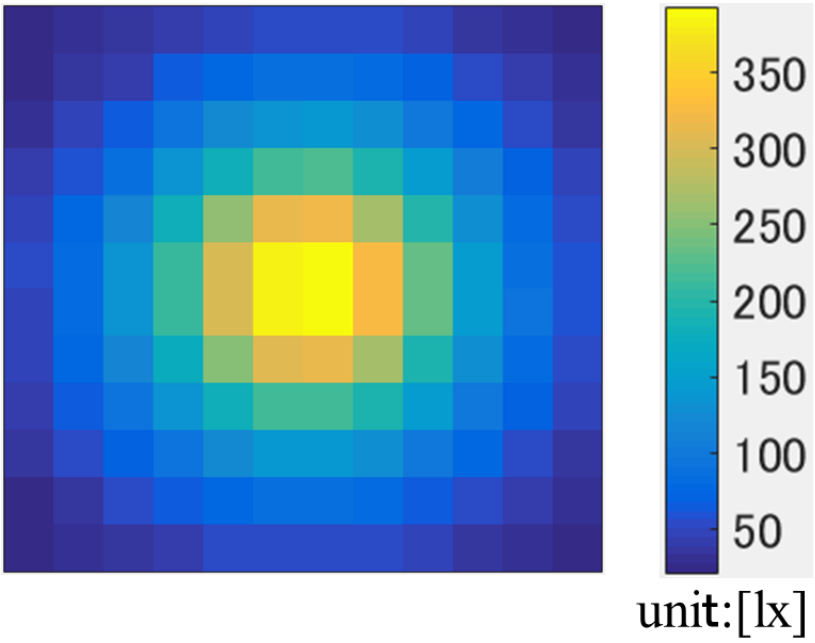

Fig. 3-14 An example of illuminance distribution chart

3-3 Validation of illuminance distribution simulator

In this work, I have imitated the fluorescent light, window, reflector and natural light sources by using the Monte Carlo ray tracing method. And finally, after the simulation, the luminous distribution for the model room was calculated. The simulation results were compared with the measured data and our simulation works were evaluated.

3-3-1 Verification of luminaires

Originally, luminaires have elements of length, width and thickness, but in the developed illuminance distribution simulator, in order to speed up the calculation, the luminaires are handled as point light sources which does not have any size. Therefore, it is necessary to verify how much the actual illuminance distribution can be reproduced by the illuminance distribution obtained by the simulation. Thus, I actually measure the illuminance distribution in the actual room, and verified the validity through the comparison with the simulated value.

1：Characteristics of lighting equipment

The lighting equipment used is a reverse Fuji type that is often used in offices, schools, etc. The fluorescent tubes of the light source are straight tube fluorescent tubes (length 1.194 cm, tube diameter .0.032 m). The total luminous flux is 7040 lm, and the instrument efficiency is 90.2%. The image of the lighting equipment used for the actual measurement is shown in Fig. 3-15, and the light distribution characteristics are shown in Fig. 3-16.

Fig. 3-15 Image of lighting equipment [14]

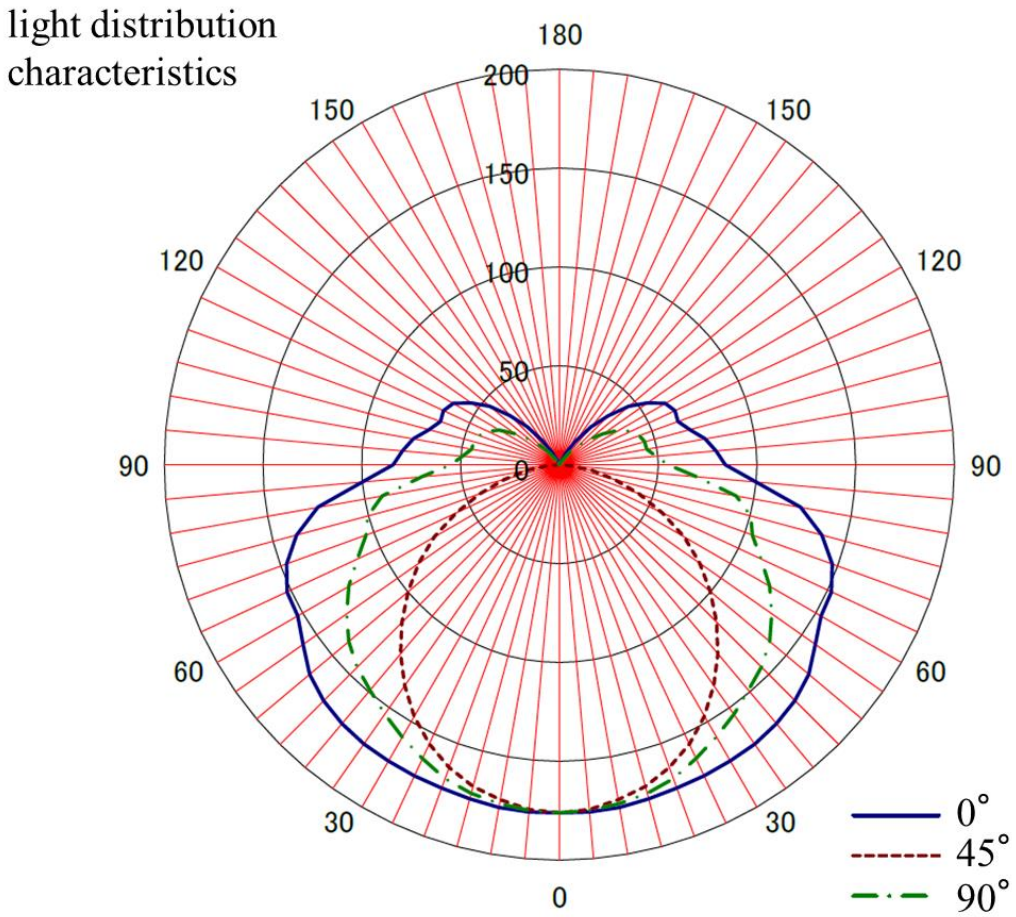

Fig. 3-16 Light distribution characteristics [14]

2：Measurement condition

The actual measurement model is shown in Fig. 3-17. Luminaires are set directly 200[cm] above the center of the floor. On the width 6.0 [m] × depth 6.0 [m] floor surface, the illuminance distribution was measured by a 4 point method using an illuminometer (ANA-F11 manufactured by Tokyo Koen Denki), equally dividing the surface into 12 × 12 squares. As shown in Fig. 3-18, the calculation method of the four point method measures the illuminance with four square points of the surface element and calculates the illuminance of the surface layer by using the expression on the right [15]. In order to measure the illuminance of only direct light from the lighting equipment, measurements were performed in the night and exterior lights were blocked from entering the room.

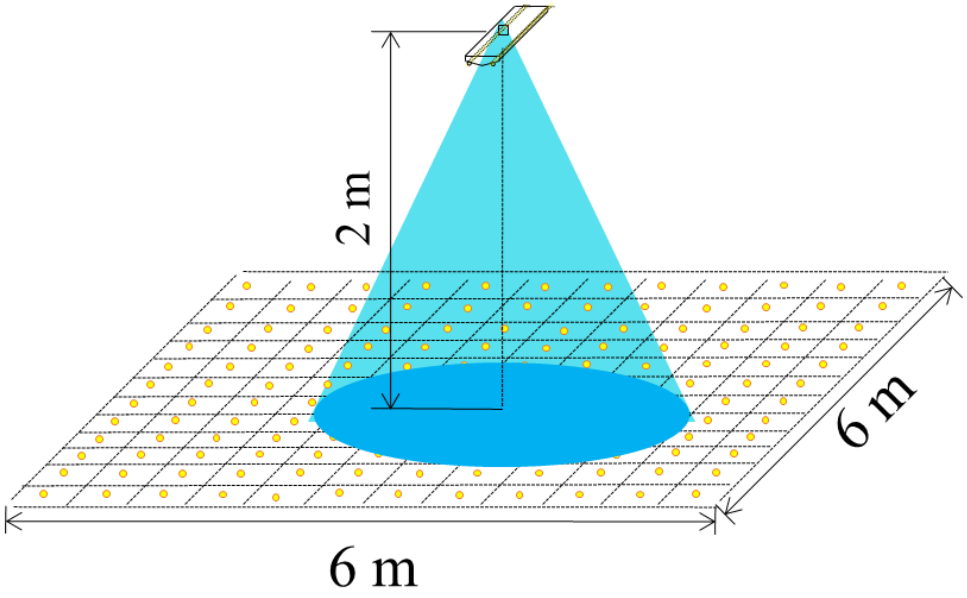

Fig. 3-17 Measurement model (lighting)

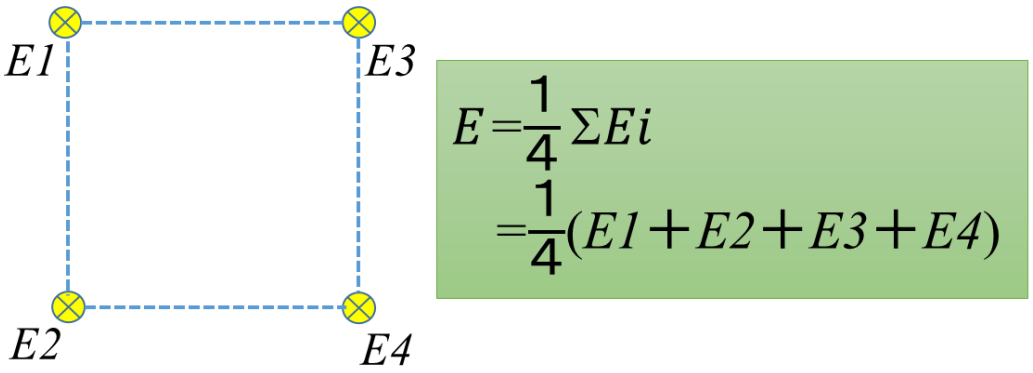

Fig. 3-18 Four point method [15]

3：Simulation conditions

A simulation model was created under the same conditions as the actual measurement described above and calculation was performed. As the number of calculations (the number of rays emitted from the light source) is increased according to the calculation principle explained above, the accuracy of the illuminance distribution chart increases. Along with that, the calculation time is increased. In this research, in order to achieve both accuracy and speed of the simulator, I set number of calculation as 20 million times per light ray.

4：Result comparison

Figures 3-19 (a) and (b) show the illuminance distributions of actual and simulated values. In Table 3-1 and Fig. 3-20, the measured values and simulated values were compared. It can be considered that the trend of the illuminance distribution of the measured values can be reproduced in the simulation value as a whole. When the average relative error of each cell with respect to the measured value was obtained, the value was 8.3%. This value is very close to the simulation value. From this result, even if the lighting equipment are handled as point light sources on the program, when the distance of the light source is sufficiently far away from the measurement place, it can be said that the program for illuminance distribution can imitate the real lighting environment.

Observing at the value of each illuminance in Table 3-1, the actual measured value is higher than the simulation value as a whole, and it gives a bright impression. As a cause of such a difference, the measurement was made assuming that the reflectance was 0% at the time of measurement, but in actual, it is thought that there was an influence of the reflection of the surface and a slight infiltration of light from the outside. A dark room is necessary to eliminate these effects.

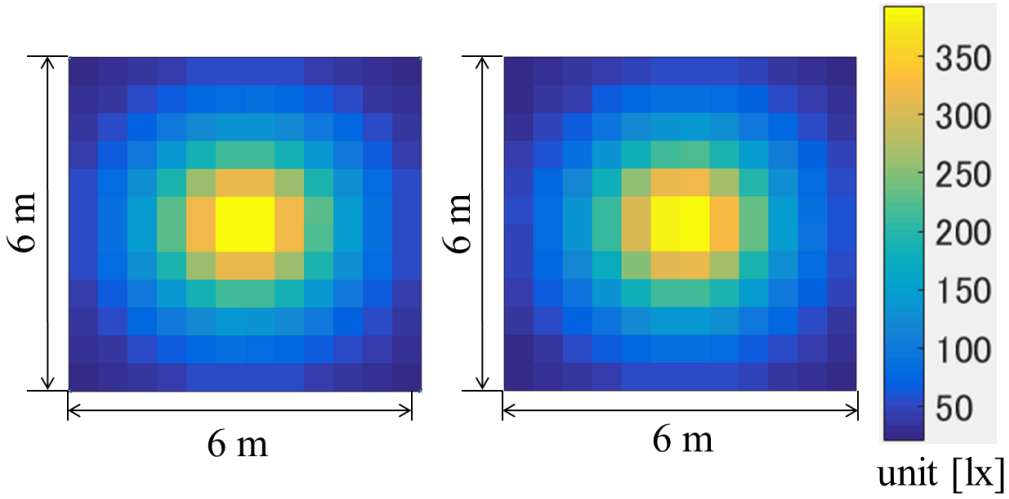

(a) Measurement value (b) Simulation value

Fig. 3-19 Illumination distribution (lighting)

Table 3-1 Comparison of the results (lighting)

	illuminance values [lx]			uniformity of illuminance
	maximum	minimum	average	
Measurement value	403	61	152	0.40
Simulation value	407	56	150	0.37

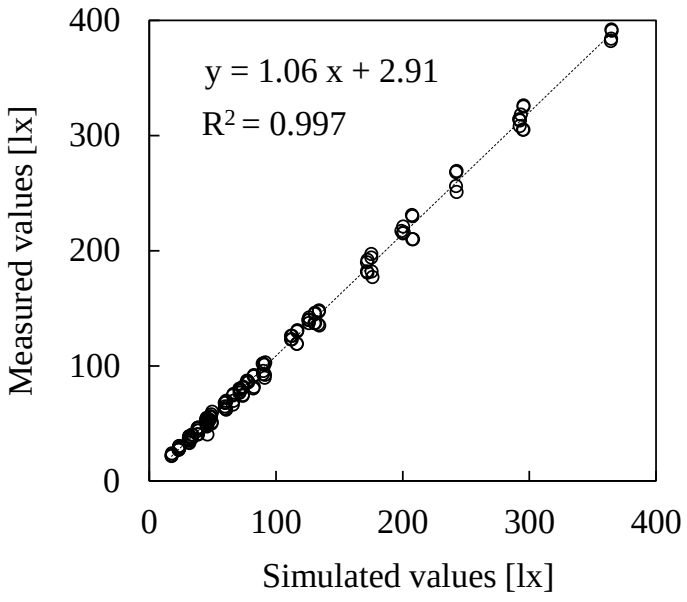

Fig. 3-20 Comparison of the results (lighting)

3-3-2 Window validation

The biggest change compared to the previous simulator in our laboratory is that the blind reflector can be installed in the windows and use the sunlight from the windows. Therefore, it is necessary to verify how much actual illuminance distribution can be reproduced by the illuminance distribution obtained from the surface light source in the simulation. Therefore, I measured the illuminance distribution in the actual room, and verified the validity by comparison with the simulation value.

1：Measurement condition

In order to verify the validity of the window, I measured the illuminance distribution of the work surface in a laboratory with a width 6.0 m × depth 7.0 m × height 2.7 m as shown in Fig. 3-21. The work surface should be 0.7 m above the floor. For the measurement method, the illuminance was measured using an illuminometer with the 4 points method described in the previous section, and created an illuminance distribution chart. However, based on the actual measurements, as the amount of incident light quantity varies according time, it is difficult to measure when there is direct light. Also, simulating natural diffused light with the Monte Carlo ray tracing method, one can confirm that indoor reflection and light route tracking are correct. In the case of direct light, it only unifies the direction of the light emitted from the window in one direction, that is, if it can be verified in the case of scattered light, it can be confirmed for the case of direct light. Here, I measured the illuminance distribution in the target room, without direct light nor reflector and lighting fixture attached (Fig. 3-22).

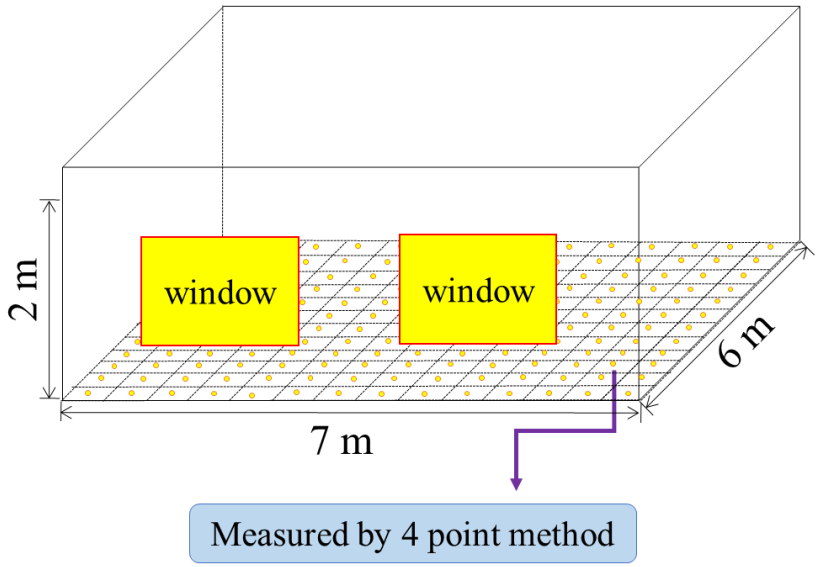

Fig. 3-21 Measurement model (Window)

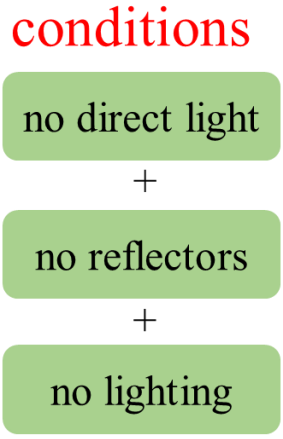

Fig. 3-22 Measured conditions (Day lighting form window)

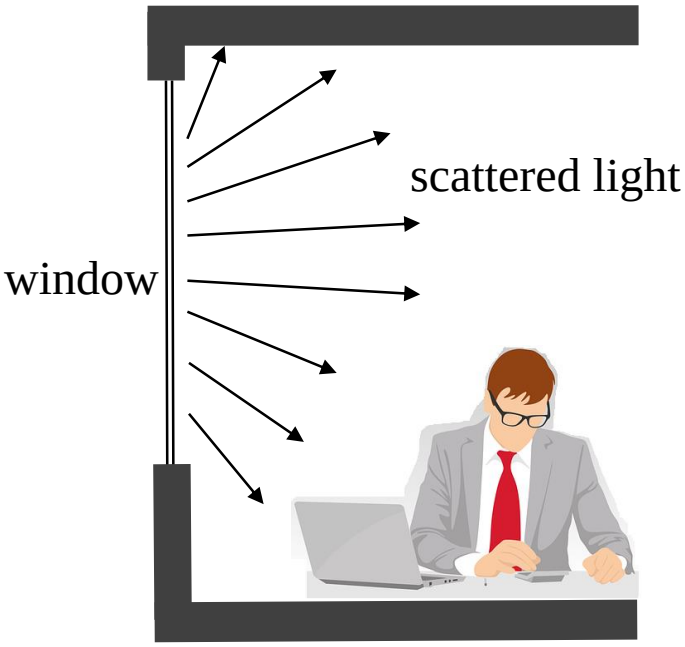

Fig. 3-23 Light emission from window (cloudy)

2：Simulation conditions

In the simulation, I simulated an actual laboratory and created an interior space with a width 6.0 m ×depth 7.0 m ×height 2.0 m, similar to the actual environment, and I installed two windows on the wall. Luminaires were not installed on the ceiling because I are verifying the validity of window. The window emits light as a surface light source. The actual measurement was measured in the condition without direct light, that is, on a cloudy day. So, the light radiated from the surface light source in the simulation is scattered light and simulates the window by

using the Monte Carlo ray tracing method (Fig. 3-23). Here, I verify the validity of the window by comparing the simulated result with the measured value.

3：Result comparison

I have performed the simulation works for daylight and without any fluorescent tube for our model room. The results of the calculation and the measured data are shown in Fig. 3-24 and their comparison can be found in Fig. 3-25 and Table 3-2. From these figures, it is obvious that the simulation results fit well with the measured data. The values of the illuminance from the simulation and the measured data show very good correlation. Thus, using daylight in interior illumination by simulating with the Monte Carlo method is achieved. It is hopefully possible to use daylight as an illumination tool for producing an eco-friendly illumination system.

By comparing the actual measurement value with the simulation value, the mean relative error of each cell with respect to the measured value is 8.7%, and it can be said that a simulation close to the actual measurement value is achieved. I assumed that the error is caused by the amount of light flux entering from the window which varies with time and it was confirmed from the slight difference seen in the flux amount of actual measurement simulated measurement. From this, I believe that natural light can be simulated by this system.

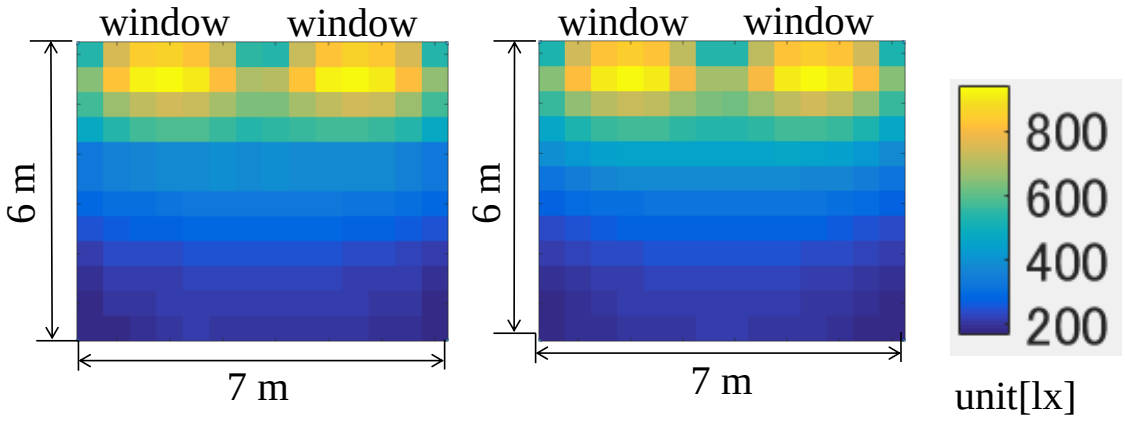

(a) Measurement value (b) Simulation value

Fig. 3-24 Illumination distribution (window)

Table 3-2 Comparison of the results (window)

	illuminance values [lx]			uniformity of illuminance
	maximum	minimum	average	
Measurement value	792	131	308	0.43
Simulation value	817	150	335	0.45

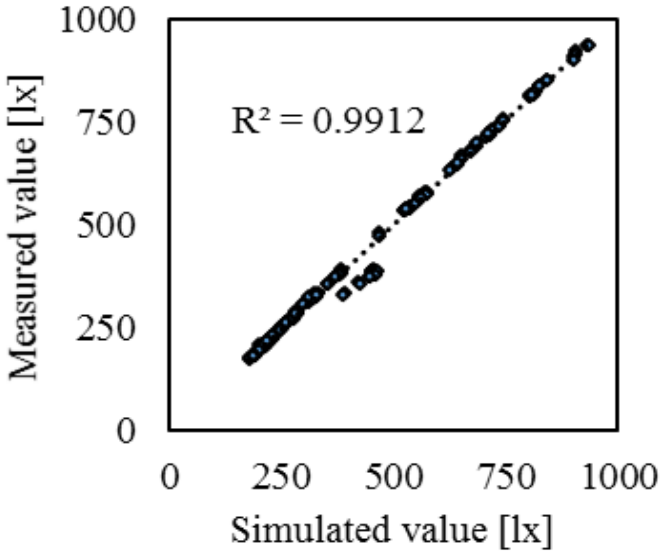

Fig. 3-25 Comparison of the results (window)

3-3-3 Verification of reflector effectiveness

1：Simulation conditions

Before simulating, it is necessary to verify the effectiveness of the reflector in the verification of the window. So, here I used a simulator to confirm the effectiveness of the reflector. The image of the reflector is shown in Fig. 3-26. Here I simulate the sun and reflector under the following conditions.

- The number of reflectors is 20
- The distance between the reflectors is 0.07 m
- The length of the window reflectors installed on it was set to 2.6 m so that the incident light can be reflected to the ceiling.
- The width of the reflector is 0.1 m
- Reflector angle is -23.0 °
- Solar altitude angle is 65 °
- Solar azimuth angle is 180 °(facing south)

2：Results

In the previous section, I have explained about the development of a simulator which uses natural light entering from the window. So, the window has turned into a light source in our simulation work and I assumed it to function as a surface light source. The simulation results will be compared with both the conditions of without reflector and with reflector. Thus the utility of the reflector will be evaluated. Fig. 3-27(a) shows the luminous distribution of the model room with no reflector in bright daylight. And Fig. 3-27(b) shows the same results from the simulation works of the model room with window shade reflector.

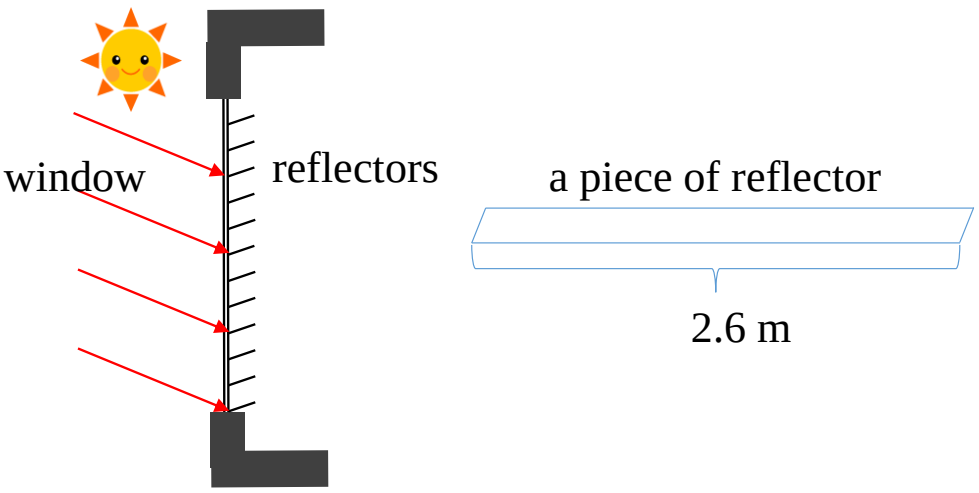

Fig. 3-26 Image of reflectors

For the condition without reflector, it can be seen that the sunlight enters the room from the window directly and it caused a concentration of luminance near to the window side of the room. The light contrast of the room is very large especially near the window for working surface and it cannot provide a uniform illuminance to whole room. It can create stress and tiredness to human body and eyes and will certainly cause bad effect in working environment.

But by using reflector in the window, these problems can be solved which can be seen from Fig. 3-27(b). The dazzling light rays are reflected to the ceiling by the reflector beside the window and then it is simulated as diffusion light to the whole room, which produces a reasonable and good illuminance distribution. The comparison of the results is shown in Table 3-3. From these results, it can be said that to use natural daylight for interior illumination, it is necessary to use reflector in a window.

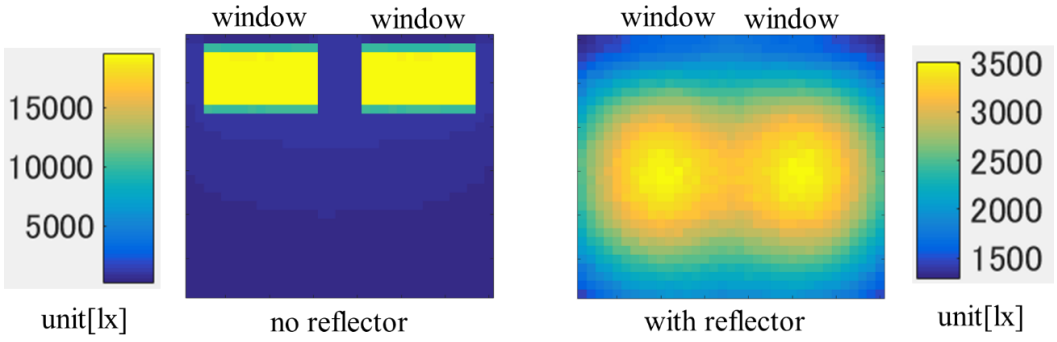

(a) No reflector (b) With reflector

Fig. 3-27 Illumination distributions (With or without reflector)

Table 3-3 Comparison of the results (With or without reflector)

	illuminance values [lx]			uniformity of illuminance
	maximum	minimum	average	
Measurement value	19281	209	2725	0.07
Simulation value	1267	811	1099	0.73

3-4 Basic knowledge of interior lighting design

In this research, when I create an illuminance distribution simulator, I need basic knowledge of lighting design and the procedures involved. In addition, it is necessary to decide the lighting standard necessary for lighting design in an actual office. These points are explained in this chapter.

3-4-1 Purpose and requirements of lighting design[16~21]

The goal of lighting design is to select light sources and lighting equipment with illuminance needed by different indoor and outdoor environments, determine reasonable lighting forms and layout plans, and create a reasonable and high quality light environment to meet the requirements of work, study and life. Residential indoor lighting is to solve people's needs in life, work and study. And it is to improve the artistic quality of indoor space environment and make people's lives better. The following requirements are to be considered when designing lighting to create an illumination environment suitable for these purposes.

1. Appropriate illuminance

The lighting design must conform to the national standards for lighting and ensure that the indoor space has a suitable illumination. In general, high illuminance is necessary when there is movement or when the size, brightness contrast and reflectance of the subject which is observed by a person are small. And it is effective to increase the illuminance when trying to increase the accuracy and speed of visual work.

For example: A place like living room, occasions of having guests or family parties, when working or studying, illuminance should be a little higher. Illuminance should also be higher in dining room to prevent accidents relating to food and plates. And the bedroom illuminance should be low, for people to rest better.

2. Appropriate light color and color rendering properties

I should try to make use of the types of lighting, lighting equipment and light colors to create an environment-friendly atmosphere and improve spatial sense. For example, a strong, concentrated contrast of luminance can be produced by using a projective lamp, which will make indoor space lively and active. Using the light trough produced by reflective lamp, the soft light color will create a peaceful, relaxed and cordial atmosphere. The classical lamps will produce a more gorgeous and elegant atmosphere. The use of simple lamps and lanterns can create a simple and flat atmosphere. The use of low color temperature warm light in cold areas, high temperature and cold tone light source in hot areas, can create an indoor with harmonic

colors filled with warmth. Lighting can also make people feel different about their surroundings. Generally speaking, rooms with high brightness feel more spacious while dark rooms with low light feel a little smaller. When the light is used as the whole lighting of the space, the space will feel bigger, and people will feel pleasant.

3. Appropriate uniformity

If there is a sudden change in the illuminance level in the space, deterioration of the visual function occurs or the feeling of uneasiness becomes large due to delay in adaptation of the visual system and insufficient time for adaptation, a person will feel less comfortable. In addition, it is desirable for the illuminance in a room to be as uniform as possible, since the arrangement of the objects like desks cannot be determined in advance or the arrangement may be changed depending on its purpose. It is desirable that the change in the illuminance horizontal plane on the work surface is as small as possible and in cases of using lighting system in office or the like, the uniformity of the illuminance in the work plane which is calculated by, degree = minimum illumination / average illuminance needs to have a value of 0.6 or more. Also, when selecting uneven lighting methods like the ambient lighting method, the illuminance required depends on the type of work but generally 250 to 600 lx is required except for visual work.

4. Prevention of glare

In order to avoid unpleasant glare from lighting fixtures and windows during the day, non-glare lighting equipment are selected according to the purpose and blinds etc. are set up in the window.

5. Harmony of artificial light and daylight

It is necessary to harmonize artificial light and daylight in when using natural light on places such as table surfaces and atelier. It is especially important to pay attention to each of the object's illuminance and balance, direction and color of light. In this research, I adopted a daylighting system that attaches a blind type reflectors on the window that guides natural light taken from the reflector to the inside of the room, and irradiates the interior from the ceiling surface, so that it is possible to incorporate more natural light to the whole room. The merit of introducing natural light is not only energy saving effect by drastically reducing power consumption but also high comfortable visual environment beneficial in terms of health and hygiene.

6. Creating an eco-friendly environment

Energy conservation and emission reduction are important measures for mankind to protect the

environment while sustaining development. For this, it is important to select energy-efficient lighting fixtures and light sources and knowing how to maintain them.

The design of indoor lighting should consider the factors of energy saving and emission reduction. I should choose lighting lamps with high light efficiency, less power consumption that last long. Due to the high power consumption and short life of incandescent lamps, its usage should be avoided as the lighting of residential area in the future. Furthermore, when setting the brightness of the light, it is necessary to take in the factors of the place and time where it is installed in order to operate it with minimum energy consumption.

3-4-2 Office lighting standards

With the development of society, the demand for lighting technology in office buildings is getting higher and higher. As far as the work of the office building is concerned, an office (such as the drawing office) can be divided into general offices and offices with special working conditions. Therefore, the lighting design of office building should be considered according to the specific work requirements. In this research, I have created a simulation for the office environment, and kept lighting design in line with office lighting standards.

The office lighting is defined by the CIE (International Commission on Illumination) 「Indoor Illumination Standard (CIE Standards 008) 」and the recommended standard is decided by the lighting committee of each country. The design of office lighting should enable the staff to work effectively. As the interest and enthusiasm to improve work efficiency are all influenced by environment, I must consider improving office lighting to achieve a harmonious working environment. Illumination standards which are considered to be particularly important are described here.

The lighting standard is the most important item in the process of lighting design. The lighting standards related to this research are as follows.

① **Illuminance**

The illuminance shows the average value of the horizontal plane illuminance including the recommended maintenance rate for each type of room in each area. When the work surface is not specified, it is assumed to be a virtual horizontal surface value of 0.8 m above the floor. As I are doing this research in an actual laboratory, the work surface was set as 0.7 m above the floor.

In a general office, people and documents most commonly enter a worker’s vision. Among these, the visual acuity of facial expression is the lowest and has the brightness of 20cd/m^2. That is to say, the minimum illuminance required for a person to see a face is 200lx, which usually requires 500-750 lx (the average reflection ratio of the face's skin is 30%). In addition, when reading words under the conditions whereby the size of the

general word is 3-4mm^2 and the eye distance is 30cm, the required illumination is about 500-800lx. Table 3-4 shows the maintenance illuminance of the work surface during indoor activities, and Table 3-5 shows the illumination standard of the office space. Based on these information, the desired illuminance of this research is 500 lx or more.

② **Uniformity of illuminance**

When there is a large change in an office's illumination distribution, it is easy for human eyes to have visual fatigue and discomfort when observing objects. Therefore, it is desirable that the change in the horizontal surface illuminance on the work surface to be as small as possible, and in the case of the general lighting system in the office area or the like, it is necessary to set the uniformity (minimum illuminance / average illuminance) of the illuminance of the work surface to be 0.7 or more.

Table 3-4 Maintained illuminance for work surface when doing indoor activities [21]

Area, type of work or activity	Maintained illuminance [lx]	Uniformity (Minimum illuminance / average illuminance)
Warehouse, very coarse visual work, emergency stairs	100	0.6 or more
Places where work is not done continuously	150	
Rough vision work, room where work is done continuously (lowest)	200	
Somewhat coarse visual work	300	
Ordinary visual work	500	
Somewhat precise visual work	750	
Precise visual work	1000	
Very precise visual work	1500	
Ultra precise visual work	2000	

Table 3-5　Lighting standard of office space [21]

Area, type of work or activity		Maintainance illuminance [lx]	Uniformity
Type of work	Design and drafting	750	0.6 or more
	Keyboard operation, calculation	500	
Working space	Design room, drawing office	750	not decided
	Office		
	Boardroom		
	Training room・data room		
	Examination room	500	
	Printing room		
	Electronic computer room		
	Kitchen		
	Central monitoring room, control room		
	Guard room		
	Reception area		
Shared space	Entrance hall (daytime)	750	
	Reception lobby		
	Meeting room, assembly room	500	
	Presentation room		
	Lounge		
	Reception room		
	Night guard room	300	
	Dining hall		
	Restroom		
	Tea room, office lounge, hot water boiler room	200	
	Electric room, machine room		
	Archive		
	Changing room, toilet, washroom		
	Staircase	150	
	Restroom	100	
	Corridor, elevator		
	Warehouse		
	Entrance hall (night time)		
	Indoor emergency stairs	50	

References

[1] Hao Chen: “Comparative Study of C, C++, C# and Java Programming Languages”, vaasan ammattikorkeakoulu vasa Yrkeshögskola University of applied sciences, pp.2-10 (2010)

[2] Mikael Olsson: “A Comparison of C++, C#, Java, and PHP in the context of e-learning”, Master of Science Thesis Stockholm, Sweden 2009, KTH Information and Communication Technology pp.1-7 (2009)

[3] Presha B. Thakkar: “Comparative Study Of Eight Programming Languages: C, C++, C#, Java, PHP, ASP, JavaScript & Visual”, Hasmukh Goswami College Of Engineering, Vahelal, A'bad, Registration No: tech_69

[4] Rana Naim, Mohammad Fahim Nizam, Sheetal Hanamasagar, Jalal Noureddine: “Comparative Studies of 10 Programming Languages within 10 Diverse Criteria”, - a Team 10 COMP6411-S10 Term Report, Concordia University Montreal, Quebec, Canada, pp.1-7 (2010)

[5] M. Suzuki, K. Akazawa and Noboru Yoshimura: “Luminous Intensity Distribution of Luminaires with Specular Reflectors”, Lighting Research and Technology, vol.88, no.2, pp.85-90 (2004) (in Japanese)

鈴木雅史, 赤澤幸造, 吉村昇: “鏡面反射を有する照明器具の配光特性”, 照明学会誌, 88 巻 2 号, pp.85-90 (2004)

[6] M. Suzuki, T. Yamaguchi, H. Nakajima and Noboru Yoshimura: “The Back Light Simulation of the Direct Method LCD - Consideration in the Arrangement of the Fluorescent Lamp -”, Lighting Research and Technology, vol.85, no.5, pp.361-363(2001) (in Japanese)

鈴木雅史,山口隆志,中嶋秀正,吉村昇: “直下型液晶ディスプレイのバックライトシミュレーション -蛍光ランプの配置における一考察-”,照明学会誌,85 巻 5 号, pp.361-363 (2001)

[7] L.Chen, X.Wang, M.Suzuki and N.Yoshimura: “Comparison of Direst and Indirect Photometric Descriptions in Monte Carlo Lighting Simulation”, Jpn.J.Appl.Phys, vol.39, No.8, pp.4786-4792 (2000)

[8] L.Chen,M.Suzuki,N.Yoshimura: “Study on Optimal Lighting Configuration and Aberration of Inspection System by Monte Carlo Method”, J.Light & Visual Environment, vol.23, No.1, pp.20-28 (1999)

[9] L.Chen,X.Wang,M.Suzuki,N.Yoshimura: “Optimizing the Lighting in Automatic Inspection System using Monte Carlo Method”, Jpn.J.Appl.Phys.vol.38, No.10, pp.6123-6129 (1999)

[10] The National Astronomical Observatory of Japan (NAOJ) http://www.nao.ac.jp

[11] “Light Sources for Monte Carlo Simulation”, http://www.bli.uci.edu/vp/wiki/images/8/8f/Description_of_Light_Sources.pdf

[12] Architectural Studies No.22: Editorial Board of Architectural Studies, Shokokusha Publishing Co., Ltd (1969) (in Japanese)

建築学大系〈第 22〉室内環境計画, 彰国社（1969）

[13] MATLAB-mathworks-Documentation
https://jp.mathworks.com/help/matlab/index.html?lang=en

[14] Hitachi Lighting-Lighting Characteristics - Lamps・Lighting Fixtures
HNM4205V-MEU14-K, www.lighting.hitachi-ap.co.jp/lighting/ (in Japanese)
日立照明器具 照明特性 - ランプ・照明器具 HNM4205V-MEU14-K, www.lighting.hitachi-ap.co.jp/lighting/

[15] JAPANESE INDUSTRIAL STANDARD - Illuminance Measurements for Lighting Installations JIS C 7612 (1985) (in Japanese)
日本工業規格 照度測定方法 JIS C 7612 (1985)

[16] “Best Practices in Lighting Program 2004-chapter 4”, Department of the Environment and Heritage Australian Greenhouse Office, Queensland University of Technology (2004)

[17] “Cooper is Brochure - Lighting Design Guide”, Eaton’s Cooper Lighting and Safety Business (2013)

[18] TAKETEK : “230 V Lighting Design Guide”, Printed in USA Doc.4859 3/07 S PECIFYING A L IGHTING S YSTEM (2011)

[19] “The Lighting Handbook”, Zumtobel Lighting, 5th edition, revised and updated: July 2017.

[20] The Illuminating Engineering Institute of Japan: “New · Lighting classroom-Lighting basic knowledge-Intermediate level”, pp.49－pp.69 (in Japanese)
社団法人 照明学会 :「新・照明教室 照明の基礎知識 中級編」pp.49－pp.69

[21] The Illuminating Engineering Institute of Japan: “New · Lighting classroom-Office lighting~In order to balance energy saving and comfort~”, pp.49－pp.69, pp.90~94 (in Japanese)
社団法人 照明学会 :「新・照明教室 オフィス照明 ~省エネルギーと快適性を両立するために~」pp.49－pp.69, pp.90~94

Chapter 4

Evaluation of lighting environment (Without any direct sunlight)

In previous chapter, it is clear that the simulation results can easily imitate the illumination condition for the model room when there are illumination tools at ceiling or window at wall. The ultimate goal of this research work is to use natural light in interior illumination system. Now, I will compare the illumination condition of the model room with natural light and without natural light. In order to use natural light as described previous chapter, a window shade of blinds which acts as reflector to the incident sunlight is necessary. But on a cloudy day, the incident light through the window is not dazzling and it can be used without any reflector on the window. So in this chapter, I will discuss about the possibilities of the decrease in power consumption for the model room while using the natural light on a cloudy day. I will elaborate the simulation results for fine day in the next chapter.

4-1 Simulation conditions

Before explaining about simulation procedures, simulation conditions will be explained first.

1：Lighting standard [1]

As mentioned in the previous chapter, by referring to the「Lighting Standard JIS Z 9110: 2010」of the Japanese Industrial Standard (JIS), the lighting standard of this research is over 500 lx for the illuminance on the indoor work surface. The illuminance criterion is satisfied when the uniformity (minimum illuminance / average illuminance) is 0.7 or more in the range is more than 1 m from the wall surface. (Table 4-1)

Table 4-1 Lighting Standard (Office)

Illuminance[lx]	500~
Uniformity	0.7~1

2：Model space

Fig. 4-1 shows the outline of the model space used for simulation. The model space is assumed to be an office space, and a simulation was conducted using a work surface of 0.7 m above the floor as work surface. As described in the previous section, the reflectance of each surface should be 80% for the ceiling surface, 70% for the wall surface and 40% for the work surface [2-4]. On one of the wall surfaces, two windows of 2.6 m × 1.4 m were installed at the same height as shown in Fig. 4-2. In this study, the number of calculation set per window is 50 million to achieve an optimum accuracy of illuminance distribution and calculation time. In addition, the surface element was 0.2 m ×0.2 m in size, and the observation surface was divided into 1050 regions of 35 rows ×30 columns to obtain the illuminance.

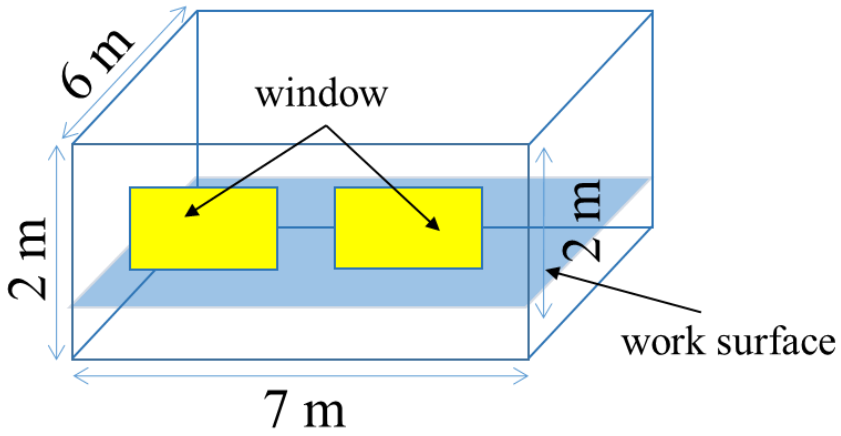

Fig. 4-1 Overview of the model space

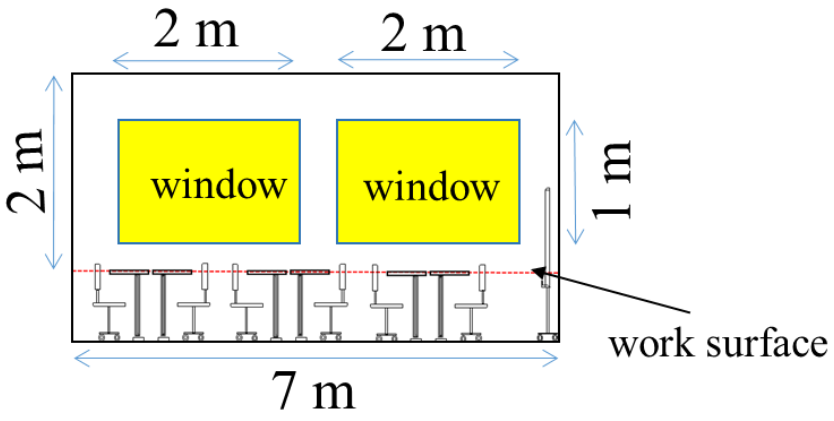

Fig. 4-2 Placement and dimension for windows

3：Lighting equipment

In the simulation, the light fixtures are installed on the ceiling surface of the model space. The installed luminaire is a Hitachi HNM 4205 V fluorescent lamp actually used in the general office as well as the writer's working laboratory. This has a total luminous flux of 7400 lm, instrument efficiency of 90.2%, and power consumption of 64 W [5]. In addition, the number of calculations per lighting fixture is 20 million cycles which is the optimum trade-off between the accuracy of illuminance distribution and calculation time. The image of this light fixture is shown in Fig. 3-15 in the previous chapter and the light distribution curve is shown in Fig. 3-16. The actual laboratory fluorescent lamp arrangement is shown in Fig. 4-2. And the size of the surface element as shown in Fig. 4-3.

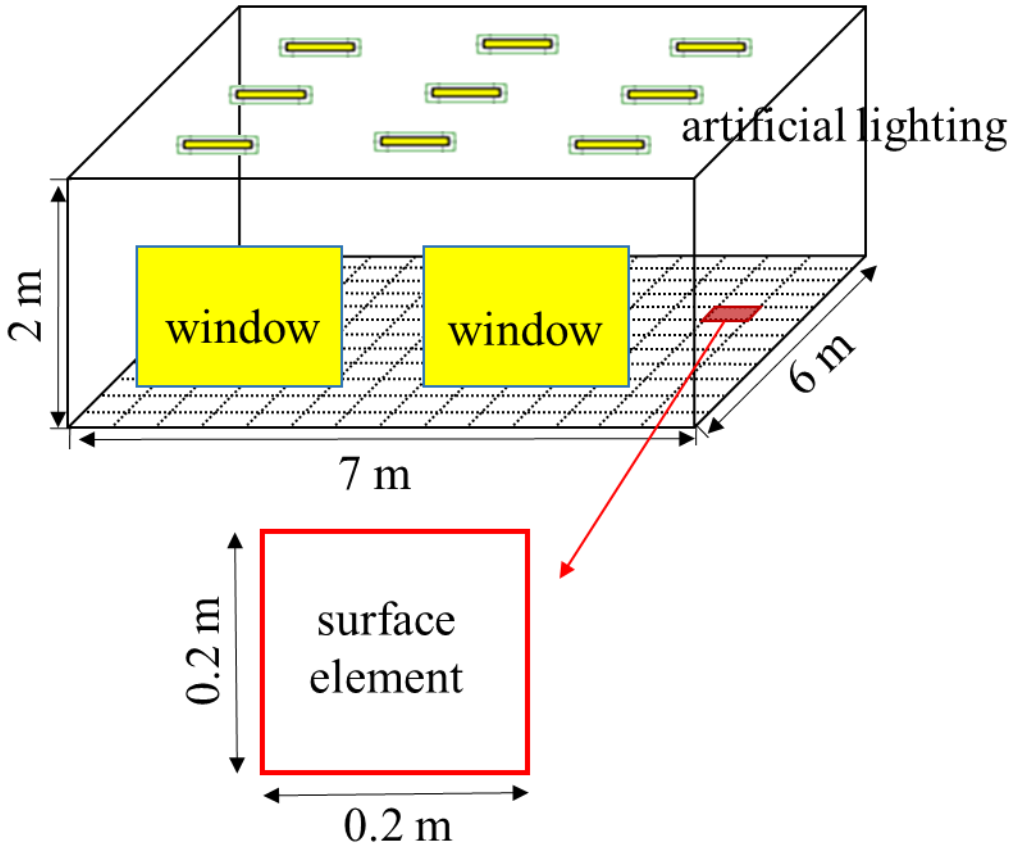

Fig. 4-3 Room model

4：Window conditions

In this study, an illumination distribution simulator which simulates the reflection of light incident of daylight window was created. Here, I will explain the idea of the window when there is no direct light (eg. cloudy). When light coming from the sun to the earth from outer space, it hits various particles and molecules in the atmosphere and scatters. This concept applies for windows too especially on cloudy days, by considering the window as a surface light source and light radiated from the surface light source will be scattered light. As shown in Fig. 4-4, a window is installed on the wall surface and light that enter through the window become scattered light due to interaction of sunlight and fine particles in the air.

By making measurements, one should know that the intensity of the scattered light fluctuates irrespective of season and time. In this study, in order to measure the luminous flux entering the room without direct light, the amount of luminous flux entering from the window was actually measured on three cloudy days before and after summer solstice, the winter solstice and the autumn equinox respectively in a classroom at Akita University. The measured average value was 10273 lm. Based on this result and by making actual calculation, the amount of light flux for simulation was set to 10000 lm in the direction of the window.

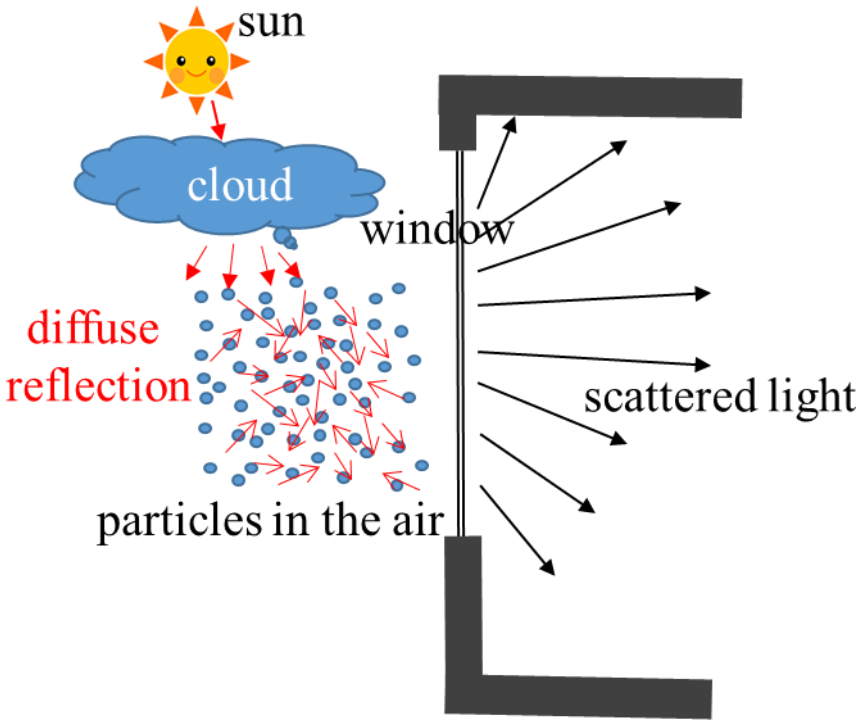

Fig. 4-4 Light emission from window (no direct light)

4-2 Installation method of lighting equipment

Under the above conditions, at first, the illuminance distribution chart was measured when light enters from window without artificial lighting on a cloudy day as shown in Fig. 4-5. Fig. 4-6 shows the measured values of the illuminance distribution on basis of the classroom window without direct light. Based on the illuminance distribution chart, it can be observed that only the illuminance at the windows satisfied the lighting standard. Therefore, it is necessary to lighten up the room.

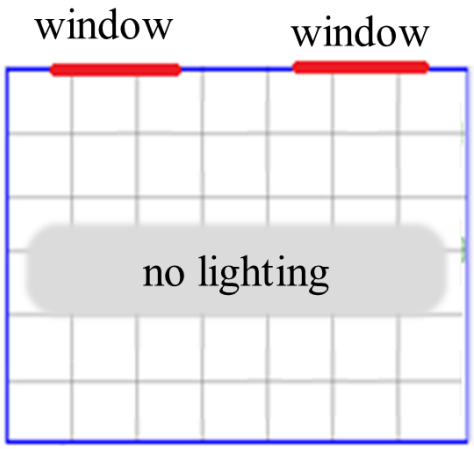

Fig. 4-5 Distribution diagram of lighting equipment (0 lights)

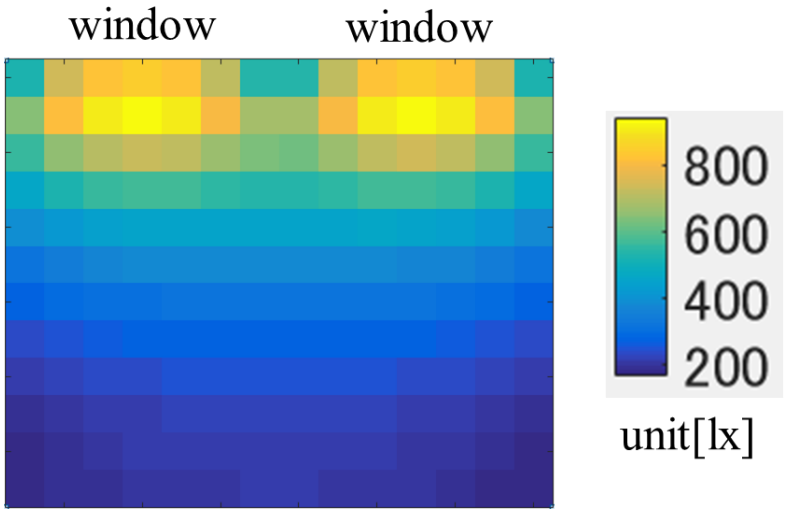

Fig. 4-6 Illuminance distribution chart (measurement)

The lighting fixtures arrangement is shown in Fig. 4-7(a ~ i). In the case of less than 9 lights, I

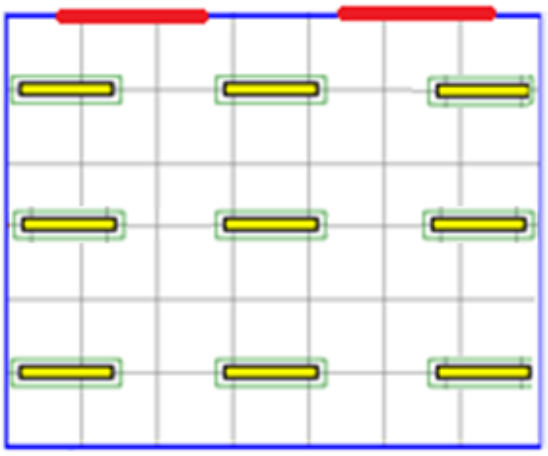

(a) 9 lights

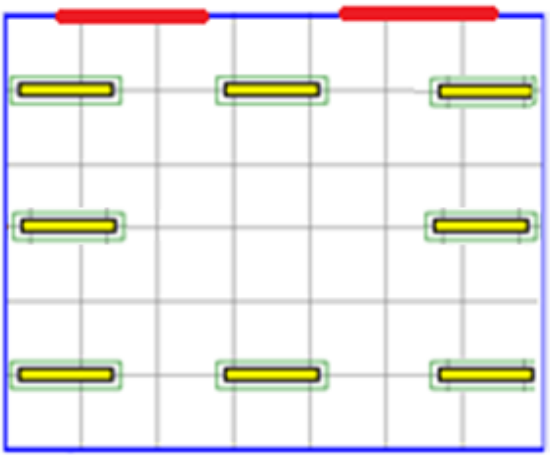

(b) 8 lights

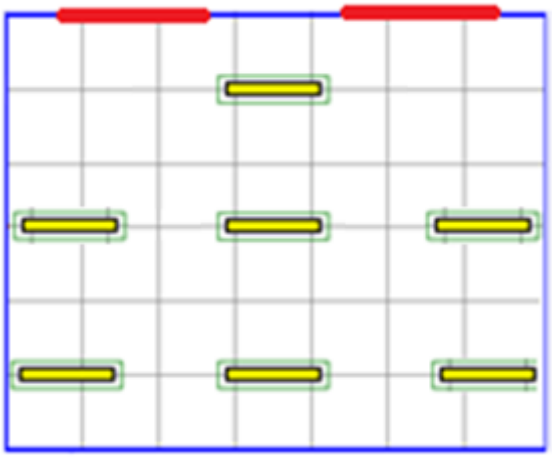

(c) 7 lights

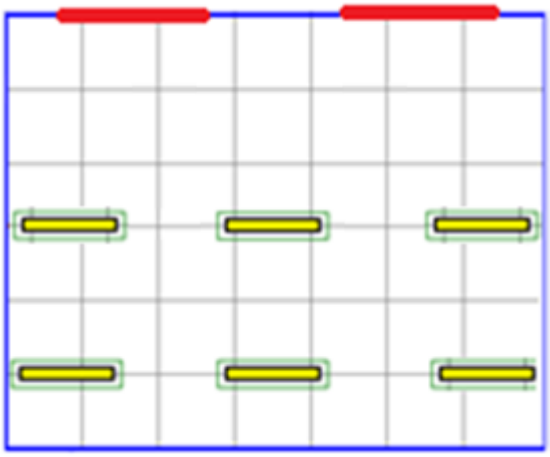

(d) 6 lights

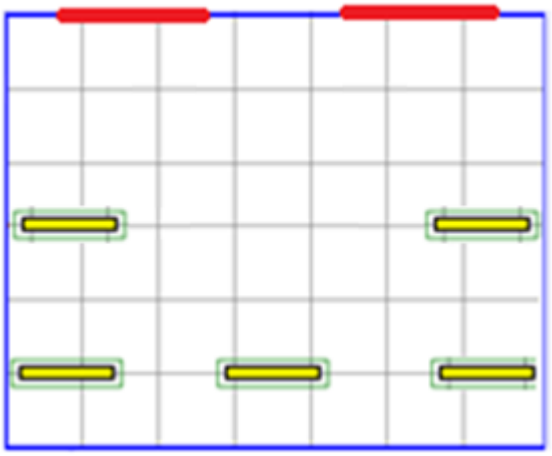

(e) 5 lights

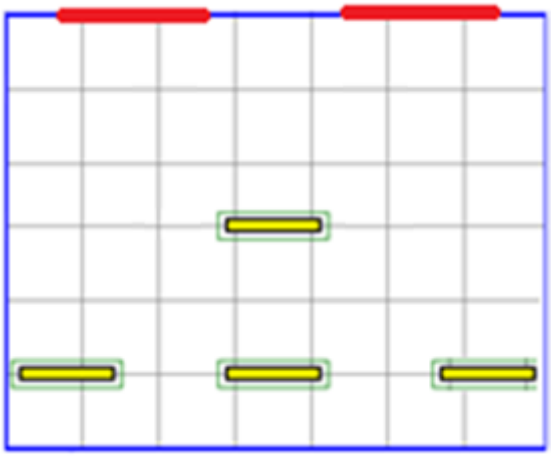

(f) 4 lights

(g) 3 lights (h) 2 lights

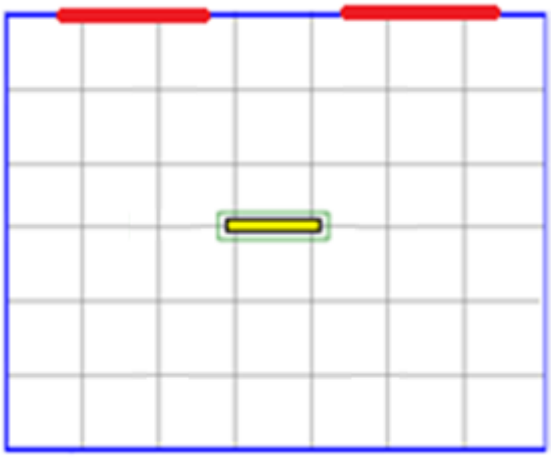

(i) 1 light

Fig. 4-7 Arrange method of lights

will reduce it one by one under the sunlight to observe the result.

There are obviously other ways to arrange the lights, but as a result of actually simulating a combination of various lights and windows arrangements, the above shows the arrangement of lights with the highest ratio of uniformity.

4-3 Evaluation of lighting environment

Based on the simulation conditions described in 4-1 and 4-2 in this research, I simulated the solar altitude in the model space for each of the four seasons. The results are shown in Fig. 4-8 and Table 4-2.

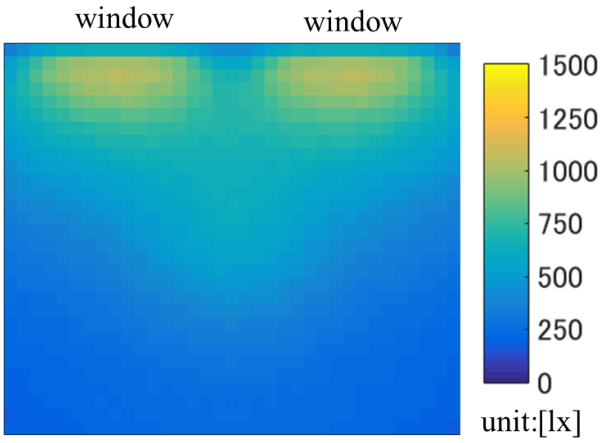

(a) 2 windows with 1 light

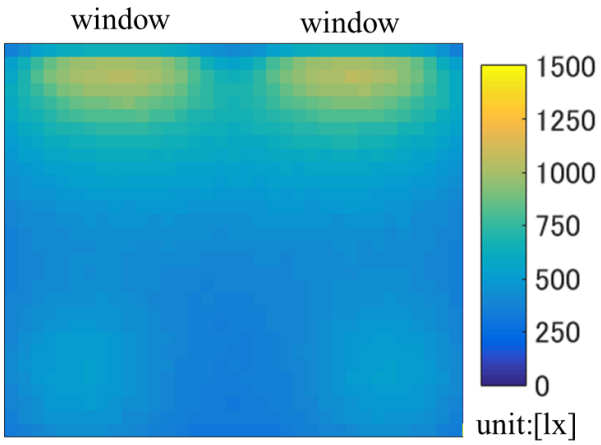

(b) 2 windows with 2 lights

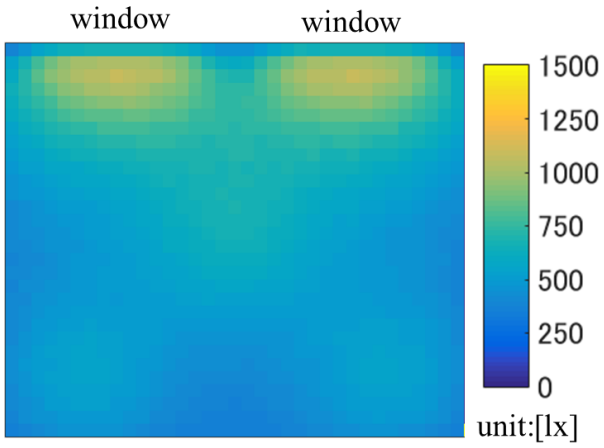

(c) 2 windows with 3 lights

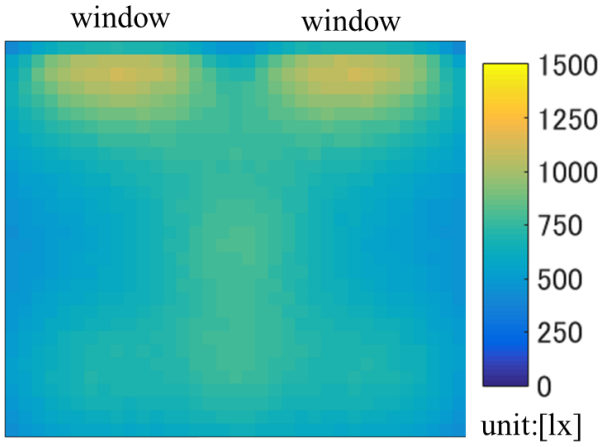

(d) 2 windows with 4 lights

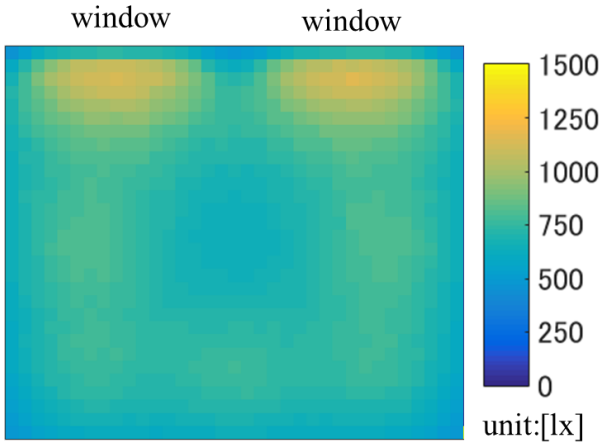

(e) 2 windows with 5 lights

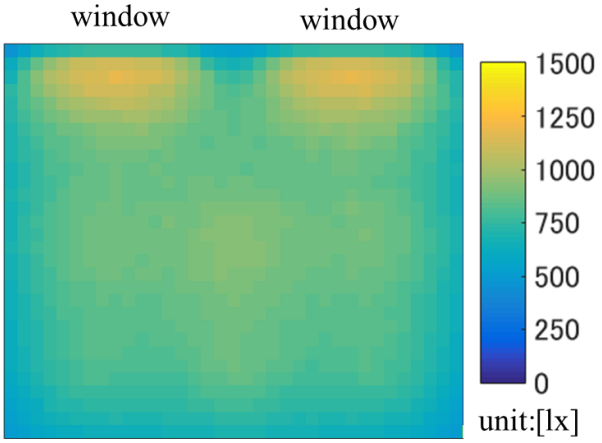

(f) 2 windows with 6 lights

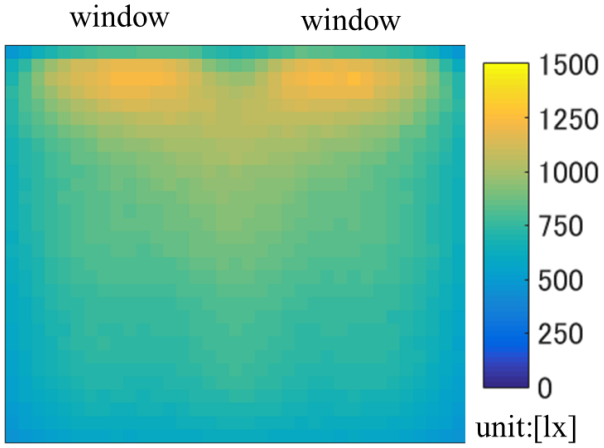

(g) 2 windows with 7 lights

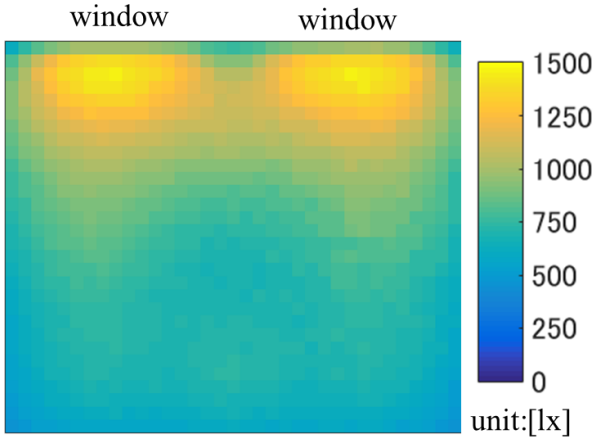

(h) 2 windows with 8 lights

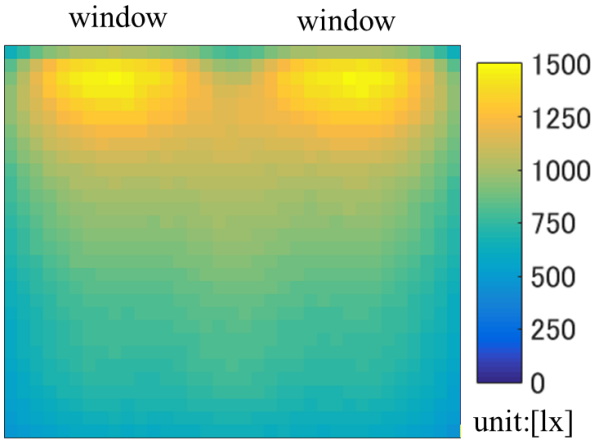

(i) 2 windows with 9 lights

Fig. 4-8 Simulation results (no direct light)

Table 4-2 Comparison of the results (no direct light)

Number of windows	Number of lights	Maximum illuminance [lx]	Minimum illuminance [lx]	Average illuminance [lx]	Uniformity
2	9	1495	590	947	0.62
2	8	1473	569	874	0.65
2	7	1242	566	842	0.67
2	6	1188	631	859	0.73
2	5	1154	612	772	0.79
2	4	1113	475	710	0.67
2	3	1088	370	599	0.62
2	2	1060	323	526	0.61
2	1	1065	199	492	0.41

Looking at the illuminance distribution diagram in Fig. 4-8, it was found that when the artificial lighting and day-lighting from the window (without direct light) are used at the same time, the lighting environment in the room becomes brighter and steadier as the number of lighting increases. It can also be observed that the brightness on the window side is the brightest. Furthermore, in order to make better comparison, the data in Table 4-2 is graphed into Fig. 4-9 (illuminance) and Fig. 4-10 (uniformity).

Fig. 4-9 shows that the maximum illuminance, the minimum illuminance, and the average illuminance decrease as the number of lighting fixtures decreases. Therefore, when decreasing the number of lights from 8 to 7, the maximum illuminance suddenly decreased, but the curve of minimum illuminance and average illuminance does not show this tendency. This is probably because under the conditions of 8 lights and 9 lights, the lighting fixture on the window side was turned on, so light reflected from the window side and other places increased the light intensity of the light directly under the lighting fixtures. In the case of 7 lights (Fig. 4-8 (g)), since the light on window side was not turn on, I believe that this factor contributed to the sudden decrease in maximum illuminance on the window side.

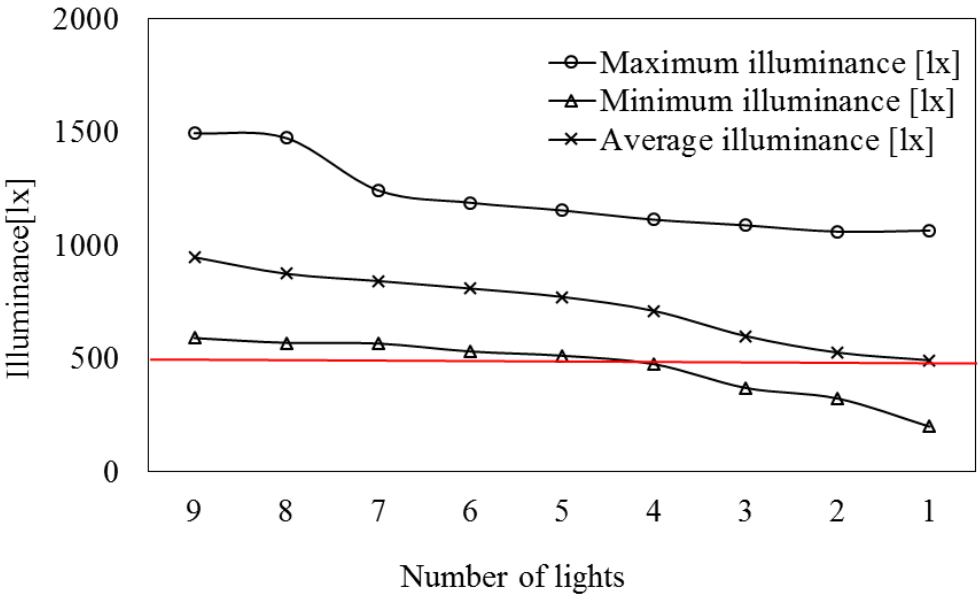

Fig. 4-9 Comparison of the results of illuminance (no direct light)

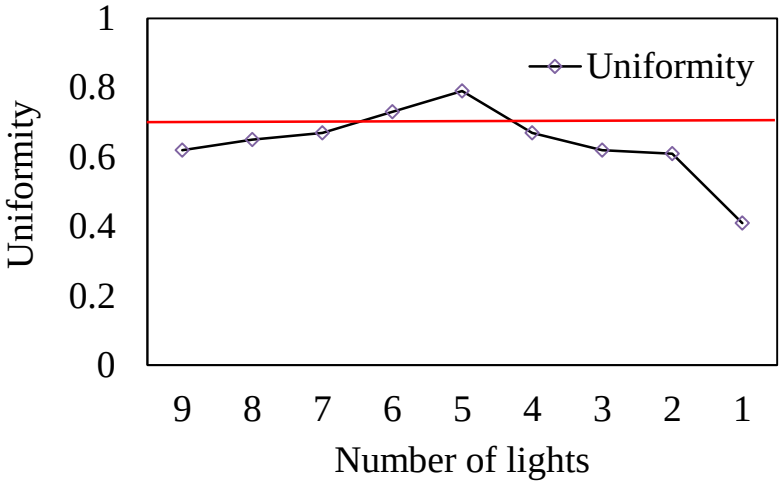

Fig. 4-10 Comparison of the results of uniformity (no direct light)

Also, looking at the curve of the minimum illuminance, in the case of 4 lights or less, the minimum illuminance is smaller than the illuminance standard 500 lx, so I think that it is necessary to have more than 4 lights in this room. Looking at the diagram of uniformity in Fig. 4-10, only the conditions of 5 lights and 6 lights obtained the lighting standard of more than 0.7. In the case of 9 lights, 8 lights and 7 lights, the illuminance was sufficient, but the uniformity of the whole room was lowered conversely. So, when lighting from the window, I think that it is necessary to attach an appropriate number of lighting equipment. If the number of lighting is insufficient, light for room lighting becomes insufficient, and if the number of lighting is too big, the uniformity of the whole room becomes low.

4-4 Consideration on power consumption

Here I will explain about the evaluation of amount of power consumption reduction of lighting. Before evaluating the power consumption of lighting fixtures, the environment of the experiment has to be decided. Generally, from the morning to the night in the office, lighting fixtures are used constantly during the operation time and in this case, 9 lights are arranged evenly on the ceiling, and the a lighting environment where no light enters through the window is set up. In other words, this is the lighting environment of a workplace in the night. The light fixtures were arranged as shown in Fig. 4-11. Fig. 4-12 shows simulation results when lighting fixtures are installed. The data is shown in Table 4-3. Here, the power consumption of one lighting fixture is 32 ×2 = 64 W.

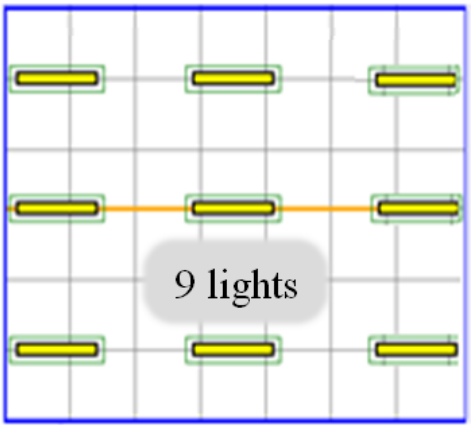

Fig. 4-11 Distribution diagram of lighting equipment (9 lights)

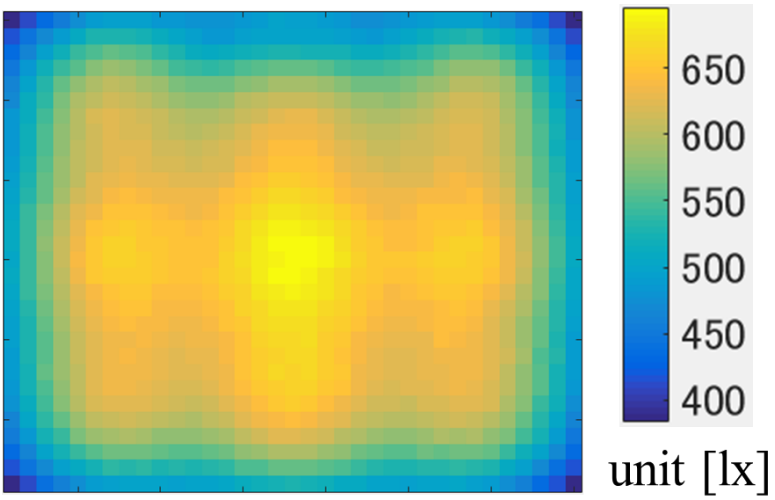

Fig. 4-12 Illuminance distribution chart (9 lights, no daylight)

Table 4-3 Comparison of the results (no direct light)

Number of windows	Number of lights	Maximum illuminance [lx]	Minimum illuminance [lx]	Average illuminance [lx]	Uniformity	Power consumption [W]
0	9	733	531	632	0.76	576
2	6	1188	631	859	0.73	384
2	5	1154	612	772	0.79	320

The data in the above table, the illuminance is over 500lx and the uniformity is more than 0.7 for all the tested conditions, so it meets the illuminance standards. Based on this, it is compared with the power consumption when light enters from the window (5 lights and 6 lights). In the case of six lamps, the power consumption can be reduced by (576-384) / 576 = 33%, and in the case of five lamps, the power consumption can be reduced by (576-320) / 576 = 33%.

As a result, in the absence of direct light, it is possible to reduce the power consumption by 33% or more by using an appropriate light in a lighting system comprised of windows and lighting fixtures.

References

[1] JAPANESE INDUSTRIAL STANDARD (JIS) - General rules of recommended lighting levels - JIS Z 9110: 2010 (in Japanese)

日本工業規格 照明基準総則 JIS Z 9110: 2010
[2] “Cooper is Brochure - Lighting Design Guide”, Eaton’s Cooper Lighting and Safety Business, pp.5-10 (2013)
[3] TAKETEK : “230 V Lighting Design Guide”, Printed in USA Doc.4859 3/07 S PECIFYING A L IGHTING S YSTEM, pp.74 (2011)
[4] Architectural Studies No.22: Editorial Board of Architectural Studies, Shokokusha Publishing Co., Ltd. (1969) (in Japanese)
建築学大系〈第 22〉室内環境計画, 彰国社 (1969)
[5] Hitachi Lighting-Lighting Characteristics - Lamps・Lighting Fixtures HNM4205V-MEU14-K, www.lighting.hitachi-ap.co.jp/lighting/ (in Japanese)
日立照明器具 照明特性 - ランプ・照明器具 HNM4205V-MEN14
www.lighting.hitachi-ap.co.jp/lighting/

Chapter 5

Evaluation of lighting environment for direct sunlight

For a bright sunny day, the direct incident sunlight from the window is too dazzling for one to use it without any reflector. By using a reflector, the sunlight from the window is reflected to the ceiling by reflectors at window and at the ceiling it will be diffused and spread to the room. Thus, the natural light can be used. In this chapter, we will discuss about the possibilities of decreasing power consumption for the model room while using the natural light on fine days for the whole year.

5-1 Simulation method

Before running simulation for all seasons, I would like to explain about the simulation conditions. As shown in Section 4-1, the illumination standard of this research is over 500 lx for the illuminance on the indoor work surface and the ratio of uniformity (minimum illuminance / average illuminance) is above 0.7. The preparing of simulation model of lighting equipment setup, etc. are all the same as the simulation in the previous chapter. Also, since the light source enters the room with dazzling sunlight from the window, it is necessary to attach blind-shaped reflectors to the window as shown in Fig. 5-1. Total sunlight entering through the window are

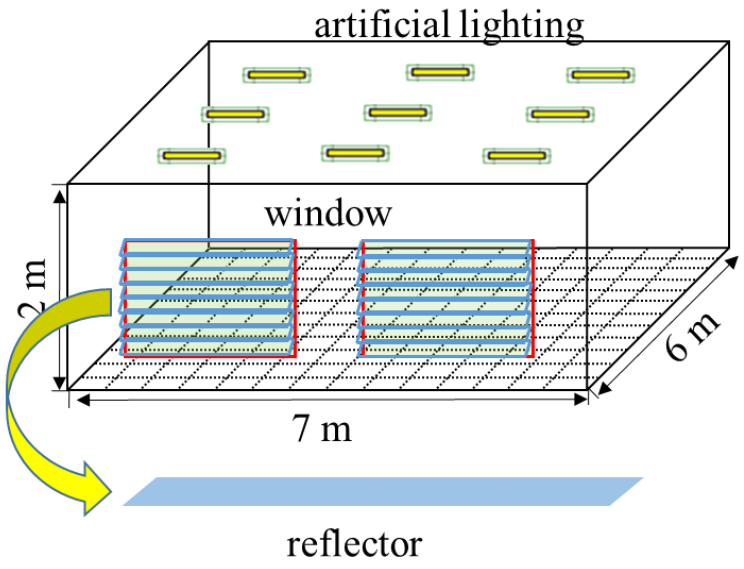

Fig. 5-1 Simulation Model for sunny day

reflected to the ceiling through the reflectors as shown in Fig. 5-2. Furthermore, in consideration of practicality, the number of blind reflection plates is set to 20 pieces as shown in Fig. 5-3, and the interval *d* between the slats is set to 0.07 m. A specific explanation of the reflector will be described later.

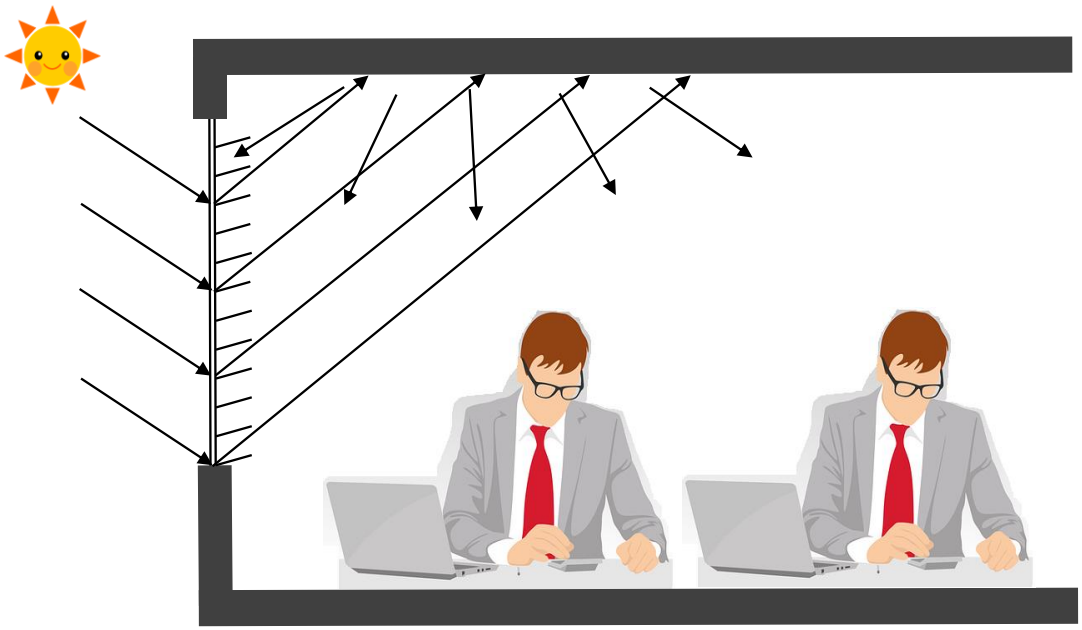

Fig. 5-2 Concept of using day light as illuminance system

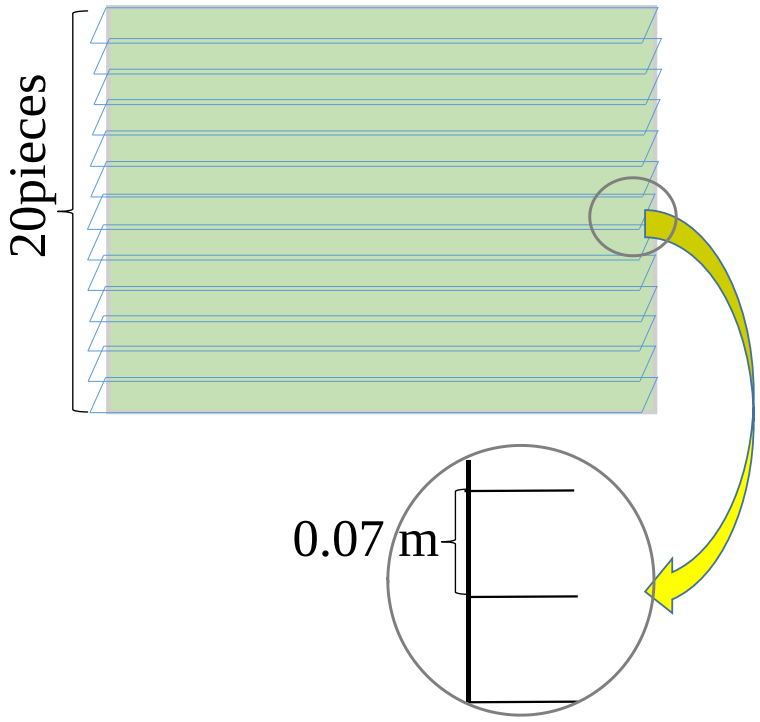

Fig. 5-3 Diagram of reflectors

5-2 Conditions for sunlight

1：Angle of sunlight

Since the earth revolves around 23.5 ° from the direction perpendicular with respect to the revolution plane, the azimuth of the sun changes throughout the cycle of 1 year [1]. The earth revolves the sun at almost the same place on the same day of every year. It means that summer and winter happens on almost the same day in each year. This concept also applies on the temperature which is high or low on roughly the same day of every year. As shown in Fig. 5-4, in the summer of Akita, the solar elevation angle is the highest is about 75° (12 o'clock) in height, and it is about 50° (12 o'clock) in the spring and autumnal. The solar elevation angle at the winter becomes the lowest, which is about 30 °(12 o'clock) [2, 3]. Also, the azimuth of the sun changes with seasons and time.

The angle of sunlight used in this simulation is the sun angle at Akita University. The longitude of Akita University is 39.7 °and the latitude is 140.1 °. Changes in solar elevation angle and solar azimuth angle which is based on the season and time zone of Akita University were calculated from this position information. In this research, daylight was used from 9 am to 3 pm in order to avoid problems such as glowing sunset. The average solar elevation angle and solar azimuth angle used in the simulation are summarized in Table 5-1 [4].

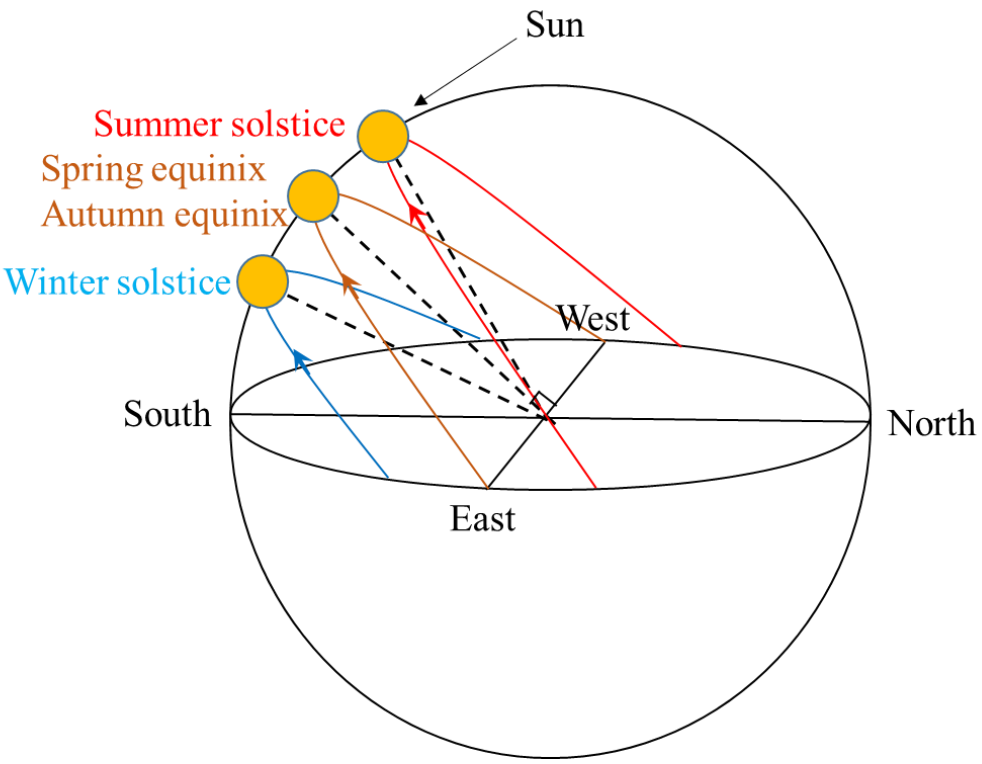

Fig. 5-4 Changes in sun altitude and azimuth angle of the day

2：Sunlight flux

The amount of sunlight flux used in this study is based on actual measurement. The intensity of sunlight coming from the window not only relates to the time zone but also to the air humidity and the thickness of the cloud. Based on the measured results, it was found that the change in daylight illuminance is large not only on cloudy days but also on sunny days. In order to reduce variations in actual measurement values used for simulation, it is necessary to average measured data. In addition, in order to prepare a simulator that can be used for all seasons, this research measured the average value of the illuminance on 10 clear days before and after the summer, the winter and the autumn day. Table 5-2 summarizes the averaged measured data.

Table 5-1 Solar angle with time for Akita University

season / time	summer		winter		spring・autumn	
	altitude angle	azimuth angle	altitude angle	azimuth angle	altitude angle	azimuth angle
9:00～10:00	55 °	110 °	20 °	150 °	40 °	130 °
10:00～11:00	65 °	130 °	25 °	160 °	45 °	150 °
11:00～12:00	75 °	170 °	30 °	180 °	50 °	170 °
12:00～13:00	70 °	230 °	25 °	190 °	50 °	200 °
13:00～14:00	60 °	240 °	20 °	210 °	40 °	220 °
14:00～15:00	50 °	260 °	15 °	220 °	35 °	230 °

Table 5-2 Solar luminous flux through a window [lx]

season / time	summer	winter	spring・autumn
9:00～10:00	26151.8	69287.7	41826.0
10:00～11:00	38186.5	73352.5	63046.7
11:00～12:00	48025.9	75656.0	75198.0
12:00～13:00	42579.9	92249.0	71753.1
13:00～14:00	36777.2	86609.6	55768.0
14:00～15:00	15911.3	83251.7	50122.6

5-3 Consideration on reflector

The solar angle varies depending on the season and time zone. Based on this information, it is obvious that the angle of light entering indoors from the window also changes, and thereby affecting the indoor lighting environment as well. The angle and the illumination environment may vary greatly depending on change in angle and type of the blind reflectors.
In order to efficiently reduce the power consumption of indoor lighting fixtures by daylighting from the window, it is necessary to know how the change in solar position affects the change of the indoor environment. In order to produce a comfortable lighting environment for all conditions, it is necessary to consider the width of the blind reflector and the slat angle. As part of this preparation, the width of the blind reflector and the slat angle is obtained by calculation in order to confirm the characteristics of the material of the reflector.

1：Material of reflector

For the reflective materials required for this research, it is necessary for them to be able to efficiently reflect light and maintain high performance under high temperature and high luminous flux, thereby making it possible to utilize a high utilization ratio of sunlight. Many companies are currently developing and producing this optical reflective silicone material. By referring to those product characteristics, the front of the reflector for this simulation is set as a mirror, and the incident daylight is reflected to the ceiling with 90% specular reflection and the remaining light is absorbed[5,6]. 90% of the light is absorbed on the back surface of the blind reflector, and the remaining light is set as diffuse reflection. (Fig. 5-5)

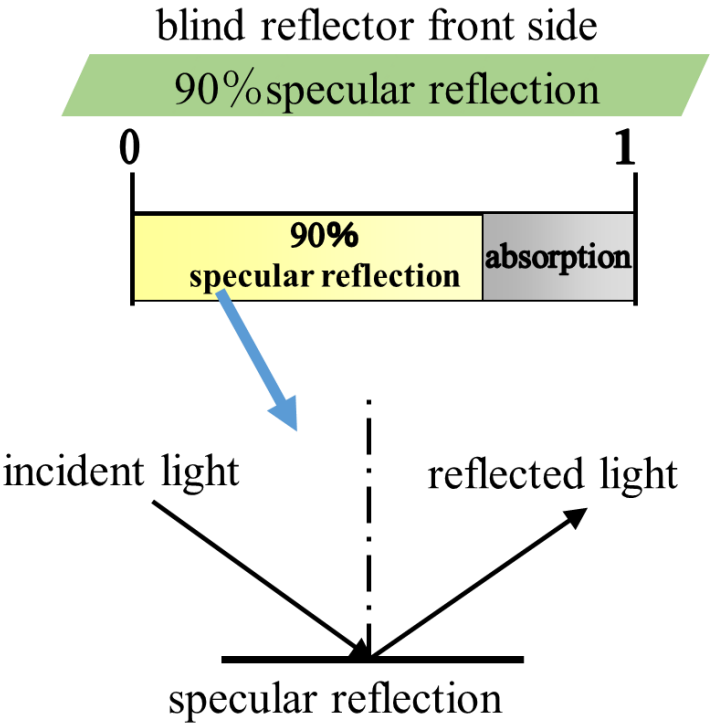

(a) Front side

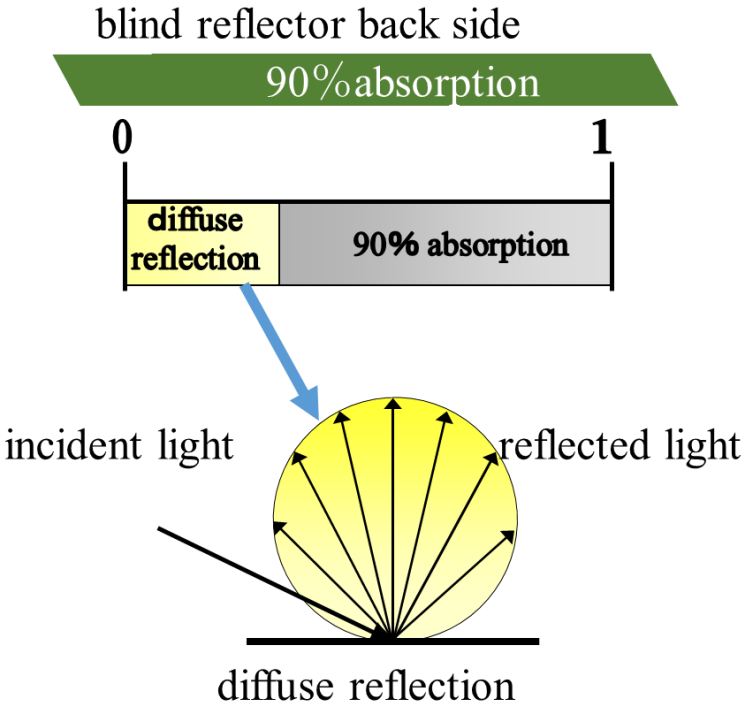

(b) Back side

Fig. 5-5 Determination of reflection and absorption

2：Reflector angle

As described in Fig. 5-1~ Fig. 5-3, incident daylight is taken into the room by a lighting system using blind reflectors whereby its type and angle can be changed. In this research, in order to improve the performance and practicality of the system, incident light is reflected on the ceiling as much as possible. For this reason, the angle of the blind reflector is determined.

As shown in Fig. 5-6, the reflectors are controlled by changing the angle about the innermost side of the reflector. The angle of the reflection plate is 0° when it is perpendicular to the window, position when turned upwards, and negative when turned downwards. In this simulation, the angle of the reflector where daylight hardly enters from the window is a_{MAX} with the maximum angle as shown in Fig. 5-7 (a). Beyond this angle, the sunlight entering the room will be reflected outside the window. As shown in Fig. 5-7 (c), let the minimum angle a_{MIN} be the angle at which the light illuminates the deepest part of the ceiling. When the angle is less than this, indoor work is affected because light is reflected on the inner side wall of the room. Also, in order to create a comfortable lighting environment in the room, incident sunlight as shown in Fig. 5-7 (b) can be reflected to the center of the ceiling. At that time, the angle of the blind reflector is a_{MID}.

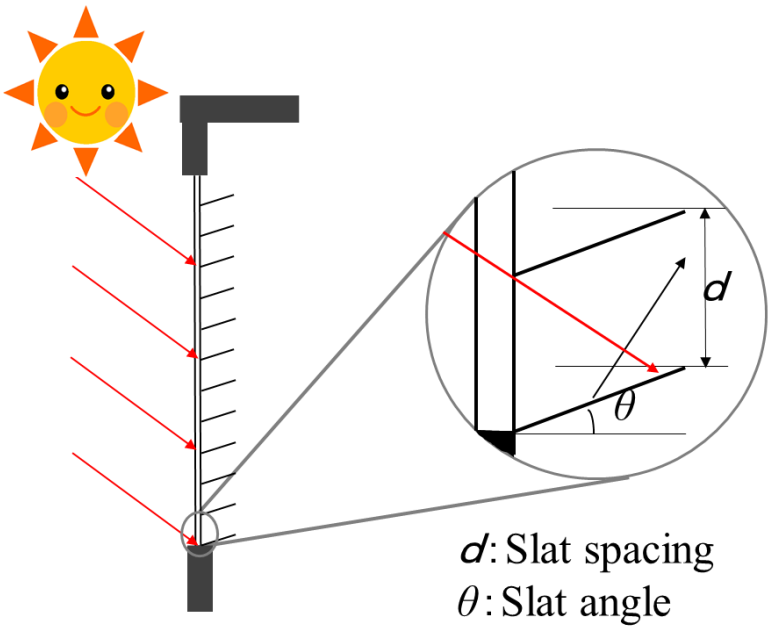

Fig. 5-6 Determination of reflector angle

As shown in Fig. 5-7, if the size of the room is known immediately and the angle of incidence sunlight to the reflector is α, the angles $a_{MAX}, a_{MIN}, a_{MID}$ of the reflector can be obtained by the following equations.

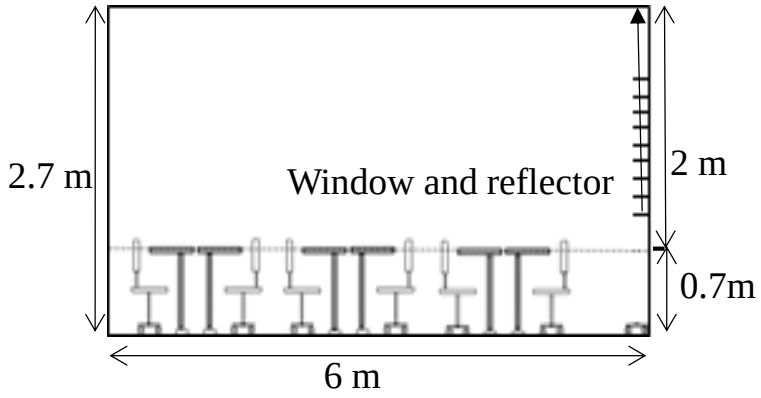

(a) Maximum angle of reflectors

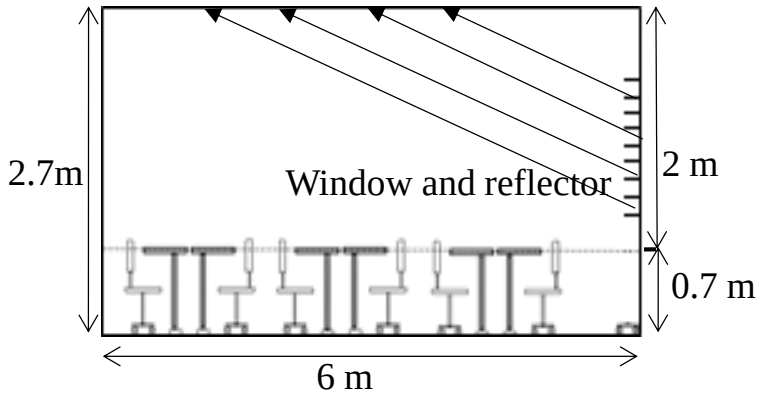

(b) Suitable angle for reflectors to reach the middle of the ceiling

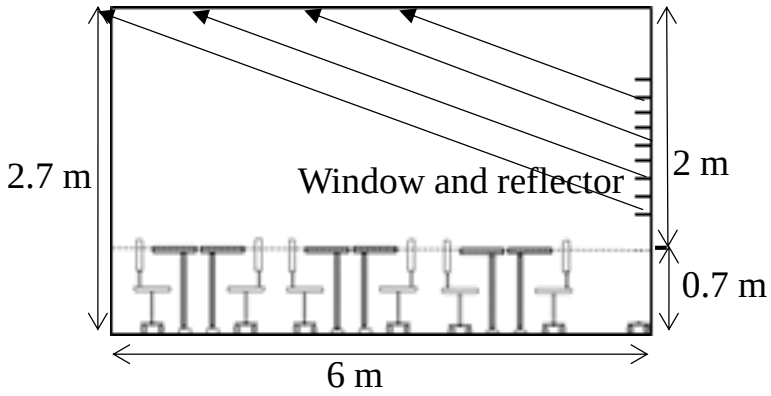

(c) Minimum angle of reflectors

Fig. 5-7 Various reflected light path with different types of reflector's angles

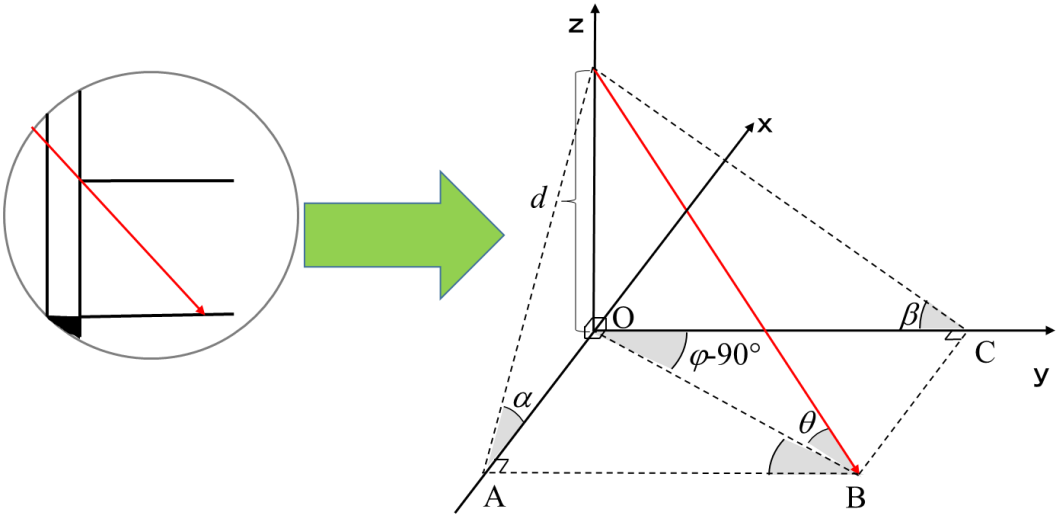

Fig. 5-8 Geometric relationship between sun angle and reflectors

$$a_{\mathrm{MAX}} = \frac{90-\alpha}{2} \quad [^\circ] \tag{5-1}$$

$$a_{MID} = \frac{tan^{-1}\frac{1}{3}-\alpha}{2} \quad [^\circ] \tag{5-2}$$

$$a_{\mathrm{MIN}} = \frac{tan^{-1}\frac{1.7}{6}-\alpha}{2} \quad [^\circ] \tag{5-3}$$

As shown in the bottom left part of Fig. 5-8, sunlight enters through the gap of the reflector and reflects on the reflector. This is converted to the right 3D coordinate system. At here,

θ : Solar elevation angle

φ : Solar azimuth angle

↑ : Sunlight

α : Projection of x-axis of the sun angle

β : Projection of y-axis of sun angle

a : Rotation angle of reflector

d : Spacing between reflectors

In this coordinate system, the distance between the reflectors is 0.07 m, and the sun angle is obtained from Table 5-1. Thus, OB is obtained by the following equation.

$$OB = \frac{d}{tan\theta} \tag{5-4}$$

OA can also be obtained from equation (5-4)

$$OA = OB \times \sin(\varphi\text{-}90°) = \frac{d \times \sin(\varphi\text{-}90°)}{tan\theta} \tag{5-5}$$

Also, α and OA have the following relationship.

$$\tan\alpha = \frac{d}{OA} \tag{5-6}$$

By simultaneous equations (5-5) and (5-6), projection α of the sun angle x-axis can be obtained by equation (5-7).

$$\alpha = \tan^{-1}\frac{tan\theta}{sin(\varphi\text{-}90°)} \tag{5-7}$$

Likewise, the projection β of the y-axis can be obtained in the same way. However, since $\tan^{-1}$ varies between -90 °and 90 °, β can be obtained in different ranges of Eq. (5-8) and Eq. (5-9).

$$\beta = \tan^{-1}\frac{tan\theta}{cos(\varphi\text{-}90°)} \quad (\varphi < 180°) \tag{5-8}$$

$$\beta = \pi + \tan^{-1}\frac{tan\theta}{cos\varphi} \quad (\varphi >= 180°) \tag{5-9}$$

By substituting the equation (5-7) into the equations (5-1), (5-2) and (5-3), angles a_{MAX}, a_{MIN}, a_{MID} of the reflector are obtained by Table 5-3. Here, the values of θ and φ are the same values shown in Table 5-3.

Table 5-3 Maximum angle and minimum angle of the reflectors

season / time	summer			winter			spring・autumn		
	θ_{MAX}	θ_{MID}	θ_{MIN}	θ_{MAX}	θ_{MID}	θ_{MIN}	θ_{MAX}	θ_{MID}	θ_{MIN}
9:00～10:00	6.7°	-29.1°	-30.4°	33.6°	-2.2°	-3.5°	18.7°	-17.1°	-18.4°
10:00～11:00	8.3°	-27.4°	-28.7°	31.8°	-4.0°	-5.2°	20.4°	-15.3°	-16.6°
11:00～12:00	7.4°	-28.4°	-29.7°	30.0°	-5.8°	-7.1°	19.8°	-16.0°	-17.3°
12:00～13:00	6.6°	-29.2°	-30.5°	32.3°	-3.5°	-4.8°	19.1°	-16.7°	-18.0°
13:00～14:00	8.1°	-27.7°	-29.0°	33.6°	-2.2°	-3.5°	18.7°	-17.0°	-18.4°
14:00～15:00	4.1°	-31.6°	-32.9°	35.4°	-0.4°	-1.7°	21.3°	-14.5°	-15.8°

3：Width of reflector

In determining the illuminance inside the room, one has to take account of the angle of the blind reflector and the width of the reflector. In determining the width of the blind reflector plate, reflection of the incident light in the indoor environment, incident daylight reflected by blind must not affect the other blinds. Therefore, it is considered that there is a limit value for the width of the blind, and its limit value can be obtained from the geometrical relationship between solar evolution angle and blind.

Considering a daylighting system with a blind reflector attached as shown in Fig. 5-9 (a), α is obtained from the equation (5-7) by the projection of the x-axis of the sun angle. At that time, the sunlight passes through the gap between the reflecting plates *a* and *b*. Let us now consider a

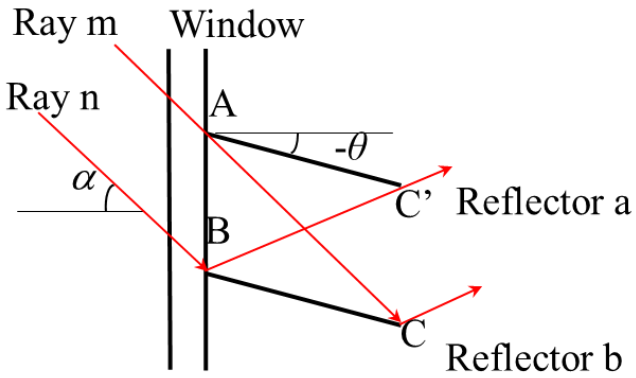

(a) Side view of a reflector's structure

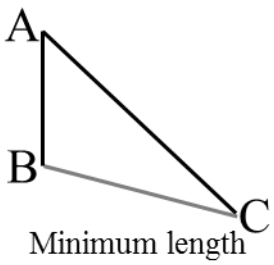

(b) The shortest length of reflector

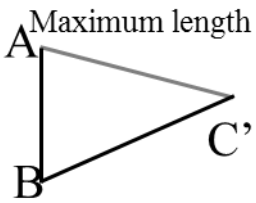

(c) The longest length of reflector

Fig. 5-9 Calculation of limit value of reflector

situation where the light beam m is reflected by the point C of the reflector *b* and reaches the ceiling. The minimum limit value of the blind width at this time is the length of the side BC. When the width becomes shorter than the length of the side BC, dazzling daylight passes through the gap of the reflector plate and it is considered to directly illuminate the workplace. Ray *n* is reflected at point B of reflector *b* and reaches the ceiling. If the width of the reflector *a* is too long, it will interfere with the reflected ray of ray n. In this figure, the maximum length of the reflector is AC'. When the blind width is longer than the side AC', reflected light reaching the ceiling is blocked, and the amount of daylight flux for illumination is reduced in the room. Therefore, in this paper we examined the width of the blind reflector.

Fig. 5-7(b) shows the ideal optical path in the daylight passing through the window. The incident ray from the window changes according to the time zone and the season, but the angle of the reflector is adjusted so that the direction of the reflected light always illuminates the center of the ceiling. The reflected light ray is indicated by the side BC' in Fig. 5-9, so ∠ABC' is set to be constant. The value can be calculated from trigonometric functions from the office model in Fig. 5-7(b), indicated by ∠ABC' in equation (5-9), which is 71.5 °.

$$\left.\begin{aligned} \angle \mathrm{A} &= 90^\circ + a_{MID} \\ \angle \mathrm{B} &= 71.5^\circ \\ \mathrm{AB} &= 7\mathrm{cm} \end{aligned}\right\} \tag{5-9}$$

$$\left.\begin{aligned} \angle \mathrm{A} &= 90^\circ - \alpha \\ \angle \mathrm{B} &= 90^\circ - a_{MID} \\ \mathrm{AB} &= 7\mathrm{cm} \end{aligned}\right\} \tag{5-10}$$

In order to obtain the limit length of the blind reflector width, ΔABC and Δ ABC' were taken from Fig. 5-9 (a). As shown in Fig. 5-9 (b), the BC side is the shortest length of the reflector width, and from the conditional formula (5-9), BC is obtained by the sine theorem. As shown in Fig. 5-9 (c), the AC' side is the maximum length of the width, and BC is obtained by the sine theorem from the conditional expression (5-10). Here a_{MID} is the angle of the blind reflector and α is the projection of the x axis of the sun angle.

The data about the limit of the reflector width is summarized in Table 5-4.

Table 5-4 Limit values of reflectors' width

season / time	summer		winter		spring・autumn	
	Maximum width [m]	Minimum width [m]	Maximum width [m]	Minimum width [m]	Maximum width [m]	Minimum width [m]
9:00～10:00	0.0900	0.0221	0.1879	0.1833	0.1142	0.0733
10:00～11:00	0.0924	0.0280	0.1736	0.1645	0.1192	0.0824
11:00～12:00	0.0909	0.0245	0.1614	0.1478	0.1172	0.0789
12:00～13:00	0.0897	0.0216	0.1776	0.1697	0.1153	0.0754
13:00～14:00	0.0919	0.02691	0.1879	0.1833	0.1142	0.0733
14:00～15:00	0.0865	0.0132	0.2047	0.20446	0.1219	0.0871

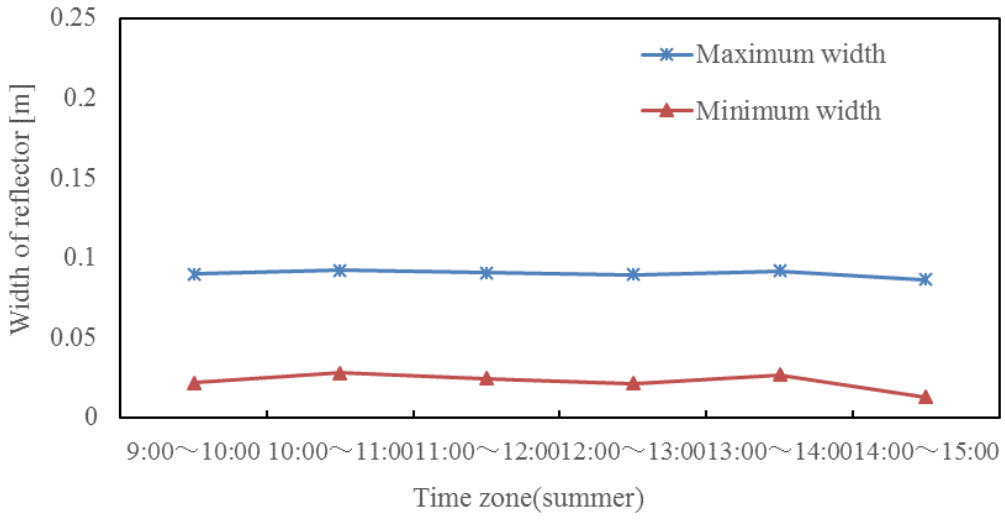

(a) Reflectors' width (for summer)

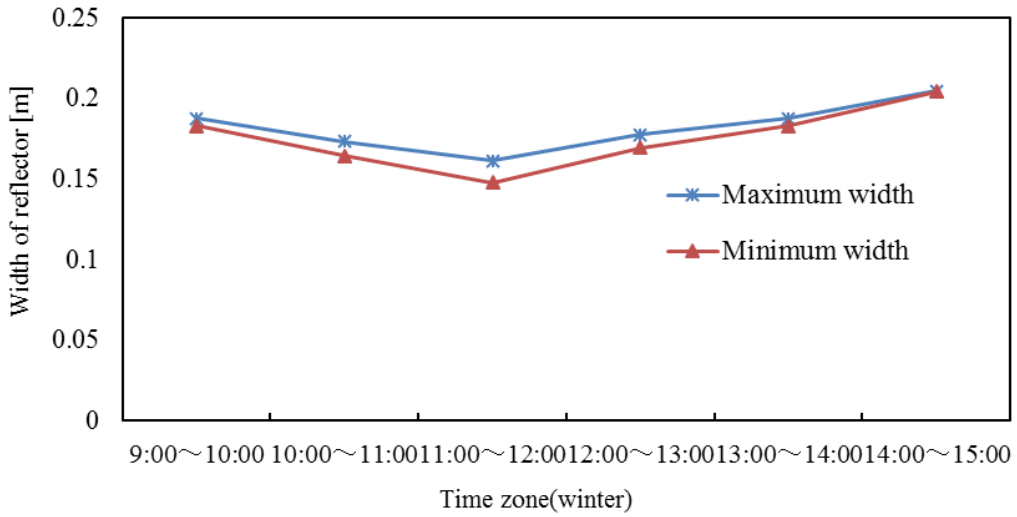

(b) Reflectors' width (for winter)

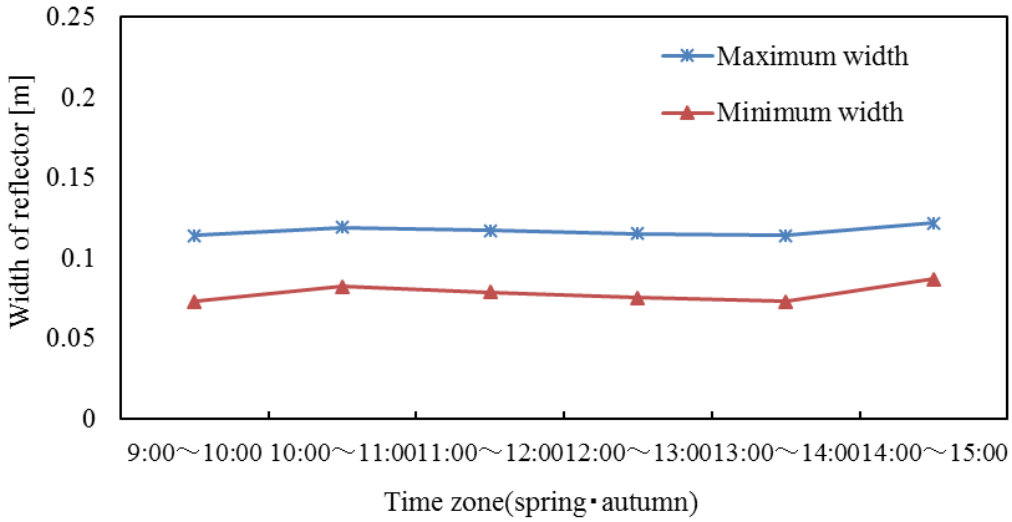

(c) Reflectors' width (for spring・autumn)

Fig. 5-10 Limit values of reflectors' width

Because it is hard to see relationship of the data in Table 5-4, the data is shown in Fig. 5-10. The blue line is the maximum width, light entering the room above this value is partially blocked. The red line is the shortest width, and when it becomes shorter, it illuminates the work surface. To improve practicality, see Fig. 5-10, it can be seen that when the width of the reflector is set to 10 cm, and can be applied to most part of the spring, summer and autumn. In the winter, based on the data in Table 5-3, the amount of daylight incident from the window of winter is larger than the other seasons. Enough lighting is obtained even if the sunlight is partially blocked, thus the width of the reflector in the winter is set to 20 cm.

4：Length of reflector

In the case of fine day, sunlight in the morning and evening is oblique and illuminates reflectors. If the length of the reflector is set to be the same as the window's length, dazzling sunlight entering the window at an oblique angle will illuminate the work surface through the gap between the reflectors. To avoid this, the length of the reflector used in this research is set to be longer than the length of the window as shown in Fig. 5-11. Here, the shortest length of the reflector in the 3D coordinate system of Fig. 5-8 was calculated by the formula (5-11). The values are summarized in Table 5-5.

$$OC = OB \times \cos(\varphi\text{-}90°) = \frac{d \times \cos(\varphi\text{-}90°)}{\tan\theta} \qquad (5-11)$$

Looking at the results in Table 5-5, the length of the reflector is required to be 2.75 m or longer in the summer, spring and autumn so that all the incident light is reflected to the ceiling, and in the winter it is necessary for the length to be more than 2.94 m . Based on the results, the length of the reflector is set to 2.75 m in the summer, spring and autumn, and 2.95 m in the winter.

5：Setting of reflector condition

Based on the above calculations, the dimensions of the reflector are set as shown below during the actual simulation.

- Number of reflector plates: 20 (each window)
- Spacing between reflectors: 7 cm
- Reflector plate length: 2.75 m in summer, spring, autumn, 2.95 m in winter.
- Width of reflector: 0.1 m in summer, spring, autumn, 0.2 m in winter.
- Reflector angle: θ_{MID} (See Table 5-3.)

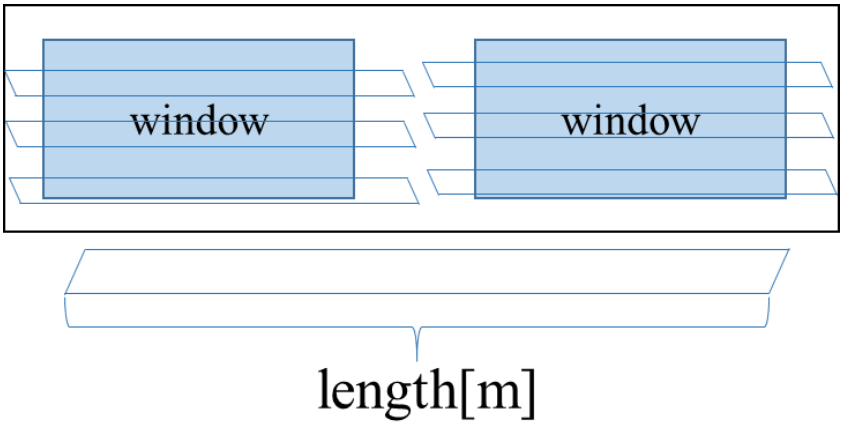

Fig. 5-11 Setting of reflectors (length)

Table 5-5 The shortest length of the reflector

season / time	summer	winter	spring・autumn
9:00～10:00	2.69 m	2.79 m	2.73 m
10:00～11:00	2.65 m	2.70 m	2.67 m
11:00～12:00	2.61 m	2.60 m	2.62 m
12:00～13:00	2.64 m	2.65 m	2.64 m
13:00～14:00	2.67 m	2.79 m	2.69 m
14:00～15:00	2.72 m	2.94 m	2.75 m

5-4 Evaluation of use of lighting in all seasons

By applying the conditions summarized in section 5-2 to the created illuminance distribution simulator, in the office model space shown in Fig. 5-1, the angle of the reflector that is attached to the front of the window is θ_{MID} changes according to the change in the solar angle and reflect incident sunlight to the ceiling. As a result, we examined the change in the illuminance of the observation surface.

1：Evaluation of daylighting utilization on summer

The simulated illuminance distribution in the summer is shown in Fig. 5-12(a~f).

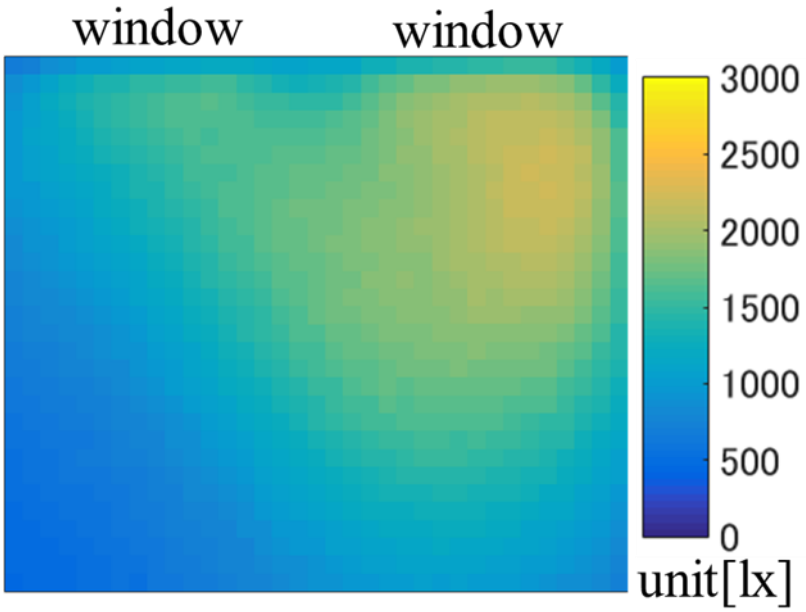

(a) 9:00～10:00 (solar altitude angle 55°, solar azimuth angle 110°)

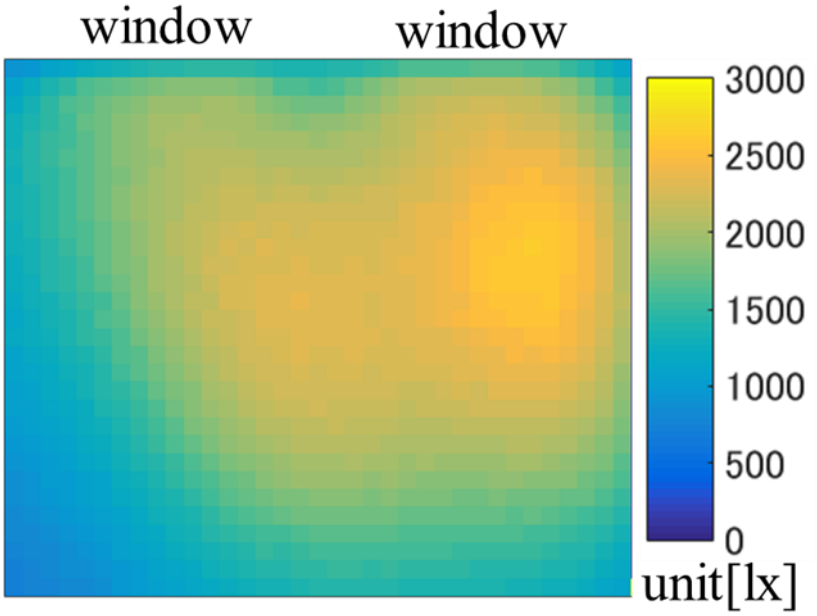

(b) 10:00～11:00 (solar altitude angle 65°, solar azimuth angle 130°)

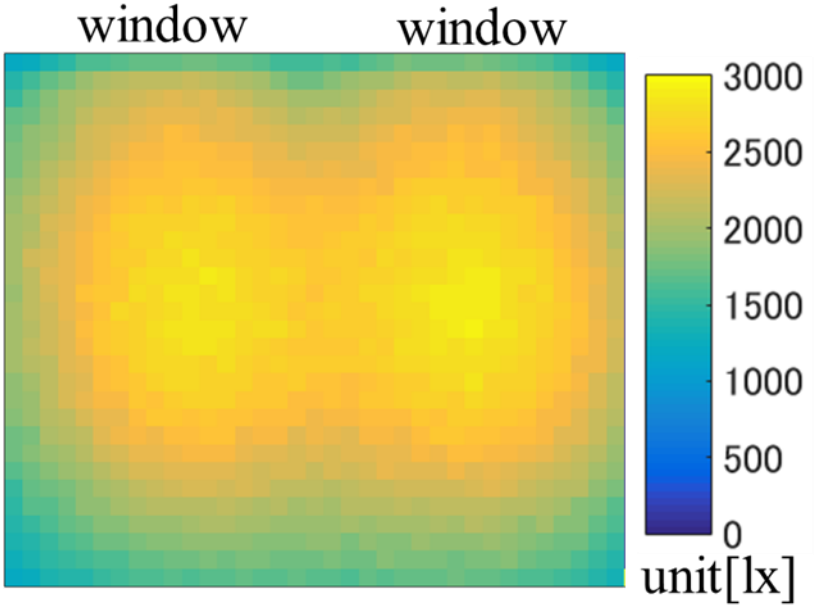

(c) 11:00～12:00 (solar altitude angle 75°, solar azimuth angle 170°)

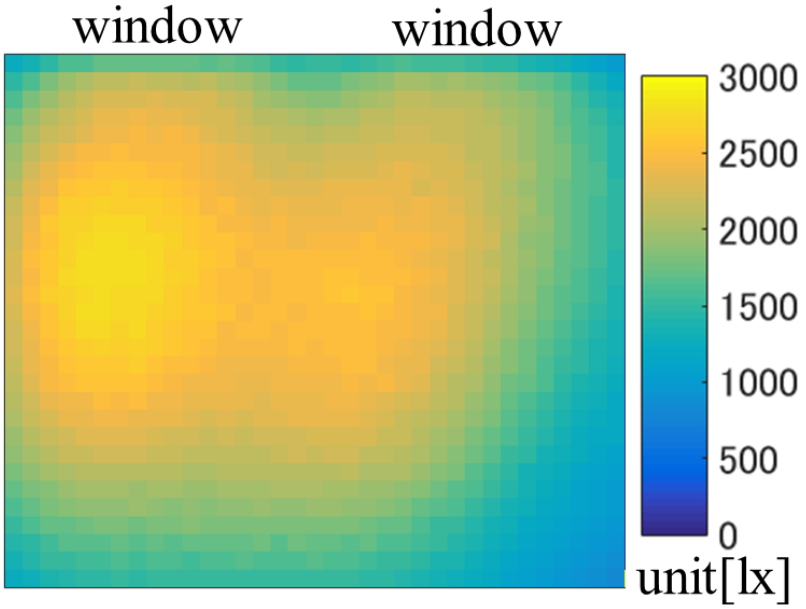

(d) 12:00～13:00 (solar altitude angle 70°, solar azimuth angle 230°)

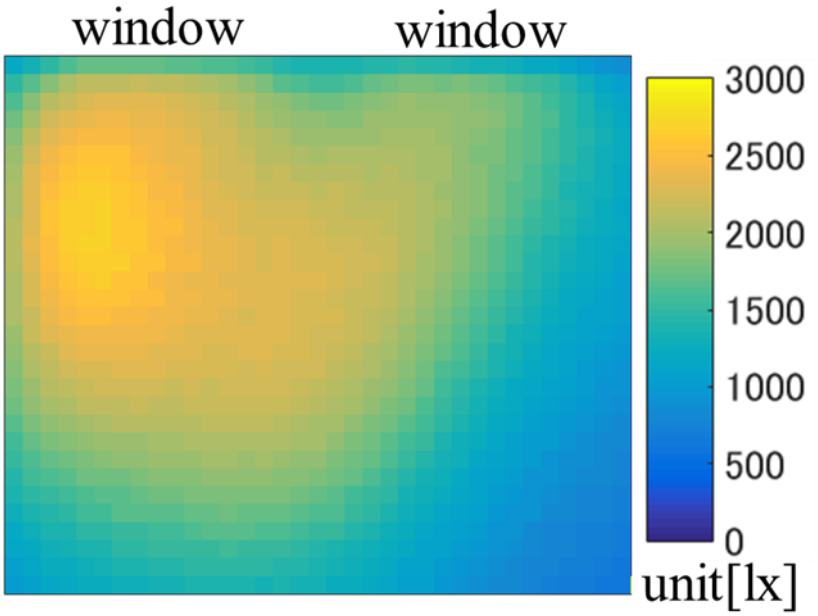

(e) 13:00～14:00 (solar altitude angle 60°, solar azimuth angle 240°)

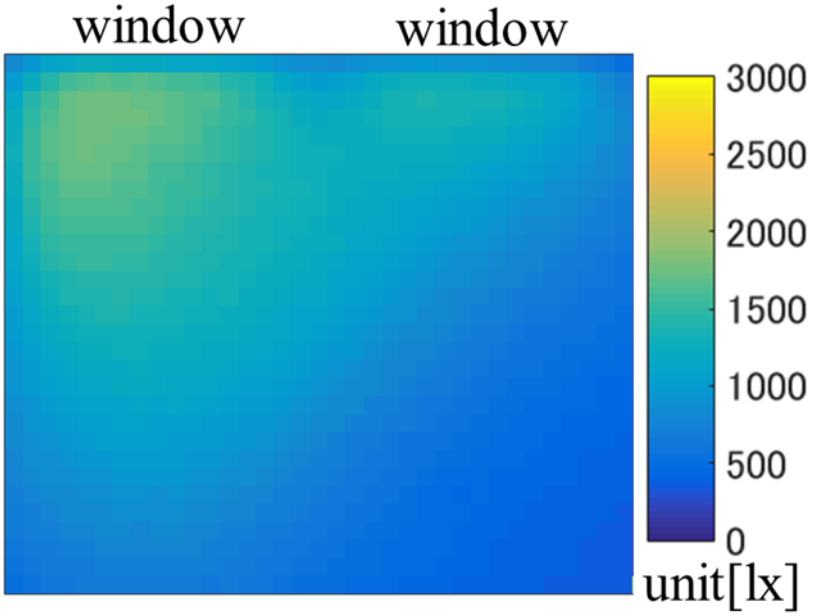

(f) 14:00～15:00 (solar altitude angle 50°, solar azimuth angle 260°)

Fig. 5-12 Illuminance distribution for summer

Observing at the illuminance distribution chart in Fig. 5-13, the center of the light entering the room moves from the west to the east (from the left to the right) as time changes from 9:00 to 15:00. It was also observed that lighting is the best between 11:00 and 12:00. The light at this time seems to be the brightest and most even. To make a more detailed comparison, the numerical results are summarized in Table 5-6, and the results of the graph are shown in Fig. 5-13.

Table 5-6 Simulation results for summer

Results / Time zone	Maximum illuminance[lx]	Minimum illuminance[lx]	Average illuminance[lx]	Uniformity
9:00～10:00	2214.3	644.2	1556.2	0.41
10:00～11:00	2627.4	1118.1	2127.6	0.53
11:00～12:00	2916.6	2084.1	2591.1	0.80
12:00～13:00	2811.9	1357.6	2337.8	0.58
13:00～14:00	2686.1	932.6	2040.7	0.46
14:00～15:00	1728.6	431.6	1099.4	0.39

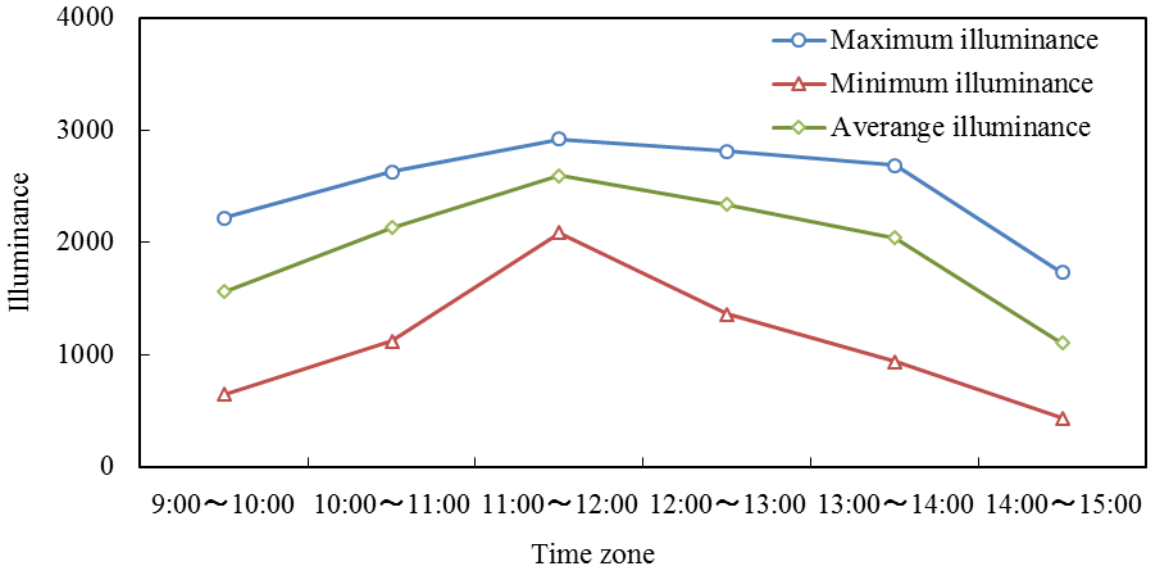

(a)Results of illuminance

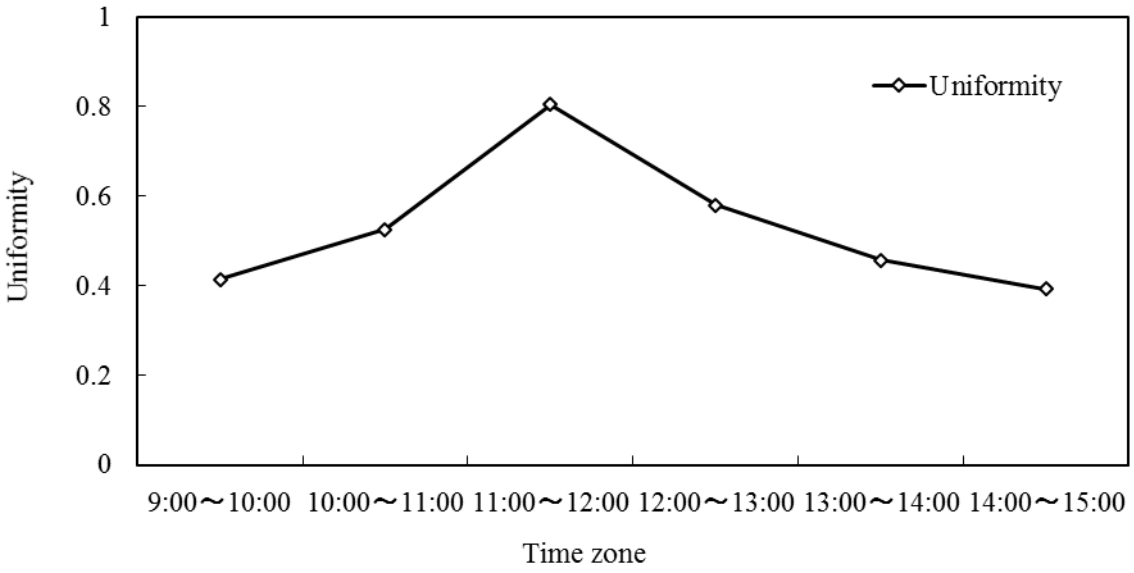

(b) Results of uniformity

Fig. 5-13 Simulation results for summer

The result of illuminance in Fig. 5-13 (a), the maximum illuminance, the minimum illuminance, and the average illuminance gradually became brighter from 9:00 and peaked at the time zone from 11:00 to 12:00, and after 12:00, it reduced gradually. And all of illuminance in any time zone met the lighting standard that is above 500 lx. Also, looking at the result of the uniformity, the ratio of uniformity also rises steadily from 9:00, which is the same as the illuminance, which peaks in the time zone from 11:00 to 12:00, and gradually reduces after 12:00. Also, when looking at the numerical values, the ratio of uniformity for the time periods other than 11:00 to

12:00 were lower than 0.7. In order to satisfy the illuminance criterion, it is necessary to increase the ratio of uniformity of the work surface by using suitable light conditions.

In order to use appropriate light, with reference to the illuminance distribution chart shown in Fig. 5-12, a light source was attached from a place with low lighting and simulated with various lighting fixture arrangement patterns. The best result of each time zone and the lighting fixture placement pattern at that time are shown separately in ①~⑥ below. (Fig. 5-14~ Fig. 5-19)

① 9:00～10:00 (solar altitude angle 55°, solar azimuth angle 110°)

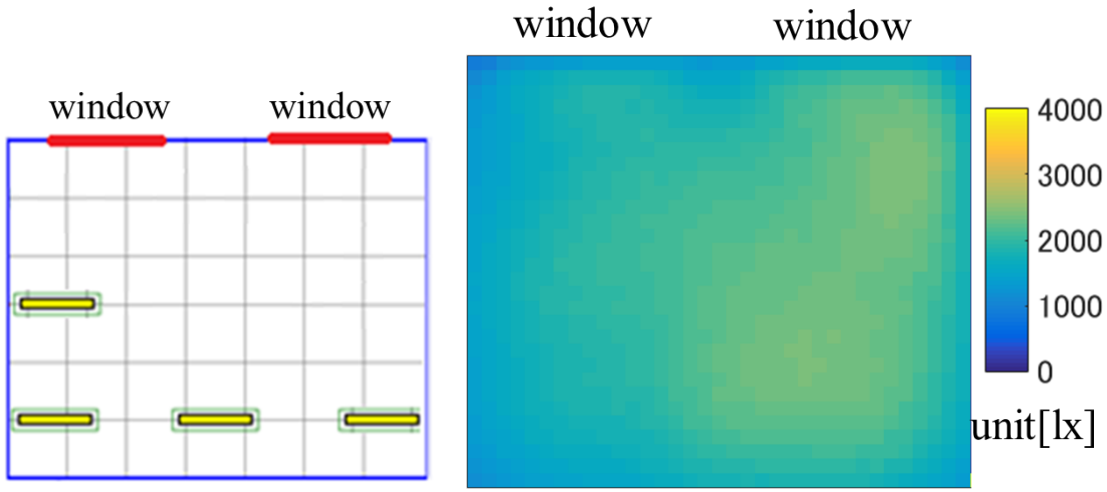

(a) Lighting fixture placement pattern (b) Supplemental illuminance distribution

Fig. 5-14 Supplemental result (solar altitude angle 55°, solar azimuth angle 110°)

② 10:00～11:00 (solar altitude angle 65°, solar azimuth angle 130°)

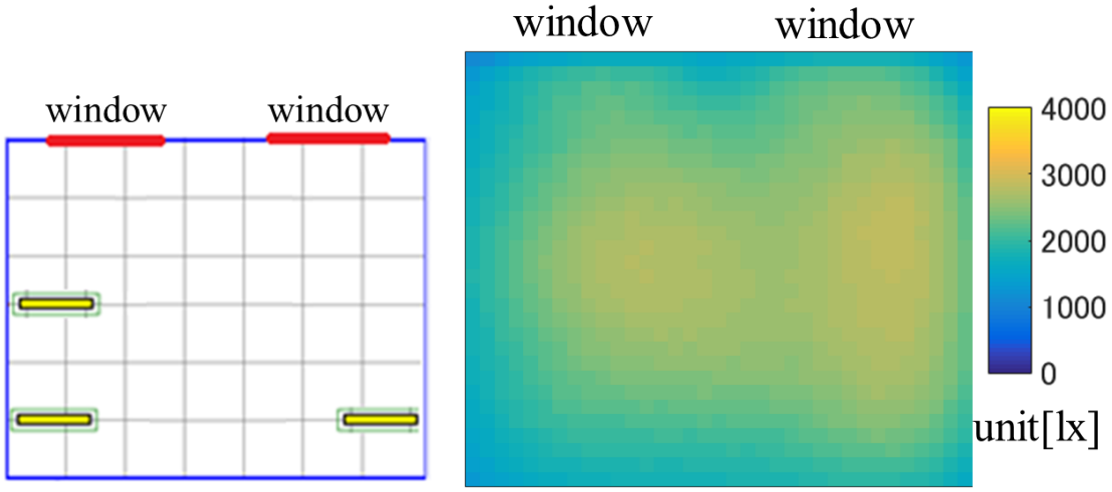

(a) Lighting fixture placement pattern (b) Supplemental illuminance distribution

Fig. 5-15 Supplemental result (solar altitude angle 65°, solar azimuth angle 130°)

③ 11:00～12:00 (solar altitude angle 75°, solar azimuth angle 170°)

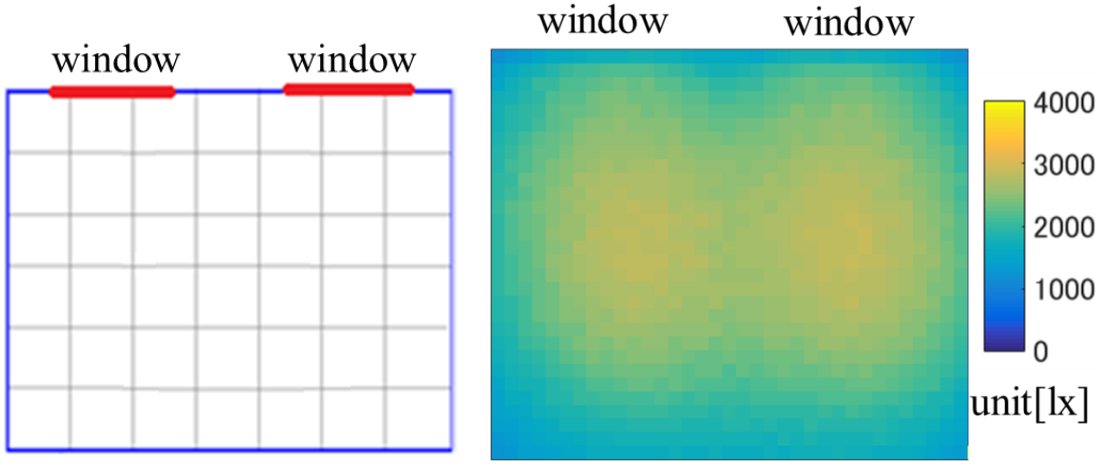

(a) Lighting fixture placement pattern (b) Supplemental illuminance distribution

Fig. 5-16 Supplemental result (solar altitude angle 75°, solar azimuth angle 170°)

④ 12:00～13:00 (solar altitude angle 70°, solar azimuth angle 230°)

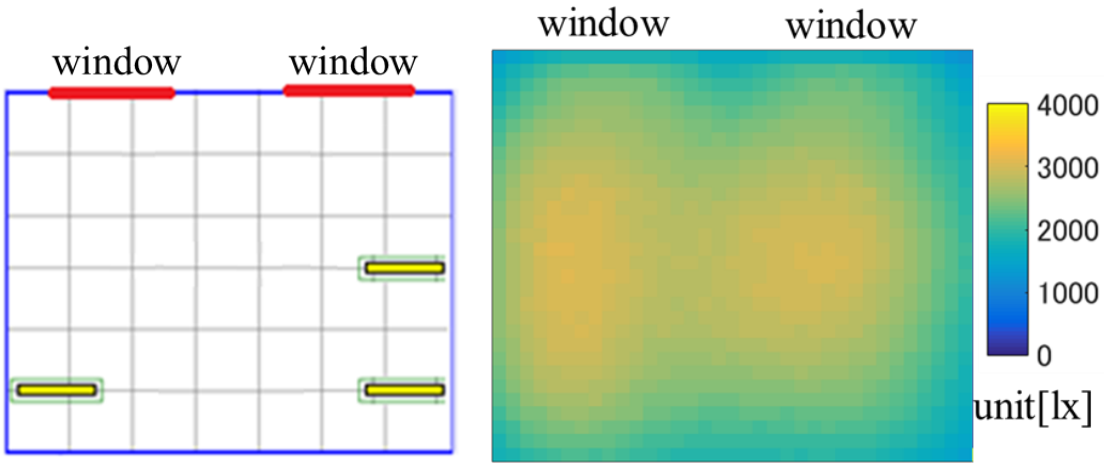

(a) Lighting fixture placement pattern (b) Supplemental illuminance distribution

Fig. 5-17 Supplemental result (solar altitude angle 70°, solar azimuth angle 230°)

⑤ 13:00～14:00 (solar altitude angle 60°, solar azimuth angle 240°)

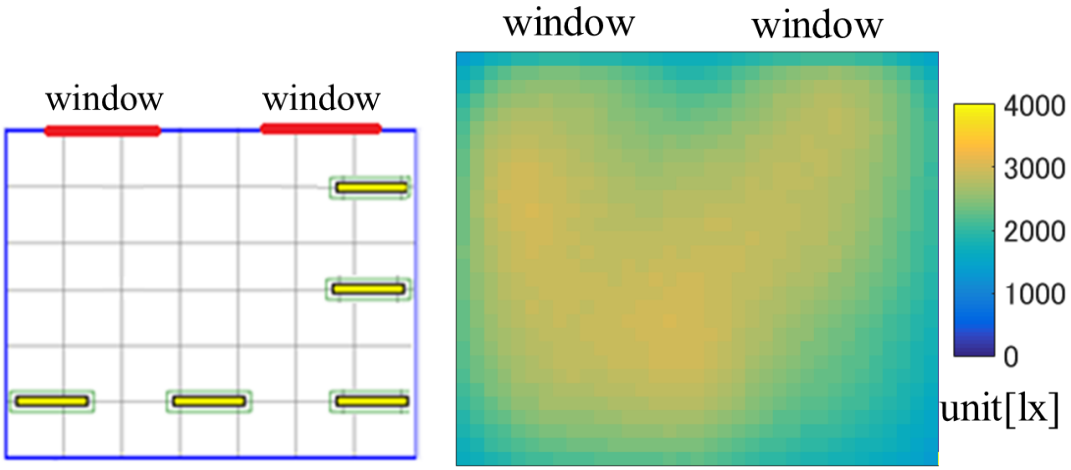

(a) Lighting fixture placement pattern (b) Supplemental illuminance distribution

Fig. 5-18 Supplemental result (solar altitude angle 60°, solar azimuth angle 240°)

⑥ 14:00～15:00 (solar altitude angle 50°, solar azimuth angle 260°)

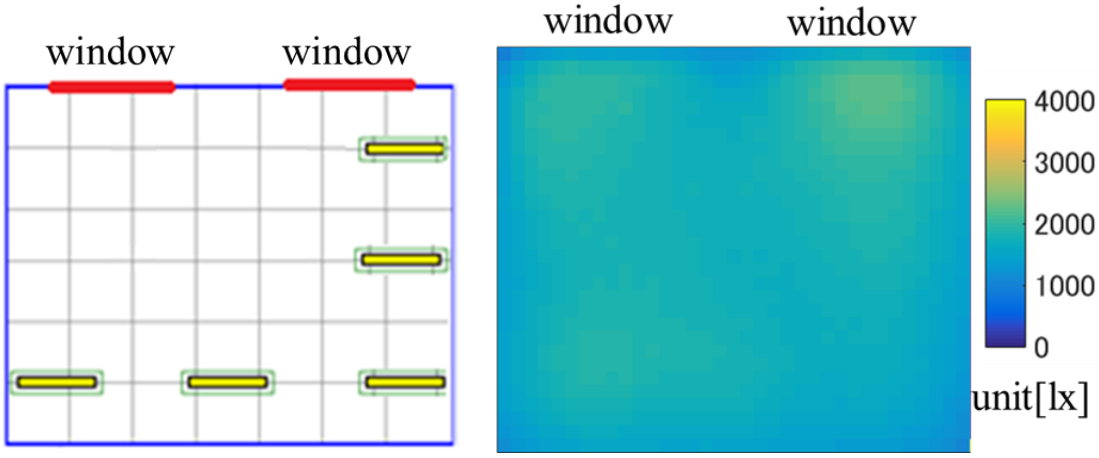

(a) Lighting fixture placement pattern (b) Supplemental illuminance distribution

Fig. 5-19 Supplemental result (solar altitude angle 50°, solar azimuth angle 260°)

Looking at the illuminance distribution charts in Fig. 5-14 to 5-19, it is clear that if lights are attached as the same as the arrangement pattern, the illuminance of the work surface will be uniform based on the illuminance distribution of the work surface as shown in Fig. 5-12 (a-f). In order to investigate whether exposure illuminance standards are satisfied, the data are summarized in Table 5-7.

Table 5-7 Simulation results for summer

Results / Time zone	Maximum illuminance[lx]	Minimum illuminance[lx]	Average illuminance[lx]	Uniformity
9:00～10:00	2423.7	1672.8	2110.1	0.79
10:00～11:00	2853.1	2074.8	2532.8	0.82
11:00～12:00	2916.6	2084.1	2591.1	0.80
12:00～13:00	3069.4	2248.3	2742.8	0.82
13:00～14:00	3021.9	2137.9	2745.8	0.78
14:00～15:00	2151.5	1630.5	1804.5	0.90

The data on the illuminance in Table 5-7, since the minimum illuminance of all the time zones exceeded 500 lx, it meets the illumination standard. Furthermore, by referring to the data on the degree of uniformity, all the time periods within the lighting time period are more than 0.7, therefore it meets the illuminance standard. Also, especially at the time zone between 14: 00 ~ 15: 00, the uniformity of the west side in Table 5-7 shows a value of 0.9, therefore it is clear that the amount of lighting under the experimented condition was very uniform. Based on the obtained result, we believe that artificial lighting and daylighting by window are possible in the summer.

2：Evaluation of daylighting usage on spring and autumnal

The simulated illuminance distribution for spring and autumn is shown in Fig. 5-20(a~f).

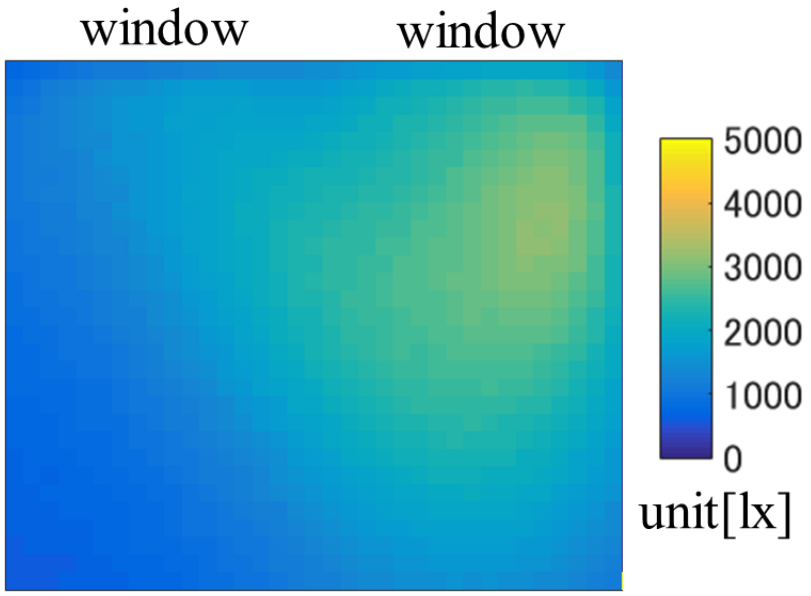

(a) 9:00～10:00 (solar altitude angle 40°, solar azimuth angle 130°)

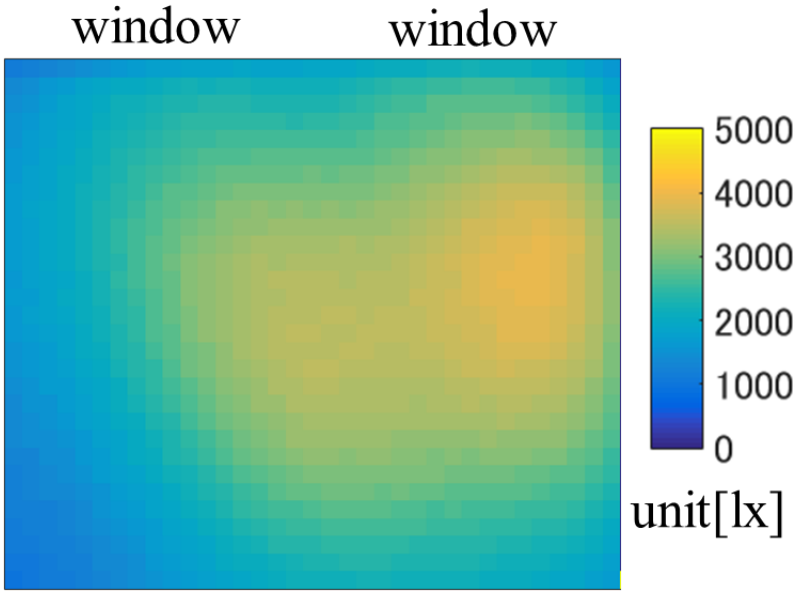

(b) 10:00～11:00 (solar altitude angle 45°, solar azimuth angle 150°)

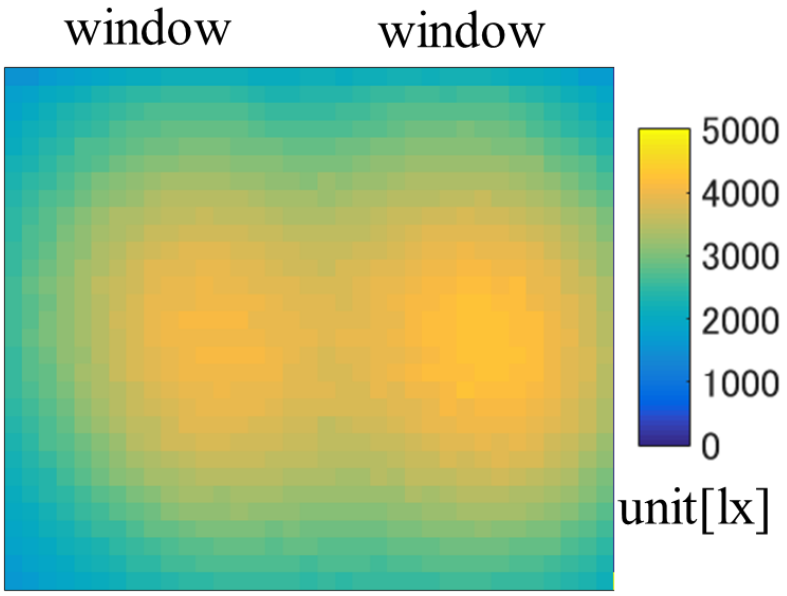

(c) 11:00～12:00 (solar altitude angle 50°, solar azimuth angle 170°)

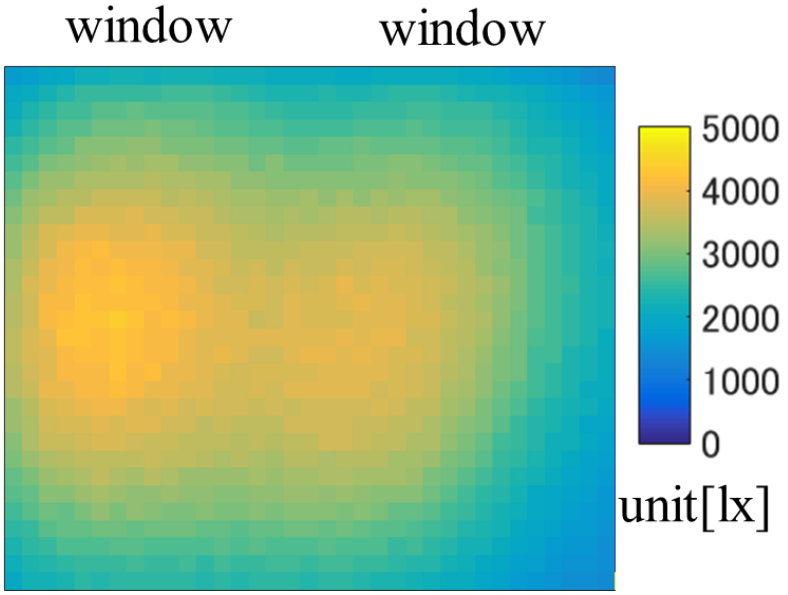

(d) 12:00～13:00 (solar altitude angle 50°, solar azimuth angle 200°)

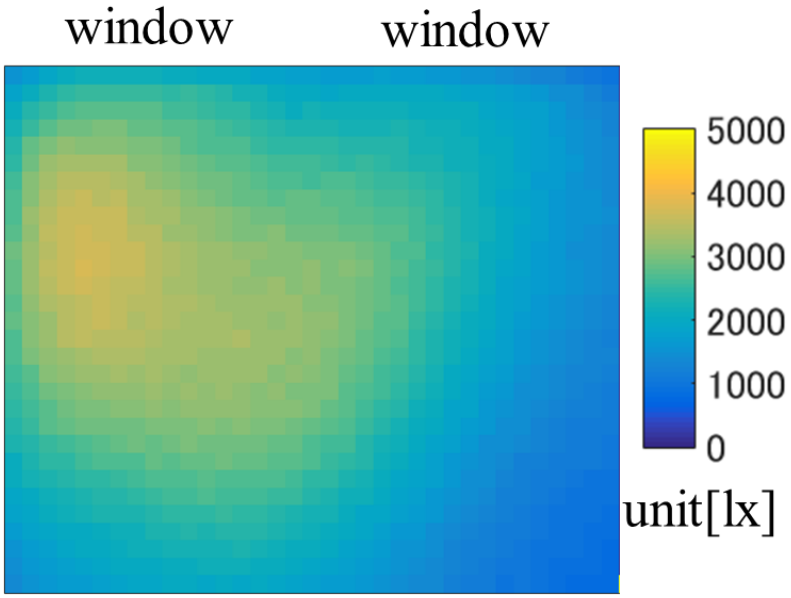

(e) 13:00～14:00 (solar altitude angle 45°, solar azimuth angle 220°)

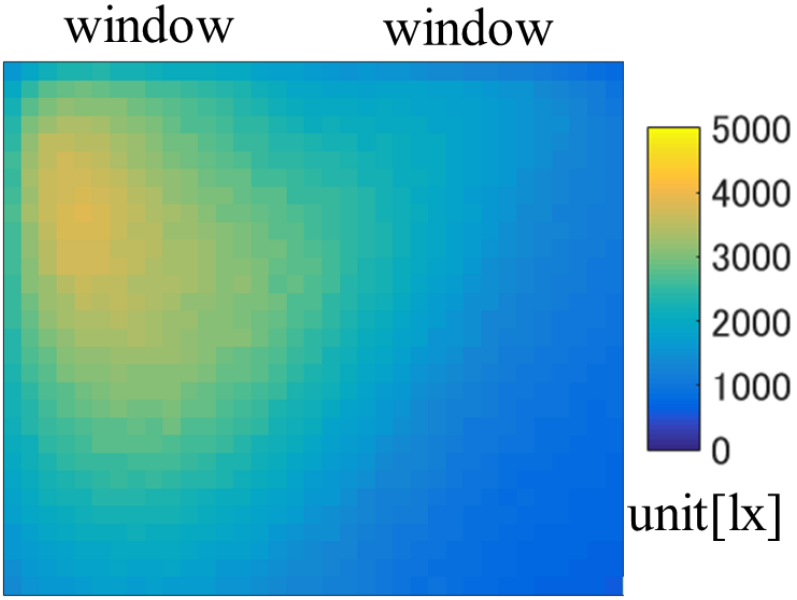

(f) 14:00～15:00 (solar altitude angle 35°, solar azimuth angle 230°)

Fig. 5-20 Illuminance distributions for spring・autumn

The illuminance distribution charts in Fig. 5-20, the center of the light entering the room moves from the west to the east (from the left to the right) as time changes from 9:00 to 15:00. The time zone when lighting is best is between 11:00 and 12:00 and between 12:00 and 13:00. The light at these time zones seems to be the most even and bright. To make a better comparison, the numerical results are summarized in Table 5-8 and the results are graphed in Fig. 5-21.

Table 5-8 Simulation results for spring・autumn

Results / Time zone	Maximum illuminance[lx]	Minimum illuminance[lx]	Average illuminance[lx]	Uniformity
9:00～10:00	3127.0	797.1	2061.5	0.39
10:00～11:00	3970.4	1642.5	3072.7	0.53
11:00～12:00	4284.4	2730.6	3646.6	0.75
12:00～13:00	4376.0	2320.3	3489.2	0.67
13:00～14:00	3705.2	1218.1	2722.1	0.45
14:00～15:00	3769.5	853.1	2350.9	0.36

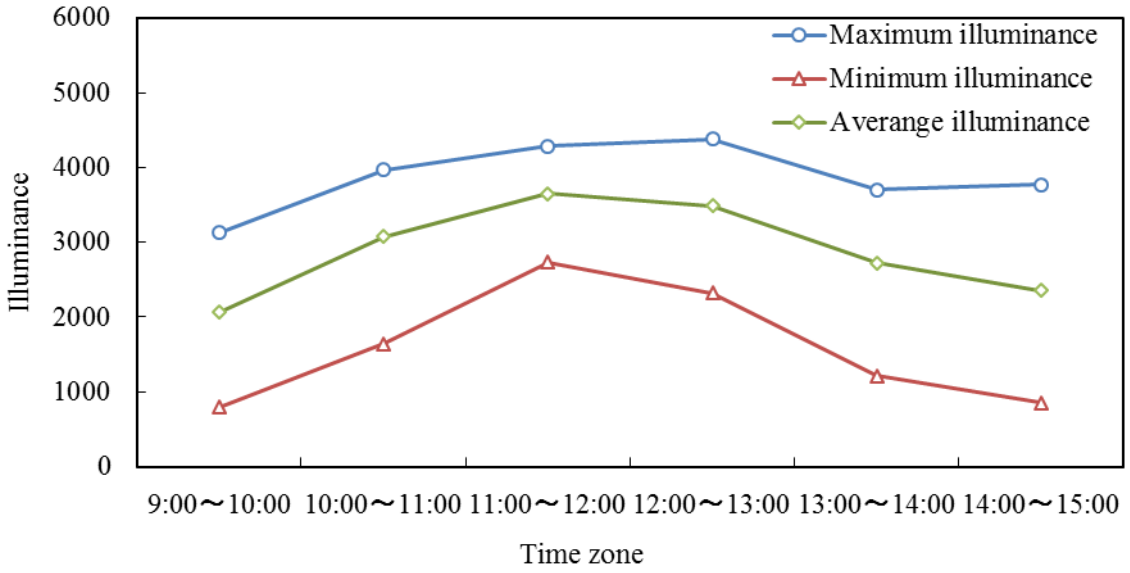

(a)Results of illuminance

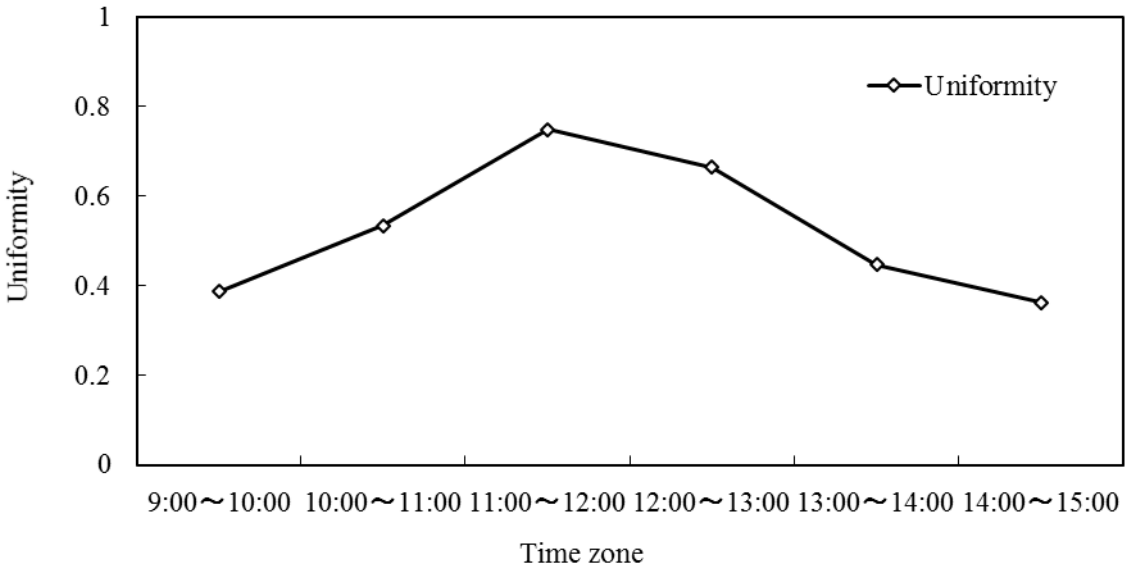

(b) Results of uniformity

Fig. 5-21 Simulation results for spring・autumn

Looking at the result of the illuminance in Fig. 5-21(a), the maximum illuminance, the minimum illuminance, and the average illuminance become brighter and lighter from 9:00, and peak in the time zone from 11:00 to 12:00, Although it tends to decrease from 12:00, the maximum illuminance from 14:00 to 15:00 is bigger than that of 13:00 to 14:00. We believe that this is due to the incident light striking a part of the east (left) wall, making the luminance around that area brighter. Moreover, the illuminances for all time zones are above 500 lx, which satisfies the illuminance standard. Also, looking at the result of the uniformity, the ratio of

uniformity rises steadily from 9:00, similar to the result obtained for illuminance. The uniformity peaks in the time zone from 11:00 to 12:00, and gradually lowers after 12:00. Referring the numerical values, the ratio of uniformity for the time periods other than 11: 00 to 12: 00 was less than 0.7. In order to satisfy the illuminance criterion, it is necessary to increase the ratio of uniformity of the work surface by adjusting the lighting conditions.

In order to search for a better lighting condition that will increase the ratio of uniformity of the work surface, simulation was performed with various lighting fixture placement patterns by attaching lights one by one starting from a place with low lighting, as shown in the illuminance distribution chart in Fig. 5-20. The best result of each time zone and its lighting fixture placement pattern are shown separately below ①~⑥. (Fig. 5-22~ Fig. 5-27)

① 9:00～10:00 (solar altitude angle 40°, solar azimuth angle 130°)

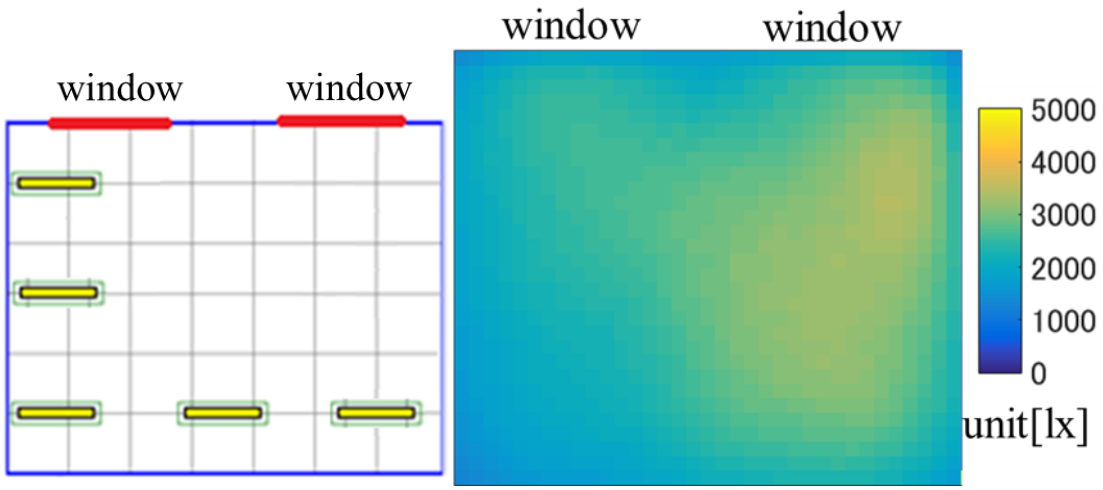

(a)Lighting fixture placement pattern (b) Supplemental illuminance distribution

Fig. 5-22 Supplemental result (solar altitude angle 40°, solar azimuth angle 130°)

② 10:00～11:00 (solar altitude angle 45°, solar azimuth angle 150°)

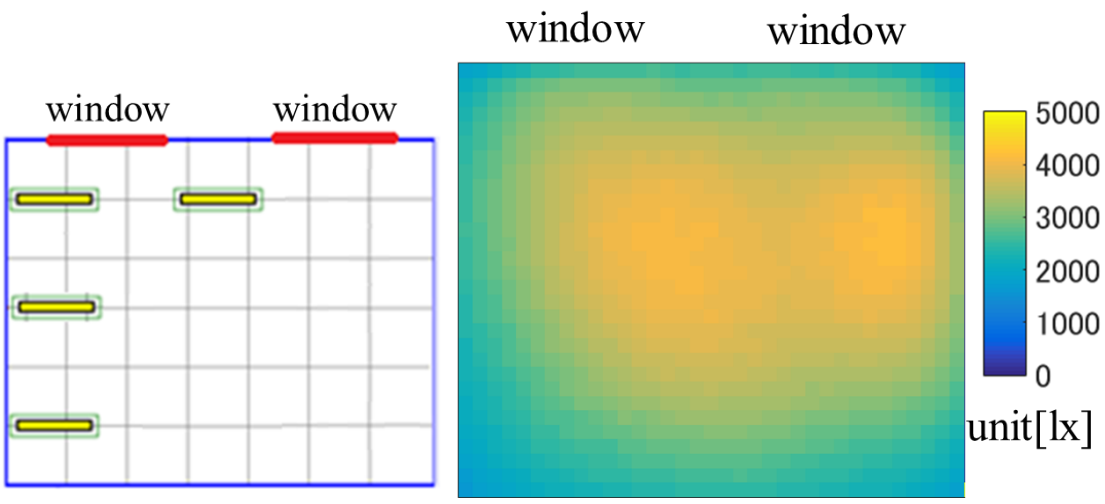

(a) Lighting fixture placement pattern (b) Supplemental illuminance distribution

Fig. 5-23 Supplemental result (solar altitude angle 45°, solar azimuth angle 150°)

③ 11:00～12:00 (solar altitude angle 50°, solar azimuth angle 170°)

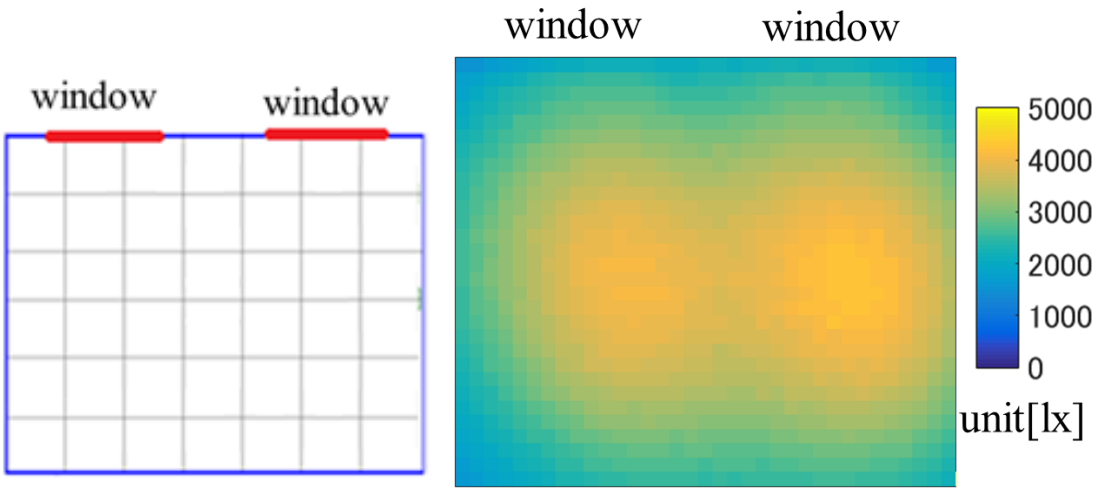

(a) Lighting fixture placement pattern (b) Supplemental illuminance distribution

Fig. 5-24 Supplemental result (solar altitude angle 50°, solar azimuth angle 170°)

④ 12:00～13:00 (solar altitude angle 50°, solar azimuth angle 200°)

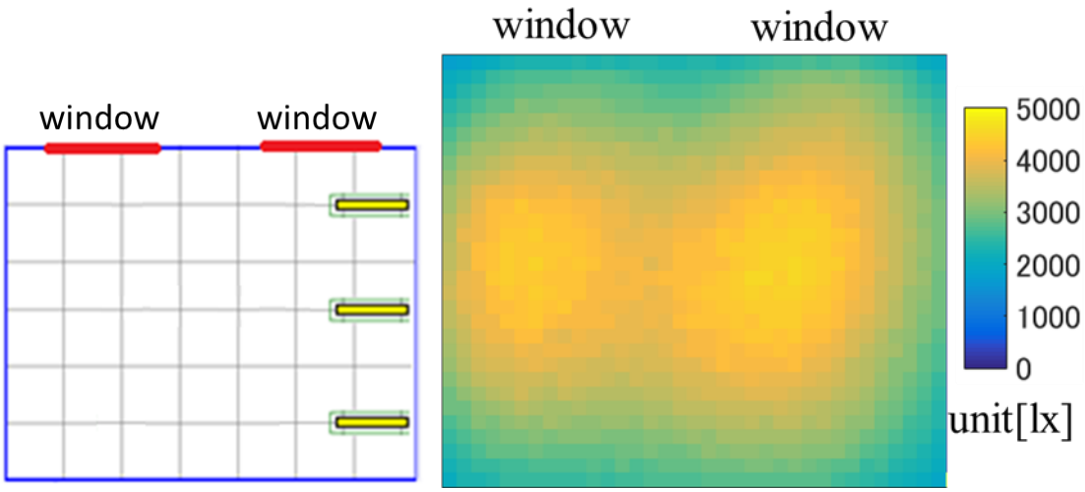

(a) Lighting fixture placement pattern (b) Supplemental illuminance distribution

Fig. 5-25 Supplemental result (solar altitude angle 50°, solar azimuth angle 200°)

⑤ 13:00～14:00 (solar altitude angle 45°, solar azimuth angle 220°)

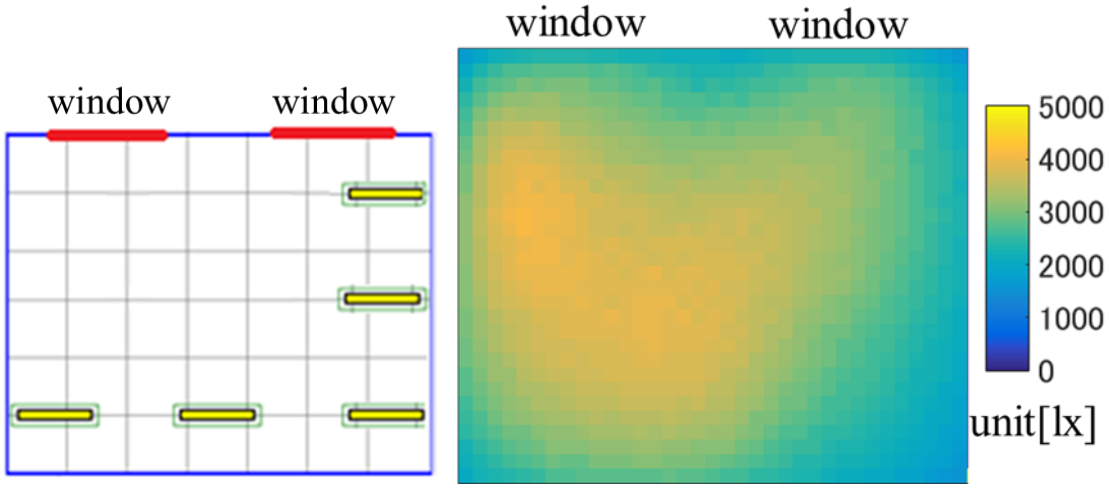

(a) Lighting fixture placement pattern (b) Supplemental illuminance distribution

Fig. 5-26 Supplemental result (solar altitude angle 45°, solar azimuth angle 220°)

⑥ 14:00～15:00 (solar altitude angle 50°, solar azimuth angle 260°)

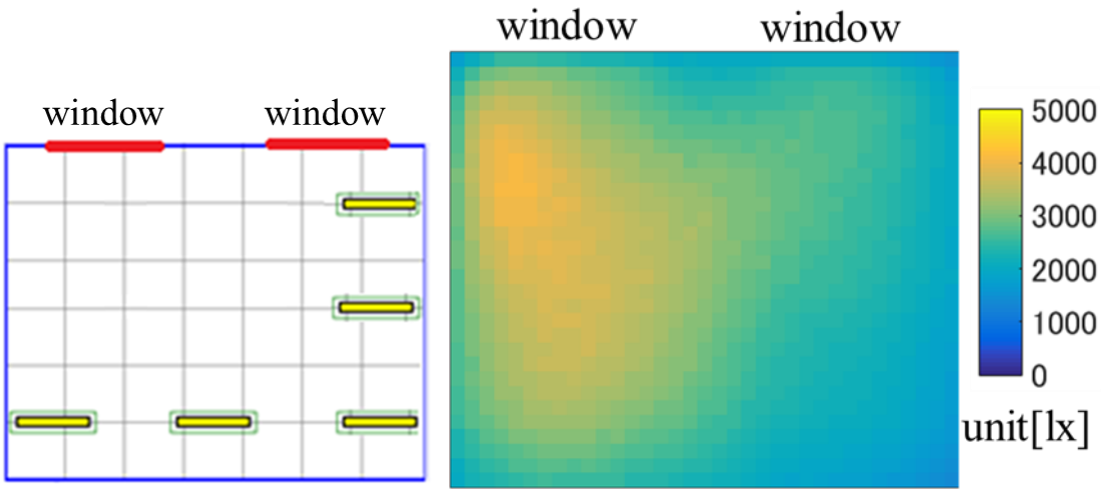

(a) Lighting fixture placement pattern (b) Supplemental illuminance distribution

Fig. 5-27 Supplemental result (solar altitude angle 50°, solar azimuth angle 260°)

Looking at the illuminance distribution charts from Fig. 5-22 to Fig. 5-27, it is clear that if lightings are arranged accordingly as the arrangement patterns, the illumination distribution on the work surface as shown in Fig. 5-20 (a~f) will be uniform. The data are summarized in Table 5-9 to analyze if the results obtained satisfy the illuminance standard.

Since the minimum illuminance of all time zones exceed 500 lx, the illuminance standard is achieved (Table 5-9). When looking at the data of the uniformity, most of the time periods within the lighting time is above 0.7 satisfying the illuminance standard. However, the uniformity of the time zone from 14:00 to 15:00 is less than 0.7 and cannot be used. We believe that this is caused by sunlight reflecting on the ceiling to the wall of the east (left) side. Dazzling lights on the east walls reflect each other causing illuminance on the wall around that area to increase and its uniformity to decrease. We believe that this problem can be resolved by

Table 5-9 Simulation results for spring・autumn

Results / Time zone	Maximum illuminance[lx]	Minimum illuminance[lx]	Average illuminance[lx]	Uniformity
9:00～10:00	3443.0	2001.7	2766.8	0.72
10:00～11:00	4203.3	2686.4	3702.7	0.73
11:00～12:00	4284.4	2730.6	3646.6	0.75
12:00～13:00	4585.7	3020.0	3931.3	0.77
13:00～14:00	4042.3	2428.0	3427.1	0.71
14:00～15:00	4066.0	2064.8	3055.9	0.68

adjusting the amount of light taken by the window, adjusting the size of the reflecting plate, or blocking the incident light. Based on the results obtained, the time zone when daylighting is possible for spring and autumn is from 9:00 to 12:00.

3：Evaluation of daylighting use at winter

The illuminance distributions chart for the simulated winter is shown in Fig. 5-20 (a~f).

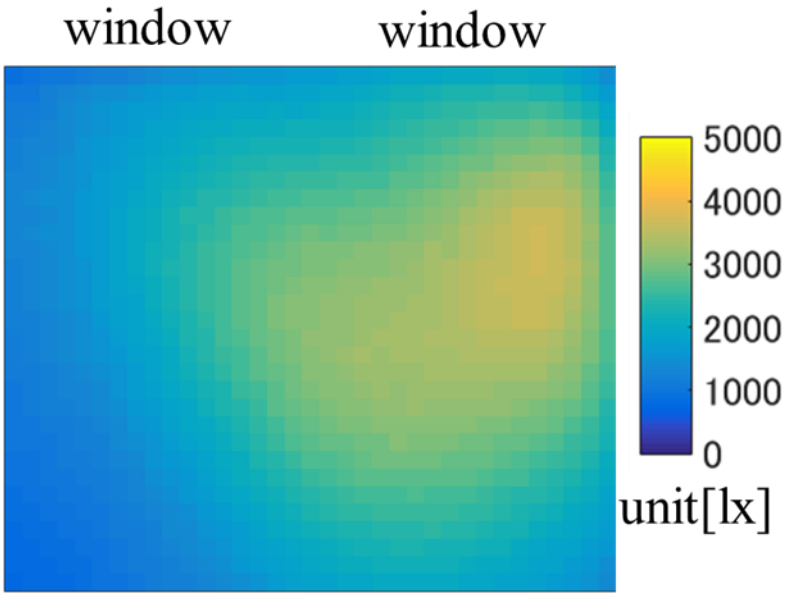

(a) 9:00～10:00 (solar altitude angle 20°, solar azimuth angle 150°)

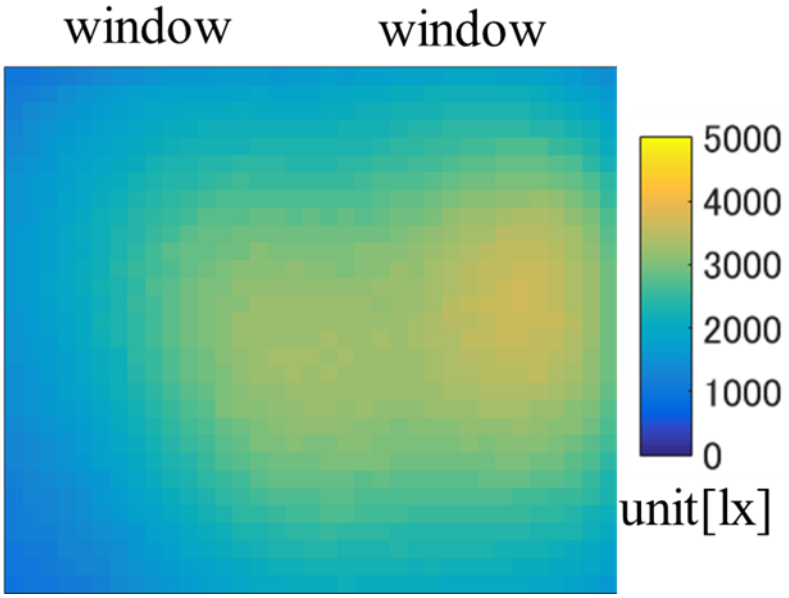

(b) 10:00～11:00 (solar altitude angle 25°, solar azimuth angle 160°)

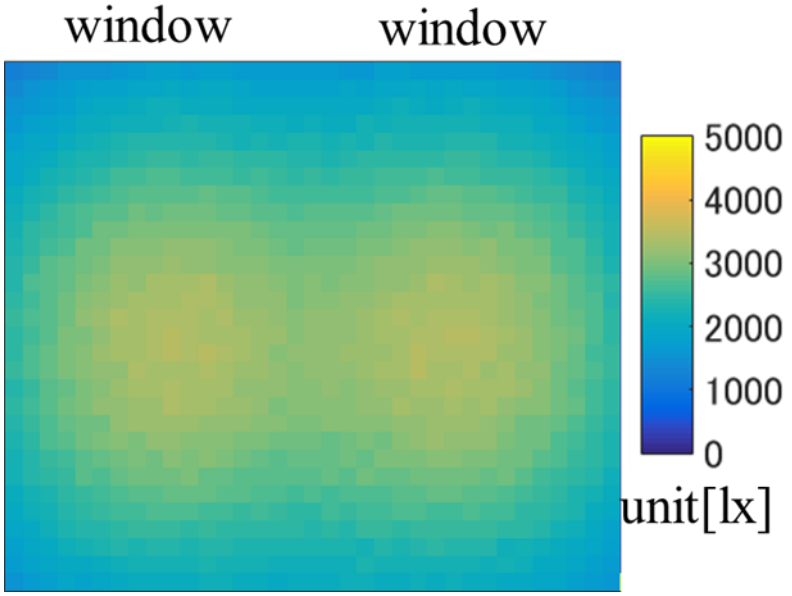

(c) 11:00～12:00 (solar altitude angle 30°, solar azimuth angle 180°)

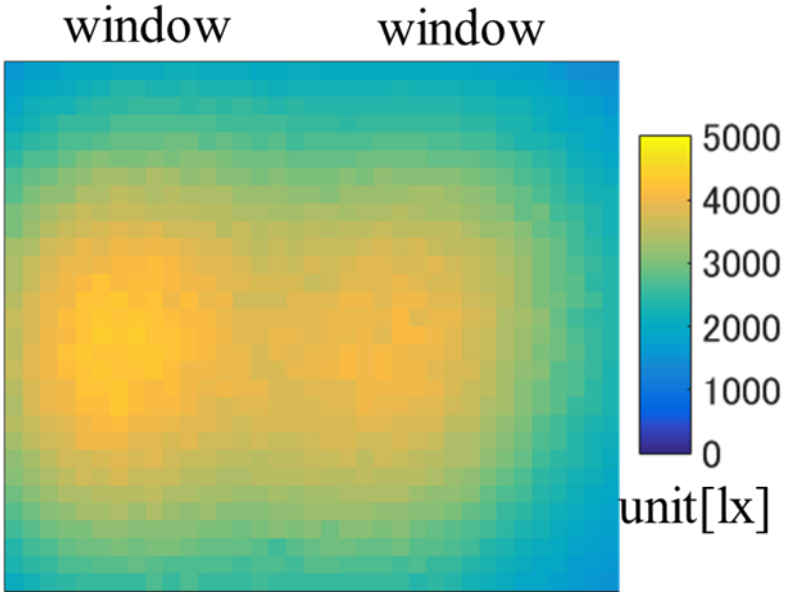

(d) 12:00～13:00 (solar altitude angle 25°, solar azimuth angle 190°)

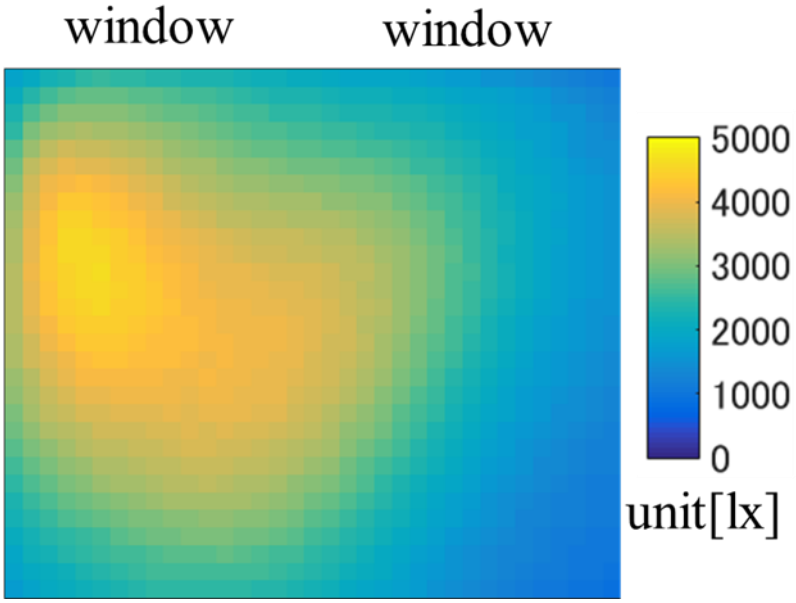

(e) 13:00～14:00 (solar altitude angle 20°, solar azimuth angle 210°)

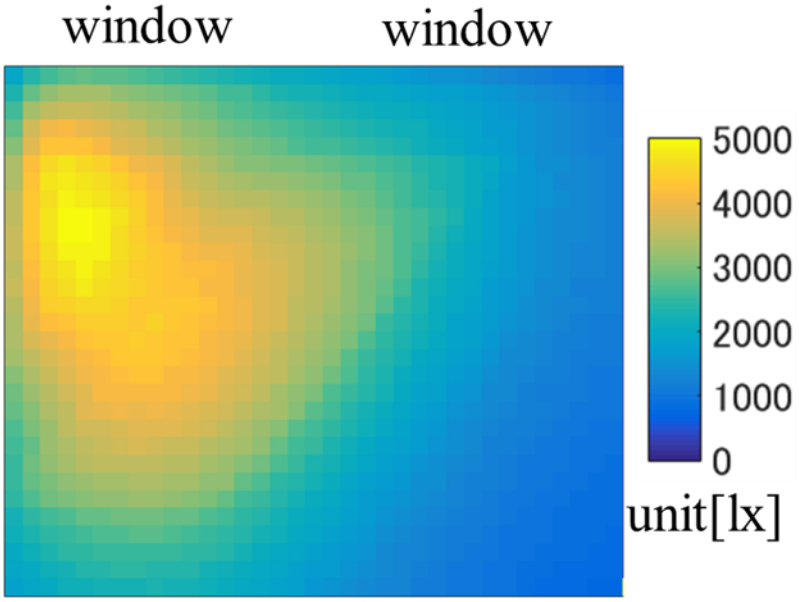

(f) 14:00～15:00 (solar altitude angle 15°, solar azimuth angle 220°)

Fig. 5-28 Illuminance distributions for winter

Looking at the illuminance distribution charts in Fig. 5-28, the center of the light entering the room moves from the west to the east (from the left to the right) as time changes from 9:00 to 3:00. The time zone in which the lighting is the best is from 11:00 to 12:00. The light at this time seems to be the most even and bright. For a better comparison, the data are summarized in Table 5-10 and the result graphs are shown in Fig. 5-29.

Table 5-10 Simulation results for winter

Results / Time zone	Maximum illuminance[lx]	Minimum illuminance[lx]	Average illuminance[lx]	Uniformity
9:00～10:00	4403.7	1402.4	3172.6	0.44
10:00～11:00	4426.1	1936.7	3425.1	0.57
11:00～12:00	4182.6	2634.9	3566.8	0.74
12:00～13:00	5278.3	2795.8	4275.9	0.65
13:00～14:00	5541.2	1731.6	3899.2	0.44
14:00～15:00	5929.7	1294.2	3616.9	0.36

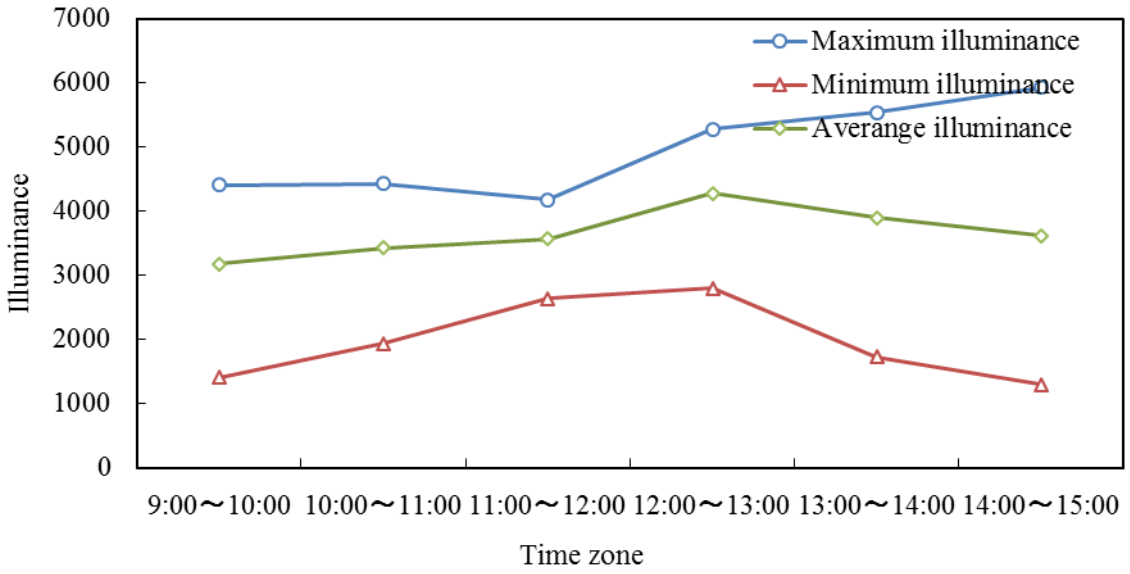

(a) Illuminance

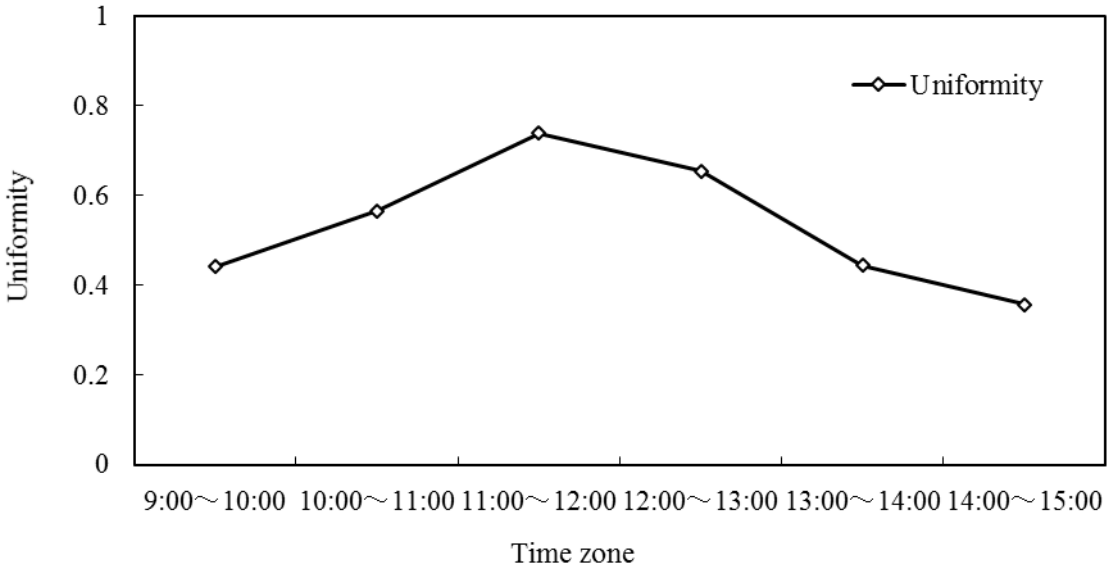

(b) Uniformity

Fig. 5-29 Simulation results for winter

Observing at the results of illuminance in Fig. 5-29 (a), the minimum illuminance and the average illuminance become brighter gradually from 9:00, peak in the time zone from 12:00 to 13:00, and tend to reduce gradually after 12:00. The maximum illuminance is almost constant between 9:00 and 12:00, but it tends to rise between 12:00 and 15:00. We believe that this is caused by the incident light striking a part of the east (left) wall, and the illuminance around that area gets brighter. And the direction of the sun relative to the window becomes diagonal gradually after 12:00 causing the dazzling sunlight to concentrate near the wall with time. Also, from the data in Table 5-10, the illuminance for all the time zones are above 500lx, and they meet the illuminance standard. Also, similar to the illuminance result, the ratio of uniformity also rises steadily from 9:00, peaks in the time zone from 11:00 to 12:00, and gradually decreases after 12:00. Also, when looking at the numerical values, other than the time zone between 11:00 to 12:00, the uniformity of all time zones were less than 0.7. In order to satisfy the illuminance criterion, it is necessary to increase the degree of uniformity of the work surface by changing the lighting conditions.

In search for better lighting conditions, with reference to the illuminance distribution chart shown in Fig. 5-28, lights were attached one by one starting from places with low lighting and simulated with various lighting fixture arrangement patterns. The best result of each time zone and its lighting fixture placement pattern are shown separately in ①~⑥. (Fig. 5-30~ Fig. 5-35)

① 9:00～10:00 (solar altitude angle 20°, solar azimuth angle 150°)

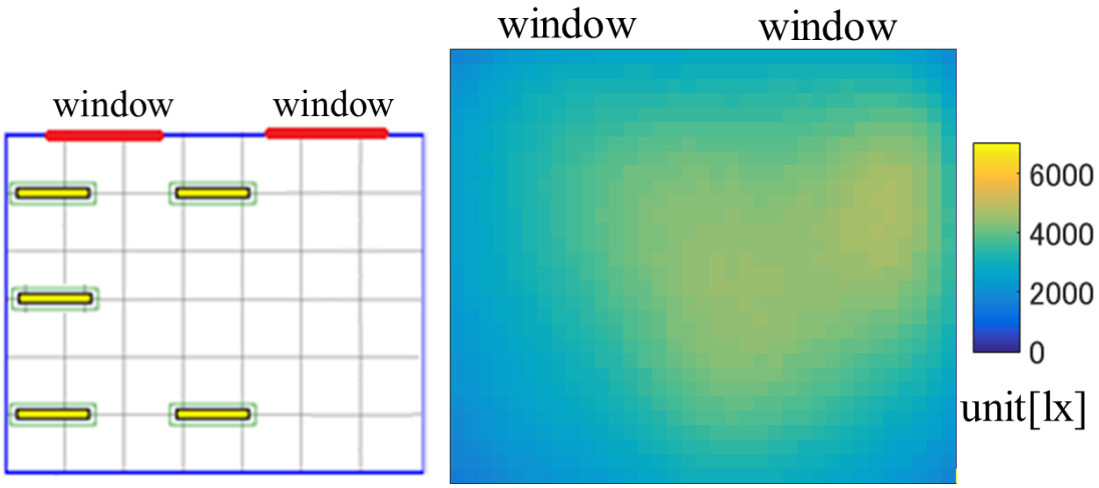

(a) Lighting fixture placement pattern (b) Supplemental illuminance distribution

Fig. 5-30 Supplemental result (solar altitude angle 20°, solar azimuth angle 150°)

② 10:00～11:00 (solar altitude angle 25°, solar azimuth angle 160°)

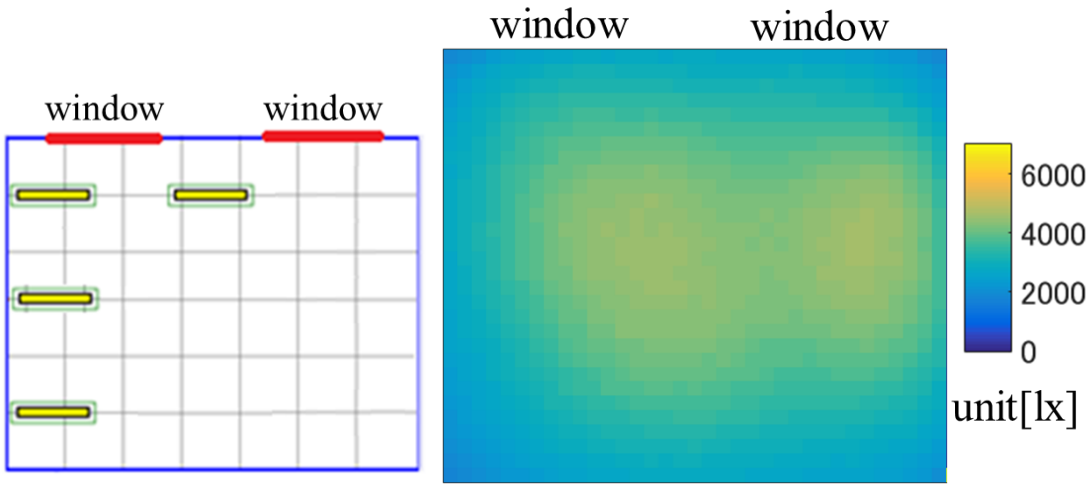

(a) Lighting fixture placement pattern (b) Supplemental illuminance distribution

Fig. 5-31 Supplemental result(solar altitude angle 25°, solar azimuth angle 160°)

③ 11:00～12:00 (solar altitude angle 30°, solar azimuth angle 180°)

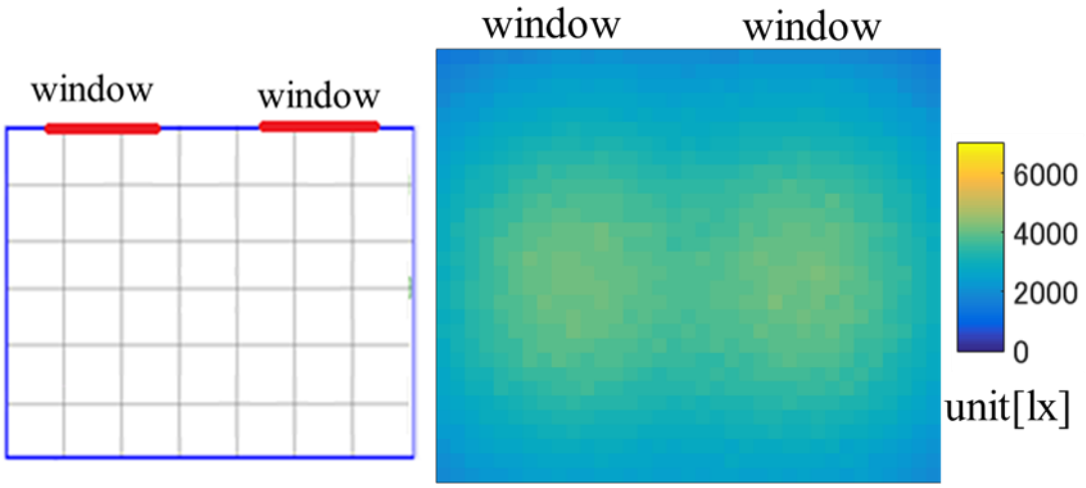

(a) Lighting fixture placement pattern (b) Supplemental illuminance distribution

Fig. 5-32 Supplemental result (solar altitude angle 30°, solar azimuth angle 180°)

④ 12:00～13:00 (solar altitude angle 25°, solar azimuth angle 190°)

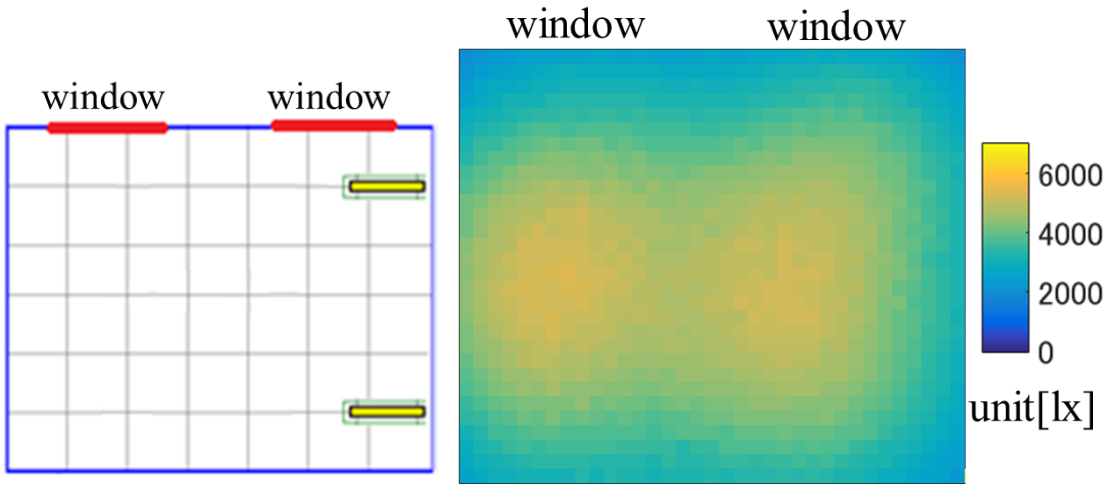

(a) Lighting fixture placement pattern (b) Supplemental illuminance distribution

Fig. 5-33 Supplemental result (solar altitude angle 25°, solar azimuth angle 190°)

⑤ 13:00～14:00 (solar altitude angle 20°, solar azimuth angle 210°)

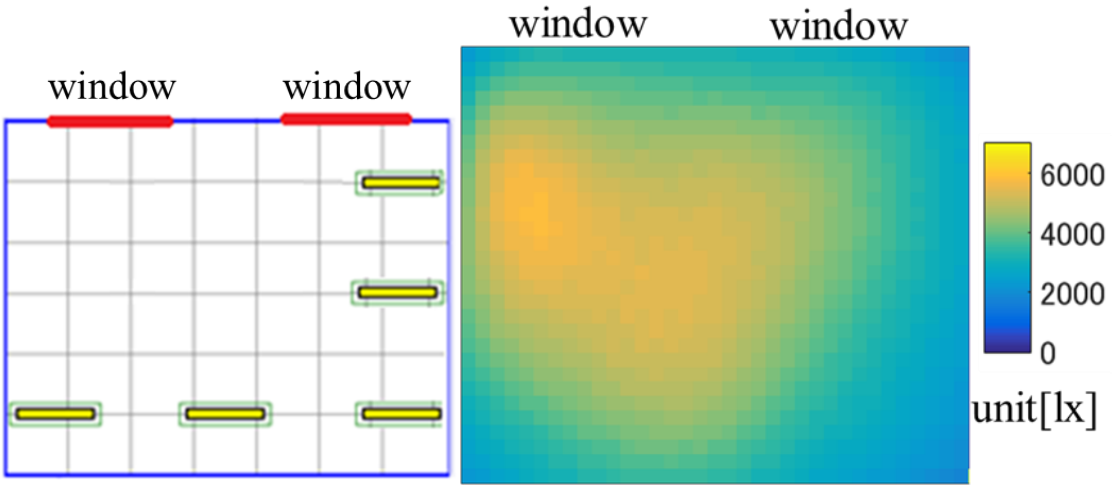

(a) Lighting fixture placement pattern (b) Supplemental illuminance distribution

Fig. 5-34 Supplemental result (solar altitude angle 20°, solar azimuth angle 210°)

⑥ 14:00～15:00 (solar altitude angle 15°, solar azimuth angle 220°)

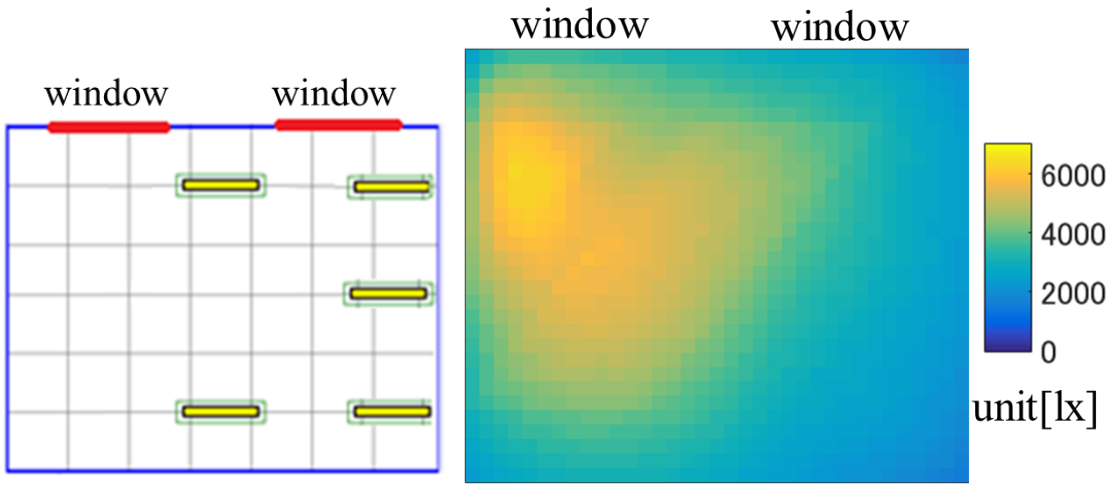

(a) Lighting fixture placement pattern (b) Supplemental illuminance distribution

Fig. 5-35 Supplemental result (solar altitude angle 15°, solar azimuth angle 220°)

Looking at the illuminance distribution chart from Fig. 5-30 to Fig. 5-35, it is obvious that if light is attached as the shown arrangement patterns, the illuminance distribution on the work surface in Fig. 5-28 (a~f) can be uniform. In order to investigate whether illuminance standard is satisfied, the data are summarized in Table 5-11.

Table 5-11 Simulation results for winter

Results / Time zone	Maximum illuminance[lx]	Minimum illuminance[lx]	Average illuminance[lx]	Uniformity
9:00～10:00	4718.6	2599.5	3951.5	0.66
10:00～11:00	4650.5	2980.7	4055.1	0.74
11:00～12:00	4182.6	2634.9	3566.8	0.74
12:00～13:00	5370.5	3312.3	4541.6	0.73
13:00～14:00	5852.6	2938.9	4677.8	0.63
14:00～15:00	6244.4	2501.5	4395.5	0.57

Since the minimum illuminance of all time periods exceed 500 lx, the illuminance data of Table 5-11 meet the illumination standard. When looking at the data on the ratio of uniformity, only the uniformity in the time zone from 10:00 to 13:00 is above 0.7, satisfying the illumination standard. The uniformity of other time zones are less than 0.7 and cannot be used. We believe that this is caused by the dazzling sunlight reflected from the ceiling onto the left and right walls in the morning and afternoon to the left and right walls. Dazzling lights on the left and right walls reflect onto each other, causing the illuminance to increase and uniformity to decrease. We believe that this problem can be solved by adjusting the amount of light taken from the window, adjusting the size of the reflector, or blocking the incident light. Based on the results above, the time period during which winter daylighting is possible is from 10:00 to 13:00.

5-5 Consideration of power consumption

If the blind-shaped reflector attached to the window is controlled as shown in Fig. 5-6, it is shown in Chapter 5-3 that the combination of artificial lighting and daylighting from the window is effective for energy conservation. Here, we examine how much energy can be saved for each lighting time zone. The environment for this comparison is described in the previous chapter whereby 9 lights are arranged evenly on the ceiling and when light does not enter from the window (see Fig. 4-11). In other words, it is the lighting environment of a typical office at night. Table 5-12 shows the amount of energy saving for each time zone. Here, the number of lights is 9 (night office environment) for boxes with diagonal lines.

Based on the data in Table 5-12, in the case of combination of artificial lighting and daylighting from the window, the number of lighting fixtures installed is the smallest for all seasons, and power can be saved most from 11:00 to 12:00, and it was found that illumination standard is satisfied even if it is not light up at this time. The power consumption at this time was compared with the power consumption when the amount of lighting fixtures was 9 lights, and it was found that 100% of power consumption could be reduced.

In the actual laboratory, the curtains are usually drawn as sunlight is too dazzling, therefore 9

Table 5-12 Percentage of energy saving

Season / Time zone	Summer		Spring and autumn		Winter	
	Number of lights	Energy saving	Number of lights	Energy saving	Number of lights	Energy saving
9:00～10:00	4 lights	55.6%	5 lights	55.6%		
10:00～11:00	3 lights	66.7%	4 lights	55.6%	4 lights	55.6%
11:00～12:00	0 light	100%	0 light	100%	0 light	100%
12:00～13:00	3 lights	66.7%	3 lights	66.7%	2 lights	77.8%
13:00～14:00	5 lights	44.4%	5 lights	44.4%		
14:00～15:00	5 lights	44.4%				

Table 5-13 Percentage of energy saving (all day)

Season / Time zone	summer		spring and autumn		winter	
	power consumption [W]	energy saving	power consumption [W]	energy saving	power consumption [W]	energy saving
9:00～18:00	3008	42.0%	3392	34.6%	3840	25.9%

lights are usually used from morning till evening. In the same time zone, it is possible to save energy by 55.5% in the morning and save at least 44.4% in the evening. Also, the power consumption during the day is calculated and summarized in Table 5-13 by assuming the working hours in the laboratory for a day is from 9:00 to 18:00. In this example, as described in Chapter 4-1, the power consumption per hour is 64 W. Therefore, the power consumption during a general day is 64 W × 9 fluorescent lamps × 9 hours = 5184 W. Compared with the daytime power consumption when combining artificial lighting and lighting from the window, the energy conservation rate was calculated and summarized in the Table 5-13.

Based on the data in Table 5-13, by attaching the blind-shaped reflector to the window and controlling it as shown in Fig. 5-6, we were able to reduce power consumption by 42% in the summer, 34.6% in the spring and autumn, and 25.9% in the winter when using a lighting system that combines artificial lighting and daylighting through a window compared to lighting. Therefore it can be said that daylighting from the window is effective in reducing power consumption.

References

[1] David Maslanka Ph.D. : “Solar Geometry”, Illinois Institute of Technology, Department of Applied Mathematics, pp.1-5

[2] The National Astronomical Observatory of Japan (NAOJ) – ECO - Koyomi Station http://eco.mtk.nao.ac.jp/cgi-bin/koyomi/koyomix_en.cgi

[3] Lee Jin You, Roger: “Yong Heavenly Mathematics GEK 1506 - Sun and Architecture” pp.3-10

[4] Masahiro Kajikawa: “On the Calculating Diagrams of Solar Altitude and Solar Azimuth on the Northern Hemisphere”, Geophysical bulletin of Hokkaido University, No.13, pp. 71-98 (1965) (in Japanese)

梶川 正弘:「北半球における太陽高度角および方位角の計算図の作成」, 北海道大学地球物理学研究報告, No.13, pp. 71-98 (1965)

[5] John Harrison: “Investigation of Reflective Materials for the Solar Cooker”, Florida Solar Energy Center, 24 December 2001

[6] MATERIAL HOUSE - Reflection Materials - http://www.materialhouse.jp/techdate/material.html (in Japanese)

MATERIAL HOUSE - 反射材料 - http://www.materialhouse.jp/techdate/material.html

Chapter 6

Evaluation of lighting environment for direct sunlight (With many rows of reflectors)

In the chapter 5, I concluded that the ratio of uniformity between 11: 00 and 12: 00 is the largest of all seasons, and the lighting fixture does not have to be lighten up in this time zone to meet illuminance standard. It is because, the solar azimuth angle is almost 180 ° between 11:00 and 12:00, and it is located south of the room. In the previous simulation works, the window is set to the south side, and the reflection plate is controlled with the angle θ_{MID} from the bottom to the top with the horizontal axis of the window plane as the axis. Between 11:00 and 12:00, the incident light is reflected to the ceiling and illuminates the middle of the ceiling. I believe that this is the reason for why the ratio of uniformity at this time is the highest. In this chapter, in order to further increase of the energy conservation rate, the reflector is not only controlled in vertically but also in horizontally in between the left and right side of the reflectors. The reflectors are to move in such a way that the sunlight of any time zone will be reflected to the center of the ceiling. This setting has chosen in the simulation works and thus, it has become possible to use the natural light throughout the whole year.

6−1 Simulation method

The simulation conditions in this chapter are almost the same as in the chapter 5, whereby the setting of simulation model, installation of lighting equipment, control of reflection plate, setting of solar altitude angle and solar azimuth angle are the same as those in the chapter 5. However, daylighting from the window is different from the simulation in the chapter 5. As shown in the coordinate system in Fig. 6-1(a), the reflector is controlled to move from the bottom to the top with the red line of the window being the axis. As shown in Fig. 6-1(b), the angle parallel to the x-y plane is 0 °, the upward angle is +, the downward angle is -. In this simulation, besides being able to control the reflector as in the chapter 5, the reflection plate is also able to turn left and right around the blue line which acts like an axis to a certain extent and it reflects the incident light to the center of the ceiling. As shown in Fig. 6-1(c), the reflector angle is set to 0 °, the angle parallel to the x-y plane is 0 °, the angle rotating to the left is +, and the angle rotating to the right is -.

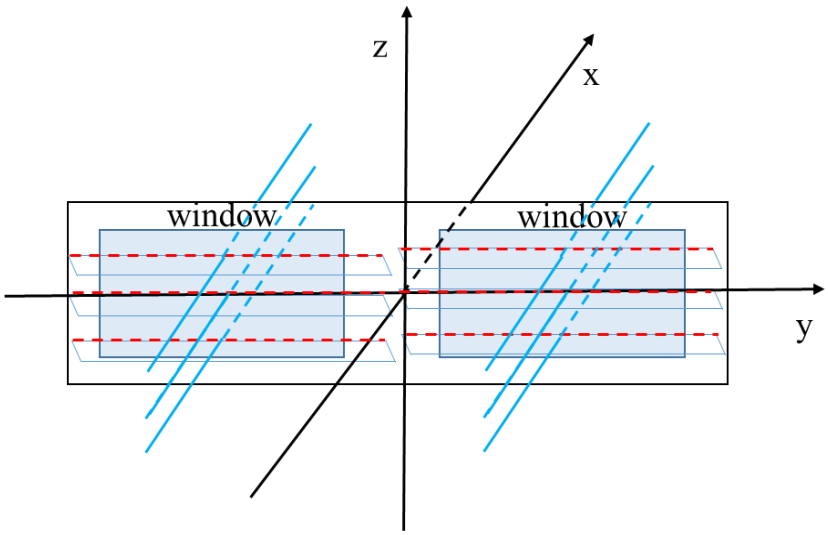

(a) Coordinates on the window surface

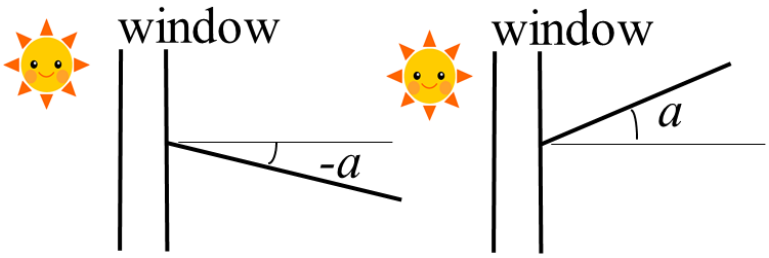

(b) Control of reflector (x-z plane)

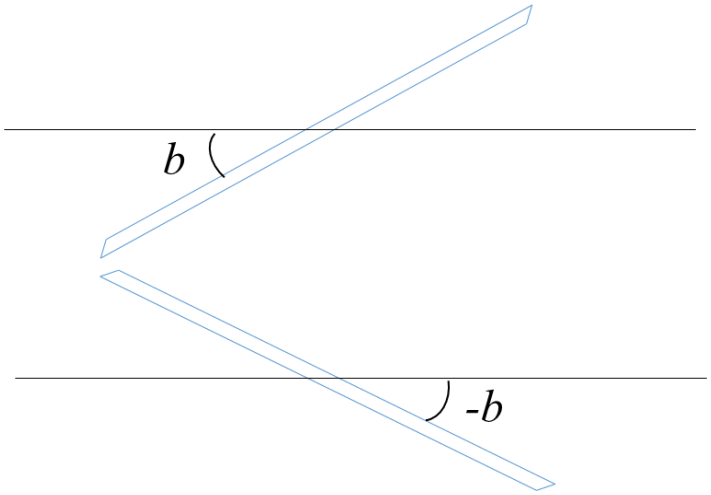

(c) Control of reflector (y-z plane)

Fig. 6-1 Fixing of angle of the reflectors

The setting of the reflector properties is the same as the simulation in the chapter 5, the front of the reflector is a flat mirror, and the incident daylight is reflected to the ceiling with 90% specular reflection and absorbs the remaining light. 90% of the light is absorbed on the back surface of the blind reflector, and the remaining light is set to be like a scattering reflection. Here, the reflector is controlled at two angles *a* and *b*, and the incident sunlight is reflected to the center of the ceiling as shown in Fig. 6-2.

By using this method, the dazzling incident sunlight is reflected to the ceiling and light diffusely reflected from the ceiling is utilized. The simulation calculation in this chapter is the same as in the chapter 5 with the number of calculations per window being 50 million. In addition, in order to obtain illuminance distribution, the surface element size was set to 0.2 m × 0.2 m, and the observation surface was divided into 1050 regions of 35 rows × 30 columns. The amount of solar flux and the solar angle for simulation in this chapter were measured and can be referred in Table 5-1 and Table 5-2 of chapter 5.

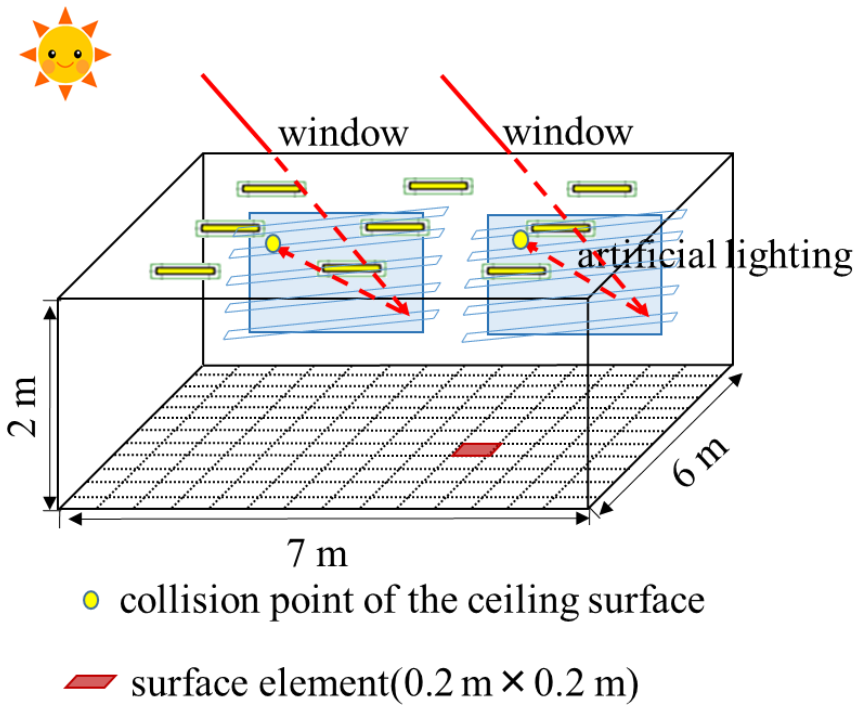

Fig. 6-2 Fixing of angle of the reflectors

6−2 Setting of reflector

As described in Fig. 6-1 to Fig. 6-2, incident daylight is taken into the room with a blind shade reflectors system. It is assumed for with natural day light and artificial light. In this chapter, in order to improve the performance, the reflector is controlled with two angles *a* and *b* shown in Fig. 6-1 so that incident light is reflected to the ceiling as much as possible. And, in order to simulate a comfortable lighting environment, incident light is reflected to the center of the ceiling. Here, the conditions of reflectors will be described.

1. Setting reflector angle

As shown in Fig. 6-3, if the horizontal angle of the reflector is *b*, the angle of the reflector when q＝90° is b_{MID}. At this time, light entering from the window reflected to the ceiling is in the

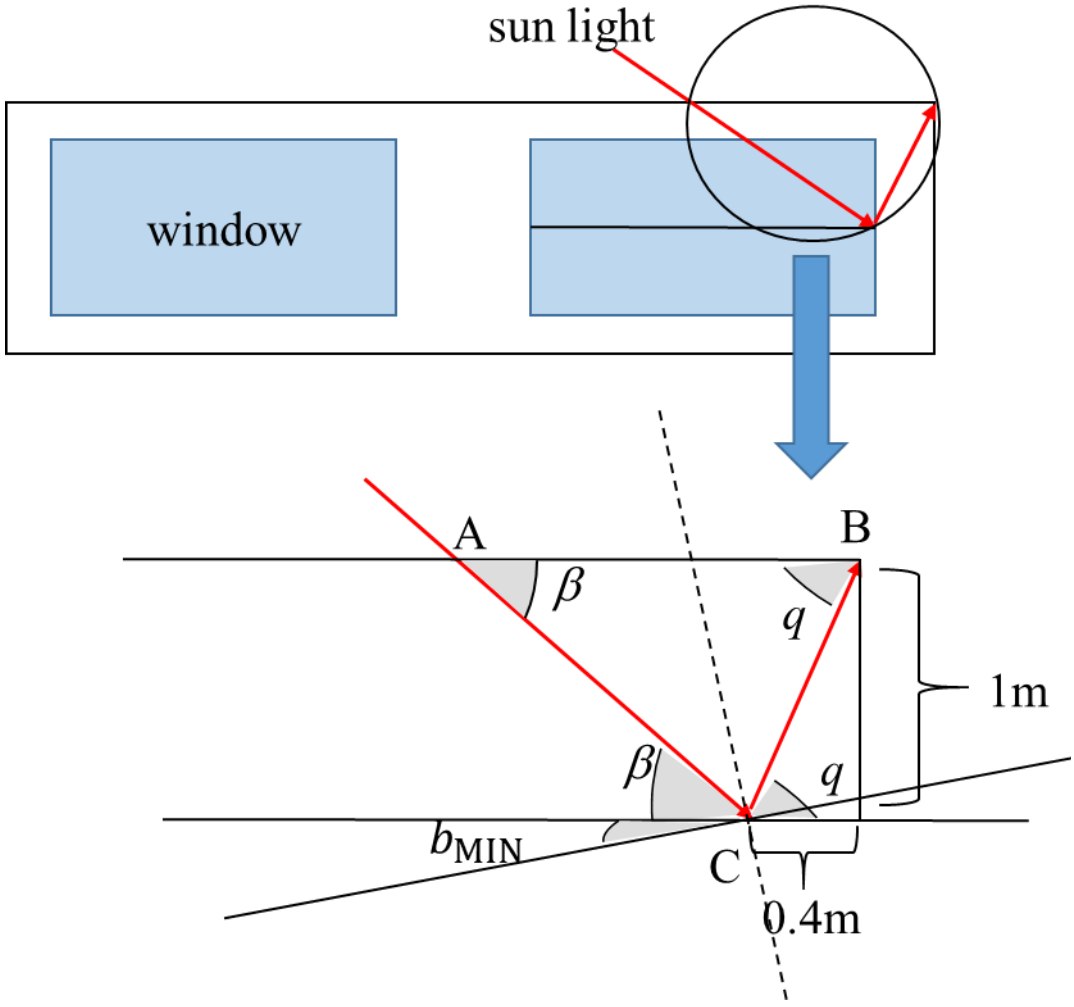

Fig. 6-3 Determination of horizontal angle of reflector

same direction as the solar azimuthal angle of 180°. From the triangular relationship shown in Fig. 6-3, the below equation can be obtained.

$$b_{MID} = \frac{90-\beta}{2} \quad [°] \tag{6−1}$$

Here, β is the projection of the y axis of the sun angle as shown in Fig. 5-8, which can be referred to the equations (5-8) and (5-9) in Chapter 5. b_{MID} can be calculated using equation (6-1).

It is also necessary to obtain the minimum angle b_{MIN} of the reflector. When the angle of the reflector becomes smaller than b_{MIN}, light reflected to the ceiling is reflected to the left wall. In order to obtain b_{MIN}, it is necessary to first obtain the ray that reflects to the ceiling and the angle q to be the ceiling, and q is obtained from the triangular relationship as shown in Fig. 6-3 by the equation (6-2).

$$\mathrm{q} = tan^{-1}\frac{1}{0.4} = 68.2° \tag{6−2}$$

Then, the minimum horizontal angle of the reflector in the case of φ<180° is obtained from the triangular relationship as follow.

$$b_{MIN} = \frac{\pi}{2} - \beta - \frac{\pi-q-\beta}{2} = \frac{68.2-\beta}{2} \ (\varphi<180°) \tag{6−3}$$

Likewise, the maximum horizontal angle of the reflector in the case of φ>180° is obtained by the following formula.

$$b_{MAX} = \frac{q-\pi+\beta}{2} = \frac{\beta-111.8}{2} \ (\varphi>=180°) \tag{6−4}$$

In the case of φ >180°, when the angle of the reflector becomes smaller than b_{MAX}, the reflected sunlight shines on the left wall of the model in Fig. 6-2. The angle of the reflector and the minimum horizontal angle of the reflector can be obtained by the above equations and are summarized in Table 6-1.

Since the simulation in this chapter can provide a comfortable lighting environment, I set the reflector such that the incident light can be reflected to the center of the ceiling by controlling the reflector at two angles a_{MID} and b_{MID} shown in Table 5-3 and Table 6-1.

Table 6-1 Maximum angle and minimum horizontal angle of the reflectors

season / time	summer		winter		spring・autumn	
	b_{MID}	range of b	b_{MID}	range of b	b_{MID}	range of b
9:00～10:00	16.7°	5.8°＜b	27.0°	16.07381＜b	21.2°	10.3°＜b
10:00～11:00	9.8°	-1.1°＜b	18.1°	7.229363＜b	13. 3°	2.4°＜b
11:00～12:00	1.3°	-9.6°＜b	0°	-10.9＜b	4.1°	-6.7°＜b
12:00～13:00	-7.8°	b＜-3.1°	-10.2°	b＜-0.68759	-8.0°	b＜-2.9°
13:00～14:00	-13.3°	b＜2.4°	-26.9°	b＜16.07381	-16.4°	b＜5.5°
14:00～15:00	-19.8°	b＜8.9°	-33.7°	b＜22.78547	-23.8°	b＜12.9°

2. Width of reflector

The width of the reflector is the same as in the chapter 5, and can be referred in Table 5-4.

3. Number of reflectors

In the simulation of this chapter, as shown in the coordinate system in Fig. 6-1 (a), the reflection plate is controlled by the axis of the blue line of the window. Therefore, if the position and the number of reflectors are the same as the simulation in the chapter 5, a part of sunlight enters the room through the yellow part shown in Fig. 6-4.

In the case of the reflector angle being b_{MID}, the length of S is calculated by equation (6-5). Calculations were made in the simulation and summarized in Table 6-2.

$$M = \tan b_{MID} \times \frac{L}{2} \tag{6-5}$$

Here, L is the length of window.

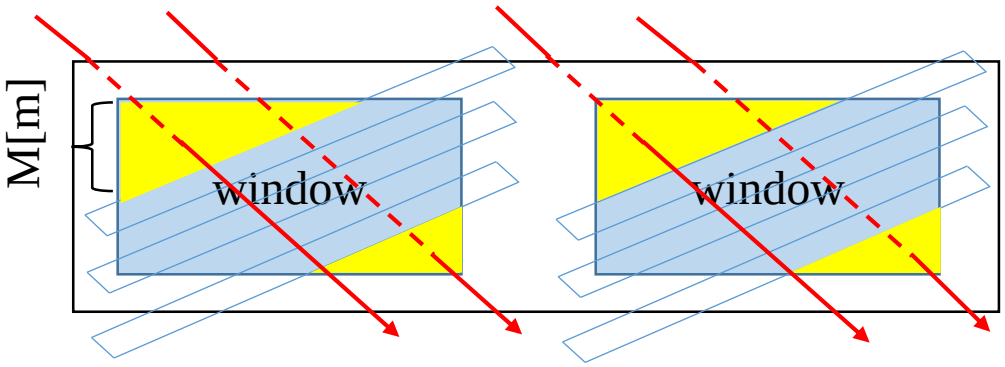

Fig. 6-4 The passage of sunlight

Table 6-2 The shortest length of M

season / time	Summer	winter	spring・autumn
9:00～10:00	0.389 m	0.662 m	0.504 m
10:00～11:00	0.225 m	0.426 m	0.307 m
11:00～12:00	0.030 m	0.000 m	0.094 m
12:00～13:00	0.178 m	0.234 m	0.183 m
13:00～14:00	0.307 m	0.662 m	0.382 m
14:00～15:00	0.468 m	0.867 m	0.573 m

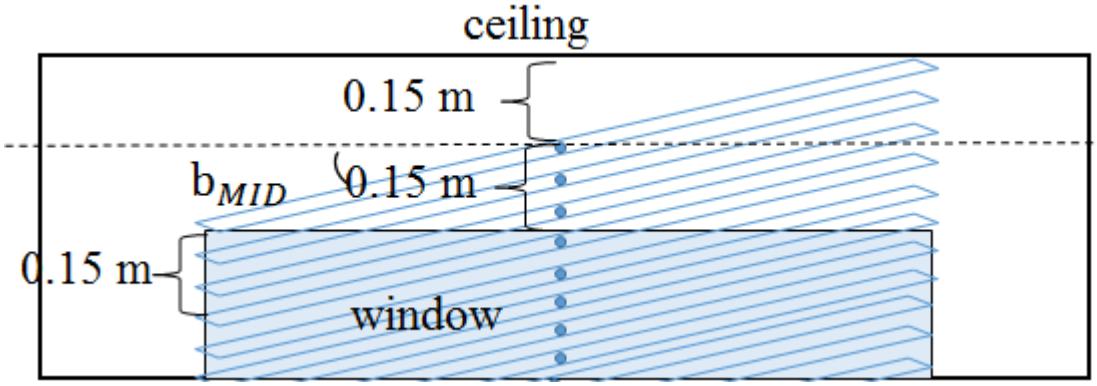

(a) The upper position of the reflector

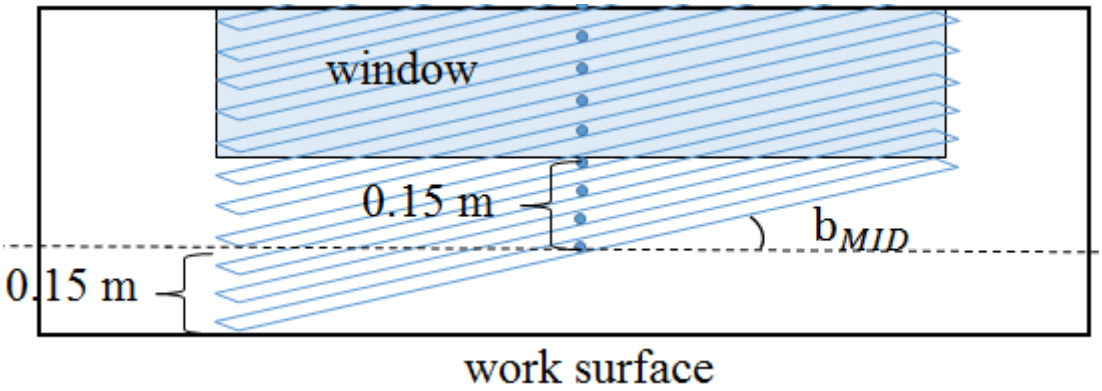

(b) The lower position of the reflector

Fig. 6-5 Reflector position

According to Table 6-2, the length of M in winter has a maximum value of 0.867 m, which is a fairly large figure. As shown in Fig. 6-5 (a), the actual maximum length of M is half the distance between the top of the window and the ceiling which is about 0.15 m. However, this distance can only be used from 11: 00 to 12: 00. In order to solve this problem, instead of controlling a single row of reflectors as shown in Fig. 6-6, I can increase the number of rows of reflectors and control the reflectors. Thus, when there is an n-column reflector, the length of S shown in Table 6-2 is 1 / n^2. Since the maximum length of is 0.867 m, it is necessary to control three rows of reflectors or more. Also, since the space between the reflectors is the same as in the chapter 5, installed at 0.07 m, it is necessary to add two reflector plates at the bottom and the top of the window. Overall, the number of rows of reflector plates is three and the number of reflector plates for every row is 24 as shown in Fig. 6-6.

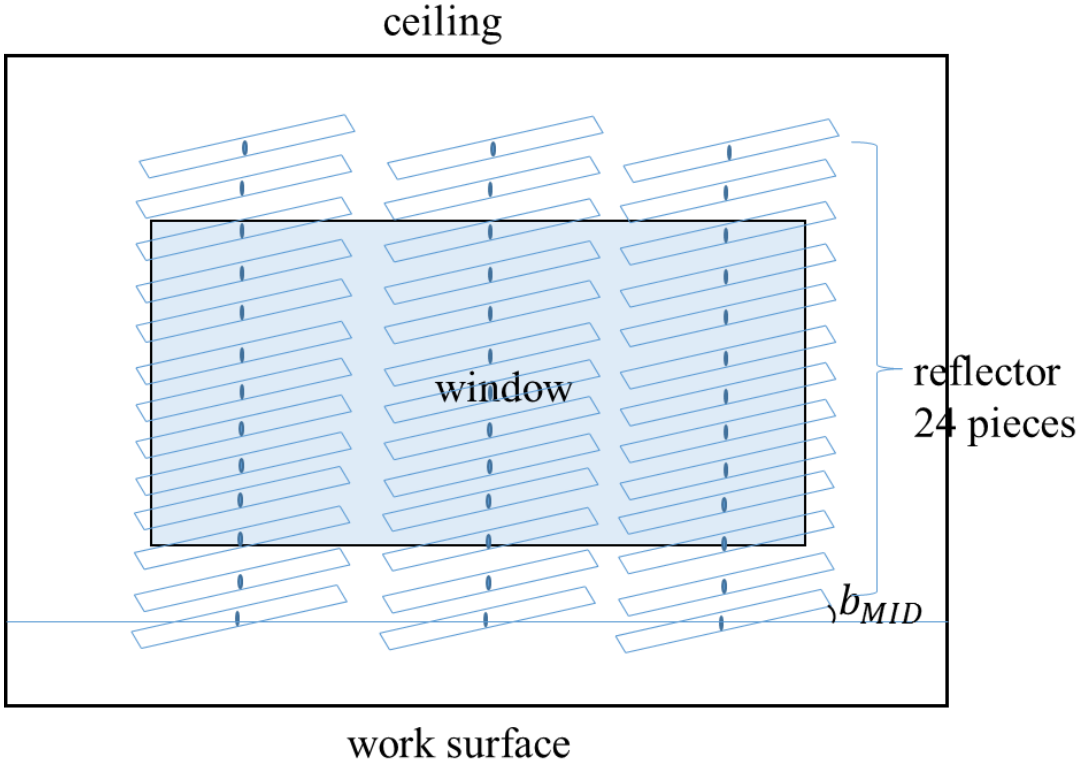

Fig. 6-6 Control of reflector

4. Length of reflector

Here, in order to prohibit sunlight coming from the gap between the reflection plates to the work surface, the length of the reflection plate has to be determined.

As shown in Fig. 6-7, in order to obtain the length of the reflecting plate, the length of BC must be obtained first. In △ABC, according to the sine theorem, the relationship is as follows.

$$\frac{AB}{sin\angle \mathrm{ACB}} = \frac{\mathrm{BC}}{sin\angle \mathrm{BAC}} \qquad (6-6)$$

From the above equation,

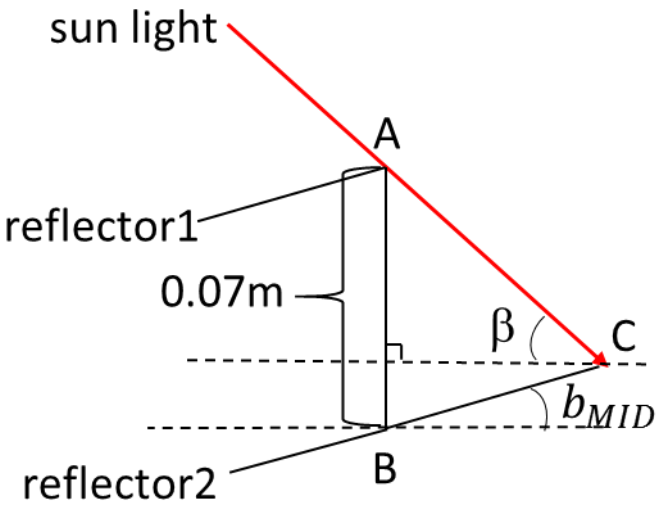

Fig. 6-7 Determination of the length of reflector

Table 6-3 The shortest length of the reflector [m]

season / time	summer	winter	spring・autumn
9:00～10:00	0.89	0.91	0.90
10:00～11:00	0.88	0.90	0.89
11:00～12:00	0.87	0.87	0.87
12:00～13:00	0.85	0.85	0.85
13:00～14:00	0.85	0.82	0.84
14:00～15:00	0.84	0.81	0.83

$$BC=\frac{AB\times sin\angle BAC}{sin\angle ACB} \tag{6－7}$$

Here, AB＝0.07m, ∠BAC＝90°－β, ∠ACB＝$\beta+b_{MID}$. β is obtained by equations (5-8) and (5-9), and b_{MID} can be referred from Table 6-1. By substituting these conditions into eq. (6-7), the following equation can be obtained.

$$BC=\frac{0.07\times\cos\beta}{\sin(\beta+b_{MID})}\ [m] \tag{6－8}$$

Also, the length l of the reflector is obtained by the following formula, with the results summarized in Table 6-3.

$$l=\frac{2.6+2BC}{3}\ [m] \tag{6－9}$$

Based on the data in Table 6-3, the shortest length of the reflector was found at 0.91 m becomes the maximum at between 9: 00 ~ 10: 00 in winter. The length of the reflecting plate is set to 0.91 m for every season so that all incident lights are reflected to the ceiling.

5：Reflector condition setting

Based on the above calculations, the dimensions of the reflectors set during the actually simulating are as shown in below.

- Number of reflecting plates: 24 (each window)
- Spacing between reflectors: 7 cm
- Length of reflector: 0.91 m
- Width of reflector: 0.1m in summer・spring・autumn, 0.2m in winter
- Angle of reflector: a_{MID}, b_{MID} (Refer to Table 5-3 and Table 6-1.)

6-3 Evaluation of use of lighting in all seasons

By applying the conditions summarized in chapter 6-1 to the created illuminance distribution simulator, in the office model space shown in Fig. 5-1, the angle of the reflector attached in front of the window changes according to the sun altitude by using angles a_{MID}, b_{MID} so that incident sunlight is reflected to the center of the ceiling. I also examined the change in the illuminance distribution of the observation surface.

1：Evaluation of daylighting usage at summer

The simulated illuminance distribution in summer is shown in Fig. 6-8(a~f).

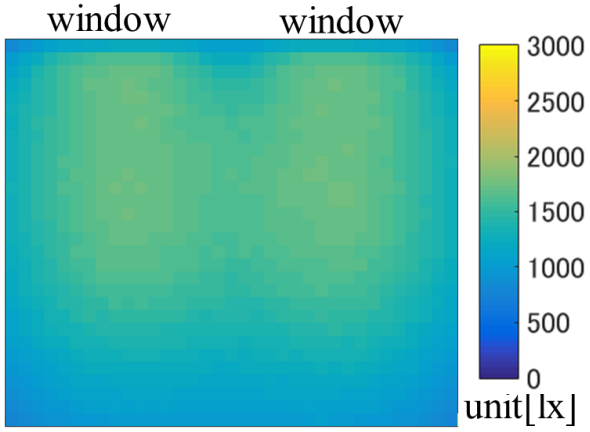

(a) 9:00～10:00 (solar altitude angle 55°, solar azimuth angle 110°)

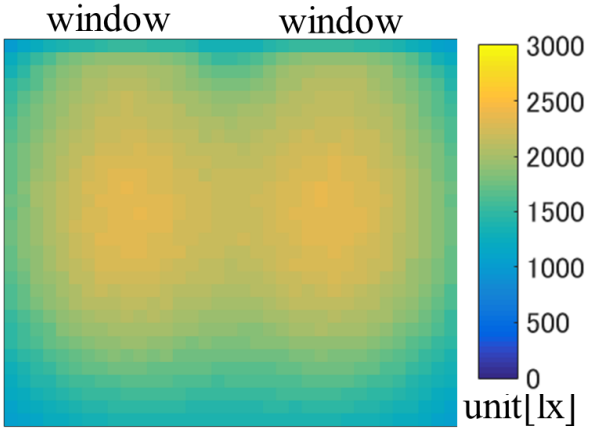

(b) 10:00～11:00 (solar altitude angle 65°, solar azimuth angle 130°)

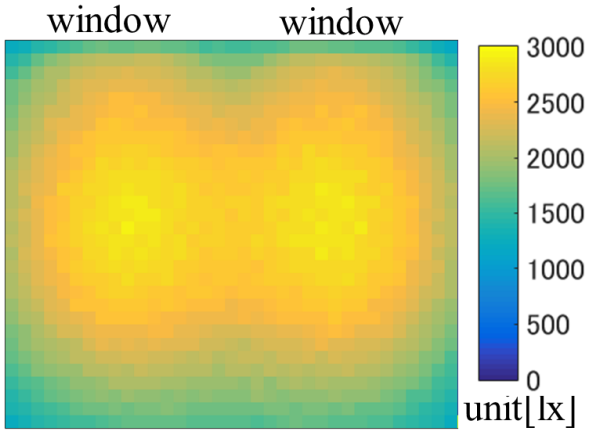

(c) 11:00～12:00 (solar altitude angle 75°, solar azimuth angle 170°)

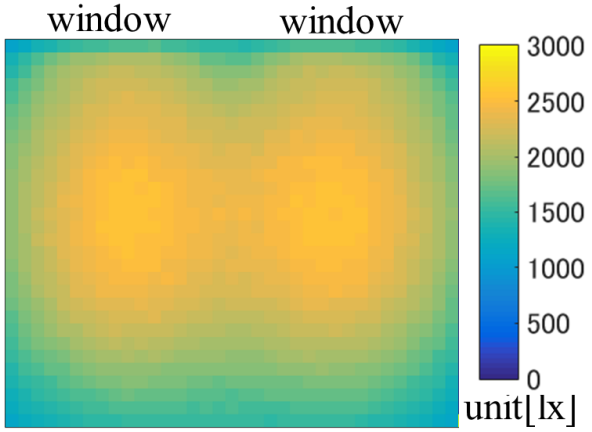

(d) 12:00～13:00 (solar altitude angle 70°, solar azimuth angle 230°)

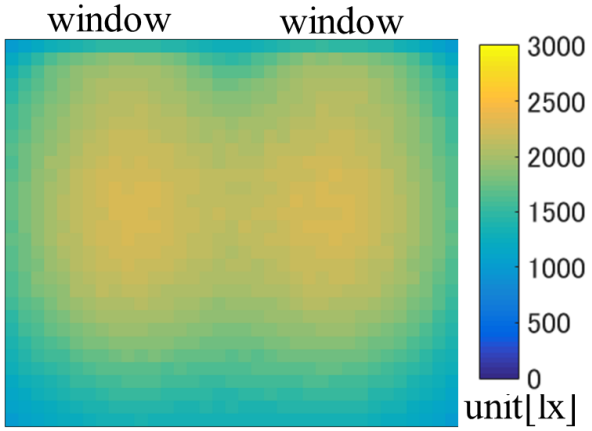

(e) 13:00～14:00 (solar altitude angle 60°, solar azimuth angle 240°)

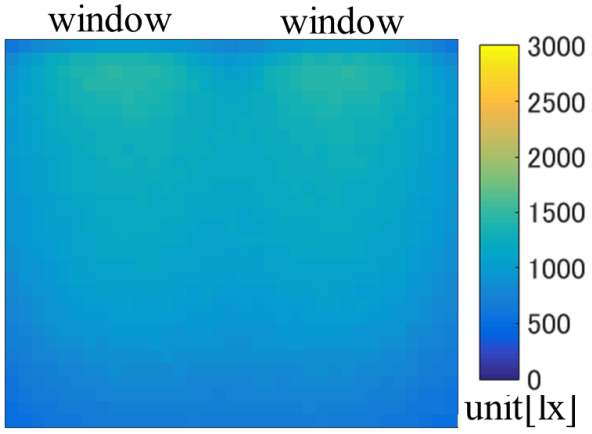

(f) 14:00～15:00 (solar altitude angle 50°, solar azimuth angle 260°)

Fig. 6-8 Illuminance distribution for summer (control 3 rows reflectors)

Looking at the illuminance distribution charts in Fig. 6-8, the illuminance distribution in the room varies with the change of time between 9:00 and 3:00. Since the dazzling sunlight entering through the window is reflected to the center of the ceiling, the illuminance distribution looks evenly visible at any time. And it became clear that the time zone with the biggest average illuminance will be between 11:00 and 12:00. To compare more precisely, the numerical results are summarized in Table 6-4 and the results are graphed in Fig. 6-9.

Looking at the result of illuminance in Fig. 6-9(a), the maximum illuminance, the minimum illuminance, and the average illuminance became brighter from 9:00, peak at the time zone from 11:00 to 12:00, and lowers gradually after 12:00. And all illuminance were above 500 lx, meeting the lighting standards. Also, from the results of the degree of uniformity, it was found that the uniformity at any time zone was about 0.8 overall. Thus, in the summer, daylighting can be performed without lighting if the reflector is controlled well between 9:00 and 15:00.

Table 6-4 Simulation results for summer (control 3 rows reflectors)

Results / Time zone	Maximum illuminance[lx]	Minimum illuminance[lx]	Average illuminance[lx]	Uniformity
9:00～10:00	1743.0	1301.4	1619.8	0.80
10:00～11:00	2351.4	1793.9	2153.8	0.83
11:00～12:00	2912.2	2143.9	2595.1	0.83
12:00～13:00	2578.0	1977.1	2354.1	0.84
13:00～14:00	2280.1	1742.9	2092.0	0.83
14:00～15:00	1372.4	867.1	1165.9	0.74

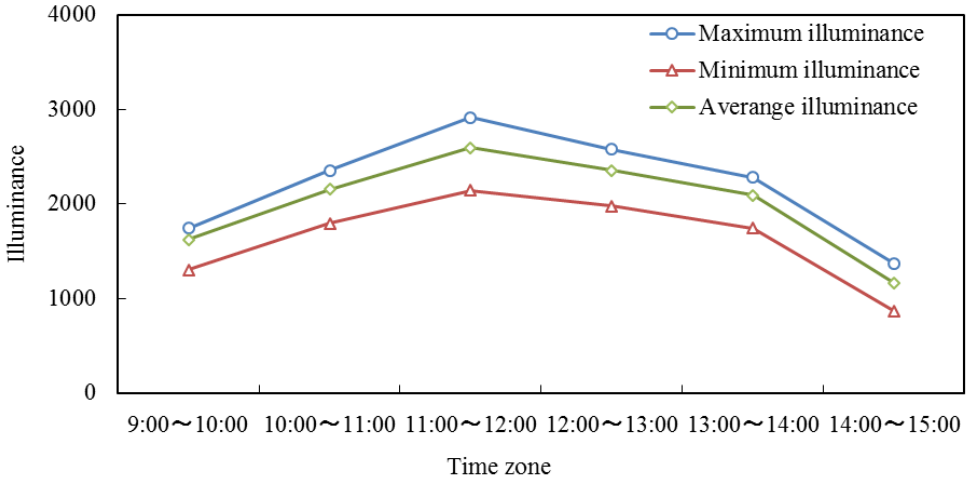

(a)Results of illuminance

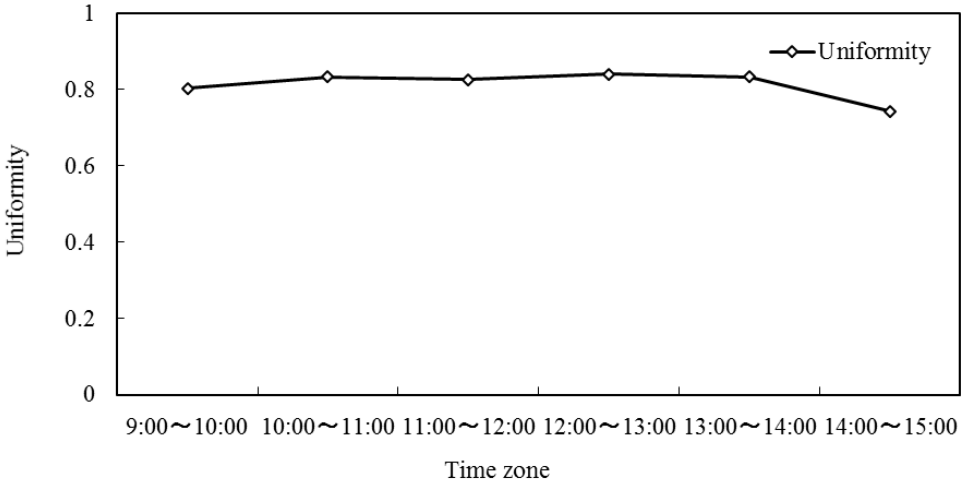

(b) Results of uniformity

Fig. 6-9 Simulation results for summer (control 3 rows reflectors)

2：Evaluation of use of lighting in spring and autumn

The simulated illuminance distribution for spring and autumn is shown in Fig. 6-10(a~f).

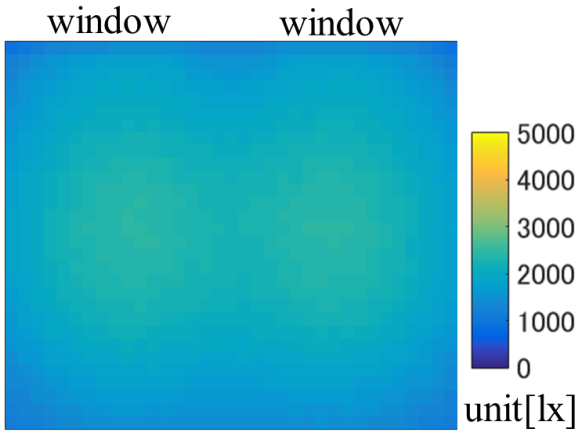

(a) 9:00～10:00 (solar altitude angle 40°, solar azimuth angle 130°)

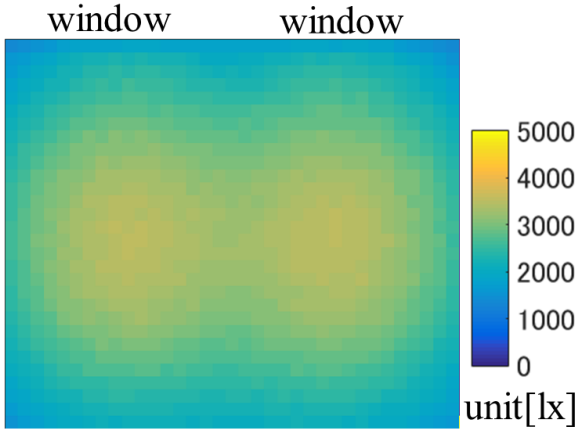

(b) 10:00～11:00 (solar altitude angle 45°, solar azimuth angle 150°)

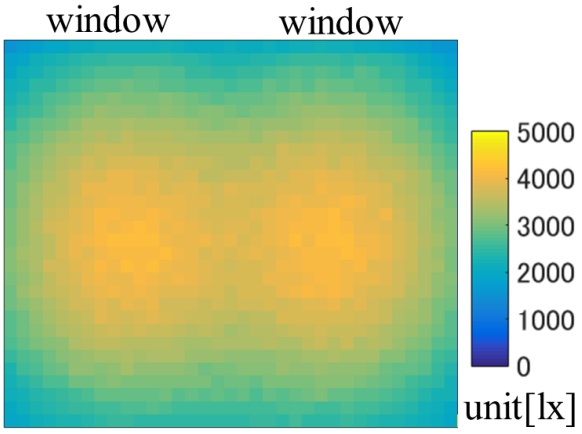

(c) 11:00～12:00 (solar altitude angle 50°, solar azimuth angle 170°)

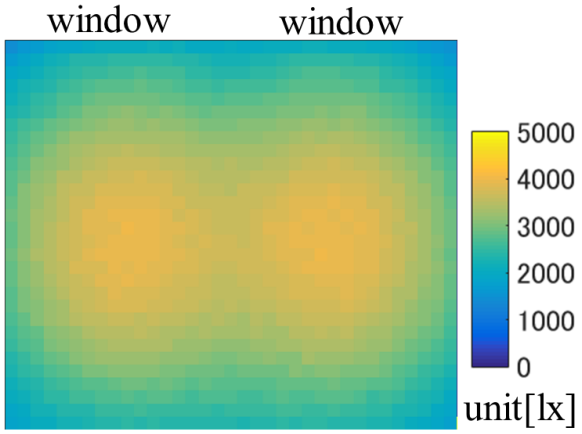

(d) 12:00～13:00 (solar altitude angle 50°, solar azimuth angle 200°)

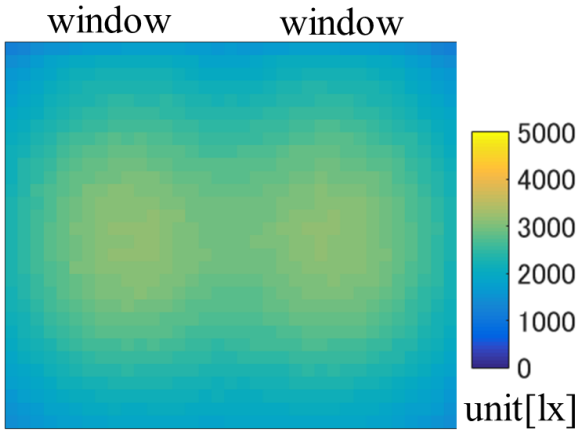

(e) 13:00～14:00 (solar altitude angle 45°, solar azimuth angle 220°)

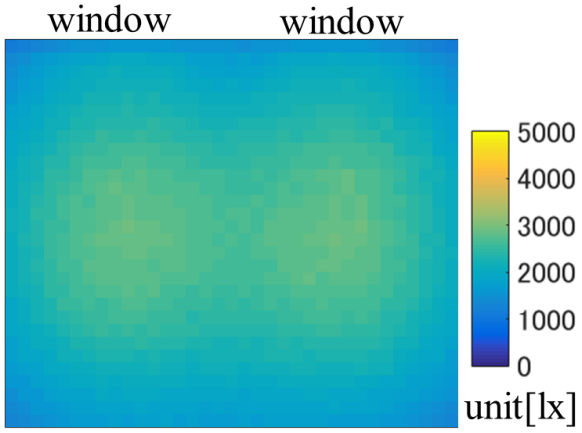

(f) 14:00～15:00 (solar altitude angle 35°, solar azimuth angle 230°)

Fig. 6-10 Illuminance distribution for spring・autumn (control 3 rows reflectors)

Observing at the illuminance distribution diagrams in Fig. 6-10, the intensity of light entering the room changes from 9:00 to 3:00 with time. The time periods when the lighting is the strongest is between 11:00 and 12:00 and between 12:00 and 13:00. The light at during this period seems to be the most even and bright. To compare the results more precisely, the numerical results are summarized in Table 6-5 and the results are graphed in Fig. 6-11.

Looking at the result of the illuminance in Fig. 6-11 (a), the maximum illuminance, the minimum illuminance, and the average illuminance became brighter from 9:00 and gradually reached the peak between 11:00 to 12:00. After 12:00, there is a tendency for them to decrease. The illuminance for all time zones is more than 500 lx, satisfying the illuminance standard. Also, looking at the result of the uniformity, all the uniformity is above 0.7, satisfying the illuminance standard. Looking at diagram Fig. 6-11 (b), the degree of uniformity is around 0.8 for all cases. Based on this result, it is clear that it is possible to create an eco-friendly lighting environment and save energy just by controlling the reflector well during the spring・autumn season.

Table 6-5 Simulation results for spring・autumn (control 3 rows reflectors)

Results / Time zone	Maximum illuminance[lx]	Minimum illuminance[lx]	Average illuminance[lx]	Uniformity
9:00～10:00	2448.5	1800.3	2197.4	0.82
10:00～11:00	3571.2	2438.5	3123.6	0.78
11:00～12:00	4205.1	2788.7	3657.4	0.76
12:00～13:00	4004.8	2690.1	3509.0	0.77
13:00～14:00	3162.2	2234.5	2807.5	0.80
14:00～15:00	2930.9	2037.1	2556.5	0.80

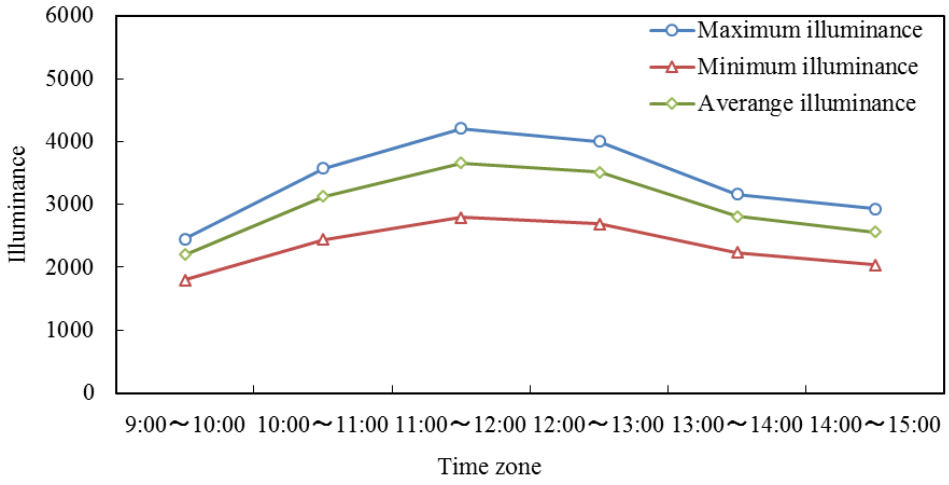

(a)Results of illuminance

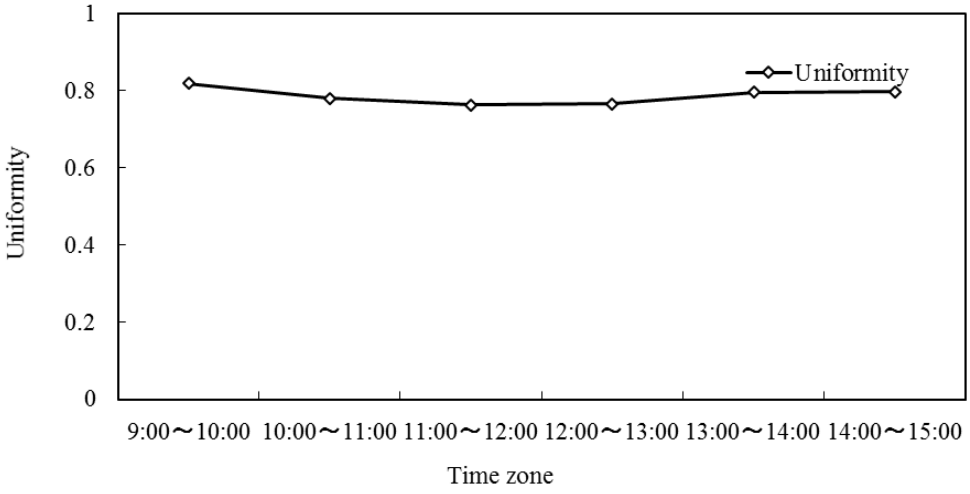

(b) Results of uniformity

Fig. 6-11 Simulation results for spring・autumn (control 3 rows reflectors)

3：Evaluation of use of daylight in winter

The simulated illuminance distribution in winter is shown in Fig. 6-12(a~f)

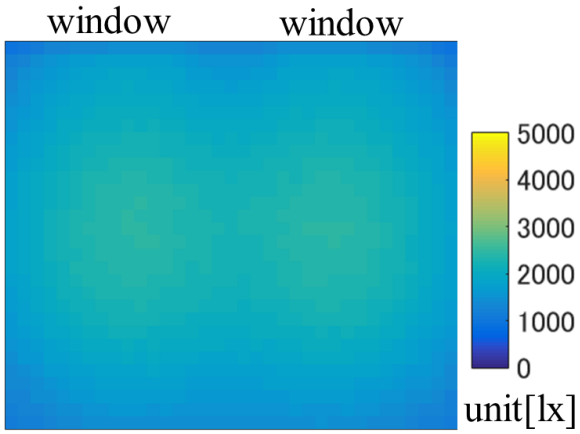

(a) 9:00～10:00 (solar altitude angle 20°, solar azimuth angle 150°)

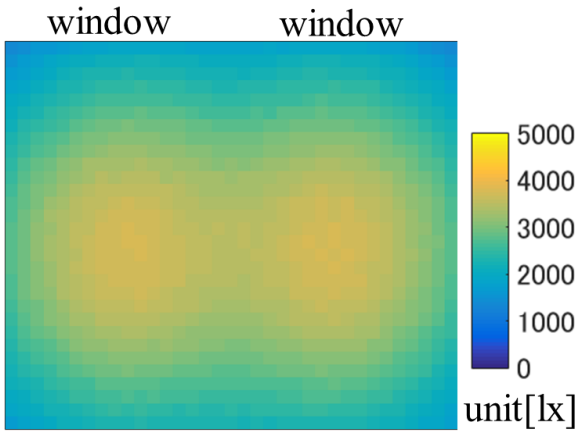

(b) 10:00～11:00 (solar altitude angle 25°, solar azimuth angle 160°)

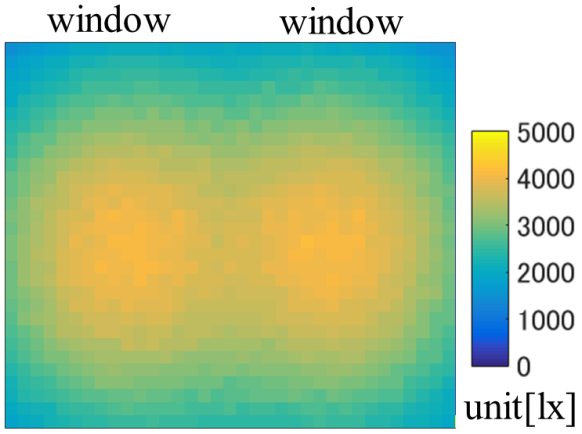

(c) 11:00～12:00 (solar altitude angle 30°, solar azimuth angle 180°)

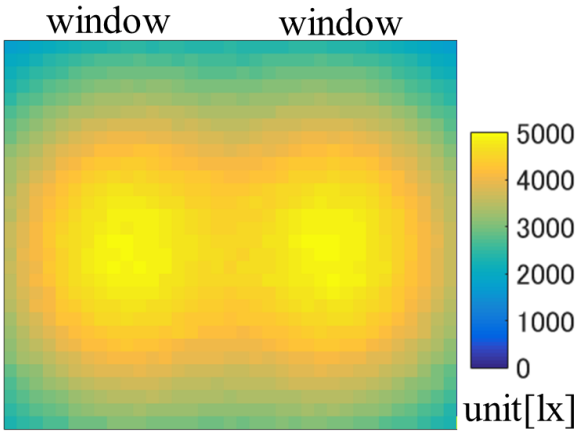

(d) 12:00～13:00 (solar altitude angle 25°, solar azimuth angle 190°)

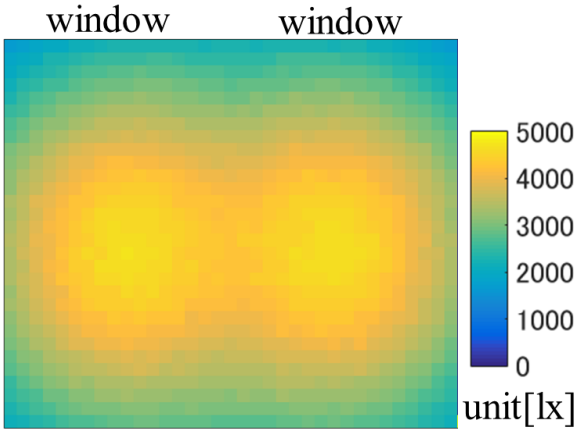

(e) 13:00～14:00 (solar altitude angle 20°, solar azimuth angle 210°)

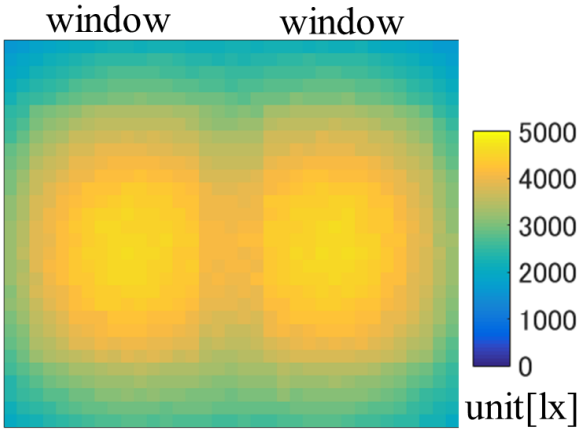

(f) 14:00～15:00 (solar altitude angle 15°, solar azimuth angle 220°)

Fig. 6-12 Illuminance distribution for winter (control 3 rows reflectors)

The illuminance distribution diagrams in Fig. 6-12, the time zone in which illumination is the best is between 11:00 and 15:00. The light of this time zone looks the most even and brightest. To compare the results more precisely, the numerical results are summarized in Table 6-6 and the results are graphed in Fig. 6-13.

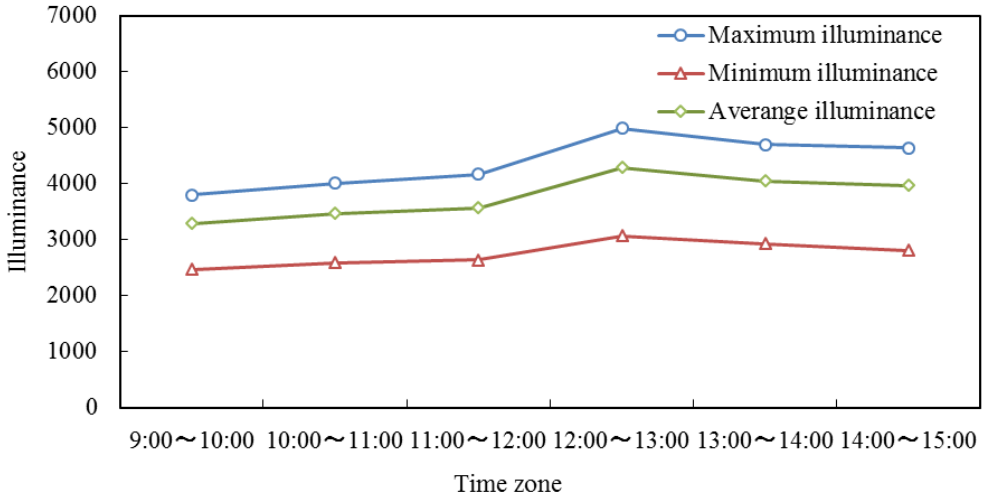

(a)Results of illuminance

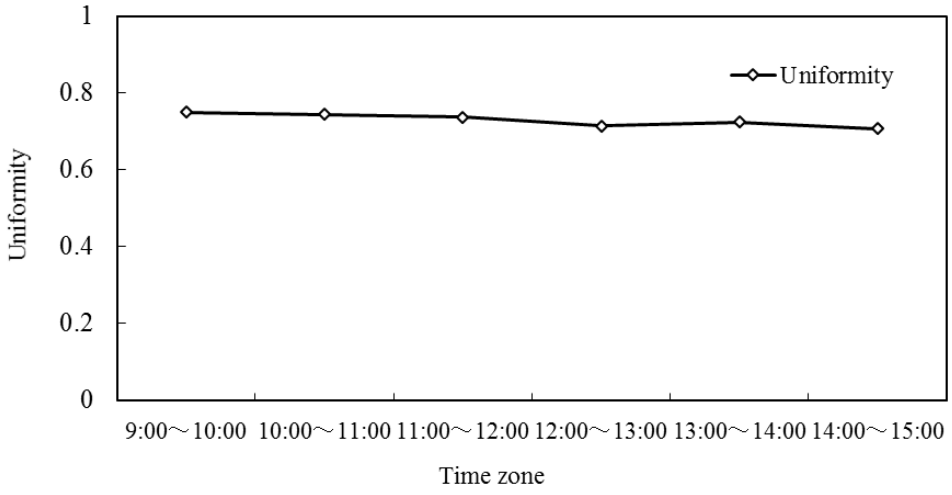

(b) Results of uniformity

Fig. 6-13 Simulation results for winter (control 3 rows reflectors)

Table 6-6 Simulation results for winter (control 3 rows reflectors)

Results / Time zone	Maximum illuminance[lx]	Minimum illuminance[lx]	Average illuminance[lx]	Uniformity
9:00～10:00	3794.5	2467.9	3291.2	0.75
10:00～11:00	4011.9	2583.2	3469.6	0.74
11:00～12:00	4164.6	2633.3	3568.5	0.74
12:00～13:00	4986.6	3069.9	4292.8	0.72
13:00～14:00	4698.6	2929.0	4045.3	0.72
14:00～15:00	4636.1	2810.0	3971.1	0.71

The result of illuminance in Fig. 6-13 (a), the minimum illuminance and the average illuminance become brighter from 9:00, peaked in the time zone from 12:00 to 13:00, the illuminance after that was almost constant. In addition, from the data in Table 6-6, the illuminance for all time zones were more than 2000lx, fulfilling the illuminance standard, but it feels somewhat high. Also, looking at the result of the uniformity, the uniformity for all time zones are more than 0.7 satisfying the illuminance standard. Furthermore, the uniformity for all time zones were almost the same, around 0.8.

6-3 Consideration of power consumption

If the blind-shaped reflector attached to the window is controlled as shown in Fig. 6-6, it is clear from section 6-2 that the combination of artificial lighting and daylighting from the window is effective for energy conservation. By controlling the three rows of reflectors attached to the window at angles a_{MID}, b_{MID}, the dazzling incident sunlight was reflected to the ceiling and an eco-friendly lighting environment was created using the diffused light reflected from the ceiling. And from the data in Table 6-4 to Table 6-6, the illuminance standard was satisfied for illuminance of all the time zones, being more than 500 lx for all seasons, and the ratio of uniformity is more than 0.7. By utilizing the reflector set in this simulation, the illuminance standard is satisfied even if light equipment are not light up in the office from 9:00 to 15:00.

By comparing the lighting environment where light does not enter from the window evenly and lighting fixtures are arranged on the ceiling as described in Chapter 4 (which is the lighting environment of a typical office at night time. Refer to Fig. 4-11), the power consumption was calculated. The working hours of an office are normally between 9:00 and 15:00, and the power consumption per day is 64 W × 9 fluorescent lamps × 9 hours = 5184 W. The power consumption when using the reflection plane for this simulation is 64 W × 9 fluorescent lamps × 3 hour = 1728 W, which increases the amount of power conservation in the day by 66.7%. Based on the results obtained, it can be said that daylighting from the window is effective in reducing power consumption.

Chapter 7

Conclusion

7-1 Results obtained in this research

The ultimate goal of this research work is to save energy in the office buildings by using daylight entering into rooms from the window. In this research, I proposed a method to utilize diffused light from the ceiling by using blind reflectors which are able to change their reflection angle freely. The reflectors are attached to the window and reflect incident light to the ceiling. This method can increase the daylighting rate from the window compared with the conventional researches, and by controlling the reflector intelligently, it is possible to make a more comfortable lighting environment for human beings. However, a versatile illumination distribution simulator was made which can reproduce the nature of light precisely on a computer. Therefore, in this research, I have created a versatile illuminance distribution simulator using the Monte Carlo method which can reproduce the nature of light precisely on a computer. I also compared and investigated the influence of daylighting on the indoor lighting environment when blind reflector plates are installed in the window. Ultimately, I found out that it is possible to conserve energy when using window lighting and artificial lighting after experimenting it under various conditions. The main results obtained are shown below.

1：Creation of illumination distribution simulator

In this research, a system that simulates an environment which can take light from windows was introduced by installing not only lighting fixtures and windows, but also a system capable of setting the sun and reflectors' angles. In this simulation system, the type of lighting equipment, the presence or absence of a window, size of simulation objects can be freely chosen, and simulation assuming night time when light cannot be taken from the window was made possible. In order to simulate the change in the solar altitude for each season, the angle of the incident light from the window can be freely changed, and the angle of the blind reflection plates attached to the window can also be freely controlled under various conditions. In addition, validity of the simulator was verified by comparing the results of simulation under various environments with actual measured values.

2：Comparison and examination of the indoor environment during daylighting from the window

An illuminance distribution simulator as described above was created and used for simulation

under various conditions. Conditions of the model space and parameters can also be changed easily. Our simulation led to the following results.

① **Evaluation of use of lighting without direct light**

Without direct light, that is, when it is cloudy, the light entering through the window is scattered light, harmless to human eyes and can be used directly as lighting for office environment, whereby in this case no reflector is attached. However, by actual measurement, in the case of only window lighting, since the area satisfying the illuminance standard on the working surface is only on the window side, it is necessary to use it together with the artificial lighting. By referring to the data in Table 4-2, if the number of the lighting equipment is too many, the uniformity of the work surface will be low. If the number of lighting is small, it will not satisfy the lighting standards and cannot be applied in working environments. As a result, I found out that in the absence of direct light, it is possible to reduce the power consumption by 33% or more in the same time zone by proper lighting using the lighting system consisting of the window and lighting equipment.

② **Evaluation of use of lighting with direct light - controlled by reflector α_{MID}**

When there is direct light, the sunlight entering through the window is dazzling and cannot be used as a work surface illumination. Therefore, it is necessary to attach blind-shaped reflectors to the window. The reflector plate is controlled by rotating it from the bottom to the top about the innermost side (the part in contact with the window) of the reflector. In order to obtain a good lighting environment, I controlled the reflector using angle θ_{MID} so that light is reflected from the window to the center of the ceiling of the room by actual calculation.

As a result, in the case of only lighting from the window, in terms of illuminance, the minimum illuminance is more than 500 lx for all time zones of all seasons which satisfies the illuminance standard, although the value was slightly higher in spring, autumn and winter due to higher daylighting rate and change of the solar azimuth angle according to time zone. In terms of the uniformity, the ratio of uniformity in the time zone from 11:00 to 12:00 is more than 0.7, but the uniformity in other time zones did not satisfy the illuminance standard. I believe that this is caused by sunlight being reflected to the left and right walls from the ceiling in the morning and evening. Dazzling lights on the left or right walls reflect on each other, increasing the illuminance around that area and decreasing its uniformity. In order to avoid it, it is necessary to brighten up the room by adding lights.

When using window lighting and artificial lighting at the same time, in summer, the uniformity and illuminance between 9:00 and 15:00 satisfy the illuminance standard. In the

case of spring and autumn, the lighting environment between 9:00 and 14:00 satisfy the illuminance standard, and the ratio of uniformity of 14:00~15:00 cannot be used because it is below 0.7. In winter, the lighting environment between 10:00 and 13:00 satisfy the illuminance standard, and the uniformity degree between 9: 00-10: 00 and 13:00-15:00 cannot be used because they were below 0.7.

In terms of power consumption, by referring to the data in Table 5-13, it was expected that the time zone of 11:00-12:00 requires the least number of lighting fixtures and the reduction of power consumption is the highest. It was found that the illumination standard was satisfied even when lighting fixtures were not light up at this time. The power consumption at this time was compared with the power consumption when the number of lighting was 9, and it was found that 100% power consumption can be reduced. And in the same time zone, energy can be saved by 55.5% in the morning and at least 44.4% in the evening.

③ **Evaluation of use of lighting with direct light - controlled by reflectors a_{MID}, b_{MID}**

Based on the previous results, the uniformity between 11:00 and 12:00 is the largest in any season, and even when light is not used in this time zone, it meets the illumination standard. The reason for this is that from 11:00 to 12:00, the azimuth of the sun is almost 180 °, and it is located a little south of the room. In order to further increase the energy saving rate, as shown in Fig 6-1, the reflector is not only moved from the bottom to the top by angle a_{MID}, but also moved horizontally between left and right by the angle b_{MID} around the center of the reflector so that sunlight in any time zone could be reflected to the center of the ceiling. And by making calculations in the actual environment, three rows of reflectors were controlled at the same time (refer to Figure 6-6) to improve the practicality of the reflector.

As a result, the illuminance in all time zones is over 500 lx for all seasons, the ratio of uniformity is more than 0.7, and the illuminance standard is met. Therefore, by utilizing the reflector settings in this simulation, the illuminance standard is satisfied even if the office is not light up in the time zone from 9:00 to 15:00.

3：Possibility of reducing power consumption

Based on the above results, it has become clear that the power consumption can be reduced by 33% or more in the same time zone when there is no direct light (such as cloudy days). When there is direct light (fine day), when controlling the reflector at the angle of a_{MID}, it is possible to reduce the power consumption by 100% at the time zone from 11:00 to 12:00. On the same day, at least 55.5% and 44.4% can be conserved in the morning and evening respectively. When three rows of reflectors are controlled by angles a_{MID} and b_{MID}, it is clear that an eco-friendly lighting environment can be created even without using any lighting fixture within the daylighting

period, and 100% power consumption can be reduced.

Assuming that the working hours of the day is from 9 am to 6 pm for a typical laboratory and the power consumption per hour for one hour is 64 W, the power consumption during the day is 64 W × 9 fluorescent lamps × 9 hours = 5184 W. In comparison with this, when controlling the reflector at the angle of a_{MID}, it is possible to reduce the power consumption by 42% in summer, 34.6% in spring and autumn, and 25.9% in winter. When three rows of reflectors are controlled by angles a_{MID} and b_{MID}, the power consumption reduction during the day is 66.7%. As can be seen from the above, it can be said that daylighting from the window is effective in reducing power consumption.

7-2 Future work

Currently, in the case of sunny conditions, a sufficient lighting environment can be achieved simply by utilizing the reflector even without artificial lighting. The illuminance and the uniformity satisfy the illuminance standard in the time zone from 10:00 to 13:00 in spring, autumn and summer, and from 12:00 to 15:00 in winter, but the illuminance is somewhat high. In order to solve this problem, we want to block incident light partially. This is probably conceivable by changing the dimensions of the reflector plate or to partially close the reflector plate from below. By adjusting the appropriate amount of light taken from the window, it is possible to create a lighting environment that is harmless to the human eyes, and also to reduce the maximum illuminance at the room center and to increase the ratio of uniformity.

Acknowledgments

I wish to express my sincere gratitude to Professor Kurabayashi Tohru of Akita University for his support and guidance throughout the whole study. I am also grateful to him for checking and correcting my thesis works.

I wish to extend my gratitude to Professor Obara Hitoshi, Professor Tajima Katsubumi and Professor Kumagai Seiji, of Akita University for their guidance and useful suggestions in this research. I would also like to express my gratitude towards the late Professor Masafumi Suzuki as I learnt the techniques and methods of simulations from him. I also pay gratitude to Professor Mitobe Kazutaka of Akita University for his advices during the research works.

I am deeply indebted to Associate Professor Mahmudul Kabir of Akita University for his constant encouragement and helpful advices. I would also like to thank Mrs. Naoko Obara, the technical staff of Akita University for her help in the research.

I would also like to thank the graduate and undergraduate students of Basic Electrical Laboratory of Akita University, for their interest and help throughout the research.

Finally, I would like to thank my beloved family and friends for their unwavering support during my research works.

Publications and presentations associated with this paper

Papers

1. Chenglin Li and M. Kabir: “Development of an Indoor Illuminance Distribution Simulator by using the Monte Carlo Method”, Global Journal of Engineering Science and Research Management, ISSN 2349-4506, Vol.4, No.3, pp.85-94 (2017)
2. Chenglin Li and M. Kabir: “The Use of Daylight for Interior Illumination System with Window Shade Reflector”, International Journal of Engineering Sciences & Research Technology, ISSN 2277-9655, Vol.6, No.5, pp.7-14 (2017)
3. Chenglin Li, M. Kabir and N. Yoshimura: “Simulation on Angle Adjustment of Blind Shaped Reflectors Installed in Windows for Daylight Utilization in Room Lighting System”, IEEJ Trans. FM (in process, in Japanese)

李 承霖,カビール　ムハムドゥル,吉村　昇：“室内照明において昼光利用のため窓に設置するブラインド状反射板の角度調整に関するシミュレーション”，電気学会誌(投稿中)

4. Chenglin Li and M. Kabir: “Simulation Works on Interior Illumination with Natural Daylight”, International Journal of Engineering Sciences & Research Technology (in process)
5. Chenglin Li and M. Kabir: “Study on Using Daylight as Lighting System According to Various Sun Angles”, International Journal of Engineering Sciences & Research Technology (in process)

International Conference

1. Chenglin Li, Mahmudul Kabir and Noboru Yoshimura: “Utilizing of Daylight in Interior Lighting System by Using Reflectors at Window Blinds”, The 8th International Conference on Materials Engineering for Resources (ICMR)(Oct.25-27, 2017) Akita, Japan, Proceedings of ICMR 2017, pp. 323-326

Domestic Conferences

1. 李 承霖,カビール　ムハムドゥル,吉村　昇：「昼光の利用による照明消費電力の削減に関する研究」,平成 29 年度電気学会全国大会（2017 年 3 月　富山大学 五福キャンパス）
2. 李 承霖,カビール　ムハムドゥル,吉村　昇：「室内照明における昼光利用の検討」,平成 29 年度照明学会全国大会（2017 年 9 月　東北学院大学　多賀城キャンパス）